THE ASTROPHYSICAL JOURNAL

AN INTERNATIONAL REVIEW OF SPECTROSCOPY AND ASTRONOMICAL PHYSICS

VOLUME 90 OCTOBER 1939 NUMBER 3

RED INDICES IN SOUTHERN SELECTED AREAS[1]

CECILIA PAYNE-GAPOSCHKIN

ABSTRACT

The red indices of nearly five thousand stars, in the Selected Areas at $-60°$, for which spectral classifications have been made at Potsdam, furnish material for a discussion of spectrum and color in relation to galactic structure.

The Potsdam system of spectral classification differs appreciably from the Henry Draper system. The accidental errors of both systems have been evaluated as functions of spectral class and apparent magnitude. The Harvard system does not contain as many subdivisions as the accidental error of classification warrants; the Potsdam system, on the other hand, is too finely subdivided. The systematic differences of classification are functions both of apparent and of absolute magnitude.

Of the twelve Selected Areas studied, six are in galactic latitude greater than 20°, where obscuration should, on the average, be negligible. For these six areas, containing eleven hundred stars, the colors are normal throughout the spectral sequence. The high-latitude areas can therefore be used as standards of normal color for comparison with other areas.

The six low-latitude areas differ in spectral makeup and in degree of obscuration. Selected Area 193 (Carina) shows extremely little reddening, and the frequency of blue stars is the greatest in this area: the negative density gradients that have been derived for blue stars in this part of the sky are partly a result of systematic errors of spectral classification. The other five areas, while differing in spectral makeup, show similar color excesses, not very different from those found by other investigators in other parts of the sky.

The principal results of the analysis is the stress that it lays on the importance of standardizing both spectral classification and magnitude systems. Otherwise, accurate and consistent conclusions on galactic structure cannot be drawn from studies of colors and spectra of faint stars.

1. *Introduction.*—Red indices for 4732 stars, in the twelve Selected Areas in declination $-60°$, have recently been determined by

[1] This paper was presented at the Symposium on Galactic and Extragalactic Structure, held in connection with the dedication of the McDonald Observatory on May 5–8, 1939.

Sergei Gaposchkin.[2] The present paper is an attempt to analyze the material so obtained, to determine what type of conclusion can be drawn from it, and to examine and summarize such results as may be legitimately derived from it.

The red indices are determined from the comparison of photographic and photo-red magnitudes. The former are directly referred to the Harvard Standard Regions,[3] which, when reduced[4] to the "1922 System," seem to be close to the "International System."[5] The photographic magnitudes of the stars in the central sequences for the southern Selected Areas were determined by Miss Leavitt but remained unpublished until they were printed with the photo-red magnitudes of the same stars.[6] When reduced to the 1922 System, these magnitudes are believed to be close to the International System. Recent redeterminations of the photographic magnitudes of many of the same stars have been made by S. Gaposchkin in his study of standards in the Selected Areas.

The photo-red magnitudes depend primarily on those recently determined[7] for standard stars in the twelve Standard Regions at $+15^\circ$ and also on the secondary standards for the Selected Areas, recently published.[6]

The red indices now discussed are all of comparable accuracy; the mean error of one red index, determined from four photographic and four red plates, is about one-tenth of a magnitude.

The spectra of all the stars for which colors have been measured in the present program are contained[8] in the *Potsdam Spektral-Durchmusterung* for the Selected Areas at -60°.

It was at first thought that the analysis of the colors would be primarily concerned with the magnitude systems. It soon became evident, however, that the principal source of difficulty in the analysis is the uncertainty of the system of spectral classification, which is, unfortunately, not so definitely specifiable as the systems

[2] To be published as *Harvard Mimeogram*, Ser. IV, No. 1.

[3] *Harvard Ann.*, **71**, No. 5, 1917.

[4] Shapley and Walker, *Harvard Bull.*, No. 781, 1932.

[5] Greenstein, *Harvard Circ.*, No. 422, 1938.

[6] S. Gaposchkin, *Harvard Ann.*, **89**, No. 9, 1937.

[7] C. Payne-Gaposchkin, *Harvard Ann.*, **89**, No. 8, 1937.

[8] *Potsdam Pub.*, **27**, No. 2, 1930.

of magnitudes and of colors. Accordingly, the present paper will be concerned first with the classification of the spectra, although these problems were the last to be encountered in the course of the research.

2. *The Harvard and Potsdam systems of spectral classification.*—Three groups of material are available for a direct comparison of the Harvard and Potsdam spectral classifications: stars common to the *Potsdam Catalogue* and the *Henry Draper Catalogue*;[9] the *Henry Draper Charts*;[10] and the classifications carried out by Miss Cannon

TABLE 1

ACCIDENTAL ERROR OF ONE SPECTRAL ESTIMATE, *Henry Draper Catalogue**

Spectrum	$]9^m$	10^m-11^m	11^m-12^m	12^m-13^m
B	±0.35 (13)	±0.00 (1)	.....	.....
A	0.84 (21)	0.87 (8)	±0.70 (1)	±0.35 (2)
F	0.90 (17)	1.50 (26)	1.76 (20)	0.00 (2)
G	0.90 (18)	1.99 (28)	1.55 (34)	2.20 (8)
K	1.10 (30)	1.16 (29)	1.47 (43)	1.82 (12)
M	±0.00 (1)	±2.03 (8)	±3.52 (2)	±3.52 (1)
All	±0.93 (100)	±1.47 (100)	±1.58 (100)	±1.74 (25)

* Mean error, derived from pairs of independent estimates.

for the *Cape Zone Catalogue*.[11] The two latter sources of material are particularly important, because it is for the fainter stars that definite spectral criteria are most difficult to apply, and it is most tempting to have recourse (consciously or unconsciously) to other, simpler criteria.

For the *Henry Draper Catalogue* (where residuals are published for spectra that have been twice classified) and for the *Potsdam Catalogue* (where reclassifications have been made and published[12] for some of the Selected Areas at $-60°$) the internal accidental errors can be immediately derived. They have been deduced from a limited number of residuals taken at random and are given in Tables 1 and 2. The unit is one-tenth of a spectral class. Evidently

[9] *Harvard Ann.*, **90–99**, 1918–24

[10] A. Cannon, *Harvard Ann.*, **105**, No. 1, Charts 1, 2, 7, and 8, 1936.

[11] Unpublished spectra, marked by Miss Cannon on charts and kindly put at the disposal of the writer.

[12] *Potsdam Pub.*, **28**, No. 3, 1938.

the precision diminishes for faint stars; at a given apparent magnitude the spectral estimates of the *Henry Draper Catalogue* have the smaller mean errors. The accidental errors indicate that the step interval for the Potsdam classification is about half as great as the precision of the estimates warrants, while that for the Henry Draper classification is a little larger than the precision demands, except for the faintest stars. The large mean errors given by Potsdam estimates for the B stars should be regarded not as errors of estimation but as gross errors resulting from classifying the star in the wrong category (B for F, or vice versa; see sec. 6).

TABLE 2

ACCIDENTAL ERROR OF ONE SPECTRAL ESTIMATE

*Potsdam Spektral-Durchmusterung**

Spectrum	$]11^m$	11^m-12^m
B	±2.62 (30)	±7.00 (1)
A	0.82 (19)	3.12 (12)
F	1.92 (21)	2.50 (38)
G	1.86 (19)	2.26 (42)
K	±0.79 (11)	±0.90 (7)
M	.....	.....
All	±1.55 (100)	±2.43 (100)

* Mean error, derived from pairs of independent estimates.

A comparison of the classification of a number of stars by Potsdam and Harvard gives the results of Table 3. The calculated mean errors are rather larger than would have been anticipated from the data of Tables 1 and 2, which indicates that the Harvard and Potsdam observers are (one or both) rather more self-consistent than would be expected from comparing their findings. Possibly memory may play some part here; or, more probably, image quality, especially for the Potsdam reclassifications, which, unlike the Harvard ones, were carried out on the same plates as the original classifications.

There is a definite systematic difference between the two systems of classification, as may be seen from Table 4. The materials of Table 4 are summarized in Table 5, which gives the adopted corrections that should be applied, at each spectral and magnitude group, to reduce Potsdam classes to the Henry Draper system. The group-

ing is by photographic magnitude.[13] It is difficult to compare measured colors with expectation without some such correction, which is appreciable at the eleventh, and serious at the twelfth, magnitude.

An interesting light on the two systems of classification is thrown by the comparison made in Table 6, which contains, for four magnitude intervals, the mean errors calculated from the dispersion of the

TABLE 3

ACCIDENTAL ERROR OF SPECTRAL CLASSIFICATION
(DISPERSION OF POTSDAM ON HARVARD)

Spectrum	$]10^m$	10^m-11^m	11^m-12^m	12^m-13^m
Fo	1.0	1.1	1.6	2.2
F2	2.2	2.3	2.8	3.4
F5	3.7	3.8	4.3	4.9
F8	4.3	4.4	4.9	5.5
Go	4.4	4.5	5.0	5.6
G5	4.2	4.3	4.8	5.4
Ko	3.1	3.2	3.7	4.3
K2	1.7	1.8	2.3	2.9
K5	0.7	0.8	1.3	1.9
K7	0.1	0.2	0.7	1.3
M	0.0	0.0	0.5	1.1
All	2.8	2.9	3.4	4.0

Potsdam spectra for a given Harvard class and from the dispersion of the Harvard spectra for a given Potsdam class. The reason for the difference is obvious when the data are plotted: the Potsdam classes have a smaller range than the Harvard classes for faint stars. To take an extreme example: suppose, at the twelfth magnitude, Potsdam assigned exactly the same spectral class to *all* stars; then all the entries in the upper line of Table 6 would be zeros, while the entries in the second line would be greater than they are. This extreme case is not approached, but there is a tendency in that direction: for stars of the twelfth magnitude in the group considered, the Potsdam classes have a range from Go to K4, while the Harvard classes for the same stars range from F2 to Mo.

In the volumes of the *Potsdam Spektral-Durchmusterung* that were

[13] *Harvard Mim.*, Ser. II, No. 3, 1937.

TABLE 4

SYSTEMATIC DIFFERENCE OF SPECTRAL CLASSIFICATION (HD−PSD)

Spectrum (PSD)	$\lvert 11^m \rvert$	$11^m - 12^m$	$12^m - 13^m$
B0	+ 3.06 (21)		
B1	+ 2.00 (1)		
B2	+ 4.5 (4)	.....	[+21.0 (2)]
B3	+ 1.3 (9)		
B4	+ 1.2 (4)		
B5	+ 1.38 (16)		
B6	+ 1.6 (8)		
B7	+ 1.64 (19)	.....	.....
B8	+ 1.06 (44)		
B9	+ 0.73 (68)		
A0	+ 0.55 (516)		
A1	+ 0.55 (89)		
A2	+ 0.09 (99)	+1.29 (21)	.....
A3	+ 1.28 (58)		
A4	− 0.22 (59)		
A5	+ 0.01 (109)		
A6	− 0.92 (28)		
A7	+ 0.43 (22)	+2.60 (7)	.....
A8	− 1.03 (12)		
A9	+ 0.95 (14)		
F0	+ 0.78 (130)		
F1	− 0.07 (71)		
F2	+ 2.95 (60)	+1.55 (23)	.....
F3	+ 0.62 (37)		
F4	0.00 (31)		
F5	+ 1.30 (33)		
F6	− 0.77 (43)		
F7	− 1.60 (39)	+0.92 (25)	.....
F8	− 0.02 (53)		
F9	− 1.66 (39)		
G0	− 3.10 (49)		
G1	− 3.75 (23)		
G2	− 1.95 (28)	−1.87 (54)	− 3.52 (10)
G3	− 1.54 (36)		
G4	− 1.01 (46)		
G5	+ 1.63 (46)		
G6	− 0.80 (54)		
G7	− 0.07 (58)	−0.72 (58)	− 5.50 (6)
G8	+ 0.01 (161)		
G9	− 0.03 (52)		

TABLE 4—*Continued*

Spectrum (PSD)	$]_{11^m}$	11^m-12^m	12^m-13^m
K0	− 0.01 (221)		
K1	− 0.43 (44)		
K2	− 0.96 (69)	−1.46 (62)	− 7.40 (24)
K3	− 0.04 (61)		
K4	− 0.77 (39)		
K5	+ 0.40 (27)		
K6	− 0.75 (12)		
K7	− 2.78 (7)	−3.00 (10)	.....
K8	− 4.67 (12)		
K9	−10.0 (1)		
M	− 1.05 (6)	+1.5 (4)	− 1.0 (1)

TABLE 5

ADOPTED SYSTEMATIC CORRECTIONS TO POTSDAM SPECTRA

Spectrum (PSD)	$]_{11^m}$	11^m-12^m	12^m-13^m
B2	+2.5	.....	.....
B7	+1.2	.....	.....
A2	+0.1	+1.4	.....
A7	−0.2	+2.6	.....
F2	+1.3	+2.2	.....
F7	−0.9	+0.4	.....
G2	−2.1	−1.7	−3.2
G7	+0.2	−0.7	5.4
K2	−0.3	−1.6	7.4
K7	−1.2	−1.6:	−7.4:
M	−1.7	.....	.....

TABLE 6

COMPARISON OF DISPERSIONS (MEAN ERROR OF ONE ESTIMATE)

Dispersion of—	$]_{10^m}$	10^m-11^m	11^m-12^m	12^m-13^m
Potsdam on Harvard	±2.8	±2.9	±3.4	±4.0
Harvard on Potsdam	±3.2	±2.8	±4.1	±6.3

first issued[14] a large number of stars were distinguished as giants and dwarfs by the letters "g" and "d." Although a definite evaluation of these absolute-magnitude distinctions will only be possible if, for example, an extensive group of data on proper motions (such as the

TABLE 7

SYSTEMATIC DIFFERENCE OF CLASSIFICATION DEPENDING ON LUMINOSITY CLASS

SPECTRUM	HARVARD SPECTRUM − POTSDAM SPECTRUM		DIFFERENCE
	g	d	
Potsdam:			
G2	.....	+1.3 (3)	.....
G3	+ 7.0 (1)	−2.2 (4)	+ 9.2
G4	+11.0 (1)	−3.6 (11)	+14.6
G5	+ 5.0 (4)	−1.3 (19)	+ 6.3
G6	+ 3.6 (15)	+0.1 (24)	+ 3.5
G7	+ 2.1 (14)	0.0 (20)	+ 2.1
G8	+ 1.7 (47)	−1.2 (125)	+ 2.9
G9	+ 1.3 (31)	−0.3 (62)	+ 1.6
K0	+ 0.7 (228)	−0.9 (112)	+ 1.6
K1	+ 0.1 (51)	−1.8 (20)	+ 1.9
K2	+ 0.3 (38)	−0.5 (25)	+ 0.8
K3	− 1.0 (23)	−0.6 (22)	− 0.4
K4	− 1.0 (10)	+0.2 (14)	− 1.2
K5	− 2.5 (2)	−0.8 (14)	− 1.7
K6	.....	+7.0 (1)	.....
K7	.....	.....	.....
K8	+ 5.0 (1)	−3.0 (3)	+ 8.0
K9	.....	.....	.....
M	.....	−5.0 (1)	.....
Harvard:			
F5	.....	0.0 (1)	.....
F8	.....	−1.5 (2)	.....
G0	+ 1.5 (2)	−6.4 (50)	− 7.9
G5	− 4.0 (36)	−3.0 (129)	+ 1.0
K0	+ 0.6 (231)	+0.6 (183)	0.0
K2	+ 0.6 (142)	+1.3 (68)	+ 0.7
K5	+ 4.0 (55)	+2.1 (45)	− 1.9
M0	+11.5 (2)	+2.5 (2)	− 9.0

Cape Zone Catalogue) becomes available for comparison, it is of interest to examine them from some more general standpoints. There is, for instance, a real difference in equivalent Henry Draper class for stars designated "g" and "d" (Tables 6 and 7). The difference for

[14] *Potsdam Pub.*, **27**, No. 1, 1929.

the d stars is very close to that shown for the stars in general by Table 4. The g stars deviate more widely, all those earlier than Ko being classified later at Harvard. Perhaps they are partly supergiants, which have long been known, from "measured" criteria, to be of much earlier spectral class than would be assigned to the spectrum from its general appearance.

The absolute magnitude criteria used by the Potsdam observers have been especially studied by Miss Hoffleit,[15] who has shown from Harvard plates that on Becker's criterion (the strength of the cyanogen absorption) the "g" and "d" designations can be duplicated for the stars to which he assigns them. She further concludes, however, that while his g stars are correctly described, his d stars may be either dwarfs or supergiants. The spectral classifications of the Potsdam d stars, in fact, differ systematically from the Harvard classes in almost exactly the same way as the average of all stars of comparable magnitude (cf. Tables 4 and 7). The g stars, however, deviate conspicuously, and there is a strong systematic run in the difference (g − d) of Table 7 with spectral class. It is to be noted that in later catalogues[16] than those just discussed, the Potsdam observers have assigned fewer stars to the g and d classes.

In examining the systematic difference in classification, depending on absolute luminosity, it is necessary to consider not only the Potsdam criteria but the stars on whose Henry Draper classes the numerical values to be used for the criteria were based. These stars, which are analogous to a "standard sequence" of magnitudes in photometric work, serve to fix the scale of a spectral system. If stars of abnormal color are used as standards of magnitude (or are measured with normal standards of magnitude), the *color equation* of the magnitude system must be taken into consideration. In considering spectral classifications we may introduce the analogous conception of a *luminosity equation* for a system of spectral classification. The last column of Table 7, for example, gives the relative luminosity equation of the Potsdam spectral system for giants and average stars. The standard stars for the spectral classification system used

[15] Dorrit Hoffleit, *Ap. J.* (in press).

[16] *Potsdam Pub.*, **27**, No. 2, 1930; **27**, No. 3, 1931; **28**, No. 1, 1935; **28**, No. 2, 1938; **28**, No. 3, 1938.

in the Selected Areas at $-60°$ are preponderantly d stars (an average mixture of low- and high-luminosity stars), and therefore the fact that the d stars of the catalogue are near to the average of all stars, in their systematic difference from Harvard (Tables 4 and 7), receives a ready explanation.

The differences in spectral classification that depend on absolute magnitude may be shown to be predictable. The Henry Draper classification, as cannot be emphasized too often,[17] rests not upon measures made upon particular features of the spectrum but upon the general appearance of the whole; it is essentially an estimate of average ionization. The Potsdam observers, however, while basing their system on the Henry Draper classes of a small number of individual stars, made their classification by means of single line ratios.[18] Between Fo and Ko they used the ratio of the G band to $H\gamma$; for classes Ko and later, they used the ratio of 4227 (*Ca* I) to the G band. Their criteria for early classes (the lines of hydrogen and helium) appear to be effective and will not now be especially discussed.[19]

All three lines or bands ($H\gamma$, the G band, and the line at 4227) used at Potsdam for classifying stars in the "later" part of the spectral sequence vary with luminosity. Hydrogen lines are stronger in giant than in dwarf stars, all along the sequence from class A_5 to class M.[20] The G band is stronger in dwarf stars than in giants;[21] and, moreover, it comes to a maximum earlier in the spectral sequence for giants (G_7) than for dwarfs (K_2).[22] Thus, for giant stars the ratio G band/$H\gamma$ will change but little from class G_7 onward, while for dwarf stars it will continue to increase as far as K_2. We have here an explanation for the fact that for giant G_5-K_2 stars

[17] See Payne, *Stellar Atmospheres*, p. 190, 1925.

[18] See, e.g., *Potsdam Pub.*, **27**, No. 1, 1929.

[19] For early-type stars (belonging to the main sequence) there is not so great an effect of absolute magnitude, except for the rare stars showing the "c character." The principal source of systematic error in classes earlier than F_5 appears to be the gross error of treating B stars as F stars, and vice versa.

[20] Payne, *The Stars of High Luminosity*, p. 269, 1930.

[21] Swings and Struve, *Phys. Rev.*, **29**, 146, 1932.

[22] Russell, *Ap. J.*, **39**, 334, 1934.

(Potsdam classification) the Henry Draper classes are considerably later (see Table 7).

The third line used at Potsdam for classification is the 4227 line of neutral calcium, which is a well-known absolute-magnitude line, considerably stronger in the spectra of giants than in those of dwarfs.[23] Therefore, in a given Potsdam class, the late K giants should be classified systematically earlier on the Harvard system, the late K dwarfs systematically later. Unfortunately, there are very few genuine late K dwarfs as bright as the limits of the spectral classification, so that the prediction cannot be tested. The standard stars themselves here are probably giants; there are very few stars with which to make the comparison, and it is here that the mean error of spectral classification is large for both catalogues (Table 1).

The systematic differences of classification, depending both on absolute and apparent magnitude, introduce great difficulties into the discussion of the colors of the stars whose spectra are known only on the Potsdam system, since the Potsdam classes cannot be discussed as though they were the exact equivalent of the Henry Draper classes.[24] It might at first be thought that the systematic difference depending on apparent magnitude (Table 1) results from the systematic difference depending on absolute magnitude (Table 7). But the quantitative differences do not substantiate this hope (which, if fulfilled, would have greatly facilitated the discussion of the material). The difference depending on apparent magnitude is greatest for the faint stars of classes G and K—the classes in which there is the greatest proportion of dwarf stars. However, the dwarf stars show the smallest, not the largest, deviation between Harvard and Potsdam spectra. The systematic differences depending on apparent and on absolute magnitude appear to be distinct and unrelated.

The following sections contain an analysis of the colors and spectra of the stars in the twelve Selected Areas at $-60°$, on the basis of the conclusions that have been reached in the present section. The results are typical of those that can be derived from color and spectrum alone. A later investigation of another group of Se-

[23] Payne, *The Stars of High Luminosity*, p. 159, 1930.

[24] Payne-Gaposchkin, *Harvard Ann.*, **105**, 384, 1936.

lected Areas will, it is hoped, show how the analysis can be amplified by the additional knowledge of the proper motions.

3. *Colors of stars in high galactic latitude.*—If the spectra of the stars of which the colors are now to be discussed were classified on a homogeneous system, and if the normal colors of the stars of the various spectral classes were known, it would be possible to proceed immediately to a discussion of the color excesses. The systematic differences between, and accidental uncertainties in, the spectral classes, which have been described in the foregoing sections, render the formation of a table of standard colors a difficult matter. It is therefore advisable to test our assumptions as to the relationship be-

TABLE 8

SELECTED AREAS IN HIGH GALACTIC LATITUDE (1144 STARS)

Selected Area	Right Ascension	Declination	Galactic Latitude	Galactic Longitude
188	$1^h 22^m.0$	$-59° 51'$	-57	261
189	3 24.0	59 38	47	241
190	5 23.0	60 3	33	236
197	19 1.4	59 42	26	303
198	20 59.2	59 56	40	303
199	22 57.8	-60 3	-53	291

tween spectral class and color, by reference to some stars that can be considered as unaffected by selective absorption.

The six Selected Areas in declination $-60°$ which are in galactic latitudes greater than $25°$ will provide such material. We are justified in assuming that the selective obscuration of stars in such high galactic latitudes will, on the average, be negligible; and we shall assume that their colors are the normal colors of stars of the corresponding spectral classes. The relevant data concerning the six Selected Areas in high latitude are given in Table 8.

The observed colors of stars in the six high-latitude areas are summarized in Table 9. Stars brighter photographically than $9^m.0$ have been excluded.

There are three steps in the comparison of these colors with expectation: (*a*) the determination of the equivalent Harvard spectra (since the normal colors are known in terms of Harvard classes);

(*b*) the determination of the normal colors, corresponding, at the different apparent magnitudes, to these equivalent Harvard spectra; (*c*) the examination of the significance of the resulting color excesses. Two subsidiary tables are needed for these steps: the normal colors for various Harvard classes (Table 10) and the mean errors of single

TABLE 9

AVERAGE RED INDICES IN HIGH GALACTIC LATITUDES

LIMITS OF PHOTOGRAPHIC MAGNITUDE	SPECTRAL CLASS (POTSDAM)								
	B5–B9	A0–A4	A5–A9	F0–F4	F5–F9	G0–G4	G5–G9	K0–K4	K5–K9
9.0– 9.9	−0.13 (1)	−0.08 (8)	+0.33 (7)	+0.60 (24)	+0.46 (11)	+0.77 (11)	+1.35 (24)	+1.84 (15)	+2.25 (2)
10.0–10.9	.....	+0.05 (10)	+0.13 (13)	+0.37 (42)	+0.45 (37)	+0.62 (39)	+1.09 (66)	+1.55 (50)	+2.05 (6)
11.0–11.9	.....	+0.17 (7)	+0.22 (3)	+0.42 (50)	+0.58 (106)	+0.71 (168)	+1.09 (100)	+1.47 (110)	+2.00 (2)
12.0–12.9	.....	.....	.....	+0.79 (12)	+0.64 (54)	+0.80 (102)	+1.12 (36)	+1.26 (25)	+1.42 (3)

TABLE 10

ADOPTED NORMAL COLORS FOR HARVARD SPECTRA

Spectrum	Main Sequence	Giants	Spectrum	Main Sequence	Giants
B2	−0.47	.....	F7	+0.43	+0.80
B7	− .14	.....	G2	0.71	1.02
A2	+ .11	.....	G7	0.91	1.25
A7	+ .21	.....	K2	+1.12	1.60
F2	+0.31	+0.53	K7	.....	+2.16

spectral estimates, converted (through the material basic to Table 10) into mean errors of color indices (Tables 11 and 12).

Step (*a*) is easily accomplished by means of Table 6. Step (*b*) is more difficult, and to perform it we need to know not only the normal colors of stars of various spectral classes but also the proportion in which giant and dwarf stars are represented. There have been but few determinations of the colors of giant and dwarf stars separately.

The most careful work has shown definitely that color is a well-defined function of spectral class and luminosity; the relation has been accurately evaluated by Morgan[25] for Bottlinger's photoelectric color indices, and he has shown that color is a linear function of spectral class over a considerable range of spectrum (for dwarfs, giants, and supergiants, separately). Our own less accurate but more extensive

TABLE 11

ACCIDENTAL ERROR OF ONE SPECTRAL ESTIMATE (*Henry Draper Catalogue*) EXPRESSED IN EQUIVALENT COLOR INDEX

Spectrum	$]10^m$	10^m-11^m	11^m-12^m	12^m-13^m
B	±0.02	±0.00	.....	.....
A	.04	.04	±0.04	±0.02
F	.02	.03	.04	.00
G	.04	.10	.08	.11
K	.09	.09	.12	.15
M	±0.18	±0.29	±0.32	±0.35

TABLE 12

ACCIDENTAL MEAN ERROR OF ONE SPECTRAL ESTIMATE (*Potsdam Spektral-Durchmusterung*) EXPRESSED IN EQUIVALENT COLOR INDEX

Spectrum	$]11^m$	11^m-12^m	Spectrum	$]11^m$	11^m-12^m
B	±0.16	±0.42	G	±0.09	±0.11
A	.04	.16	K	±0.06	±0.07
F	±0.04	±0.05			

material on the colors of stars in the system here used[26] permits the derivation of similar relationships for the system of photo-red magnitudes:

$$\text{Dwarfs: } C_{Pr} = +0^m.23 + 4^m.03\,(Sp - Fo)\,, \qquad Fo \text{ to } K5\,.$$

$$\text{Giants: } C_{Pr} = +0.48 + 4.50\,(Sp - Fo)\,, \qquad Fo \text{ to } Ko\,,$$

$$= +1.38 + 1.12\,(Sp - Ko)\,, \qquad Ko \text{ to } M\,.$$

The unit is one-tenth of a spectral class; the interval Fo to Go is expressed by the number 10.

[25] W. W. Morgan, *Ap. J.*, **87**, 460, 1938. [26] *Harvard Ann.*, **89**, Nos. 6 and 7, 1935.

The normal colors being known, the relative numbers of giant and dwarfs stars are required. These numbers (given in Table 14) have been adopted from a consideration of the work of Bok[27] and of van Rhijn and Schwassmann.[28]

Lastly, the systematic difference of spectral classification shown by Potsdam for giant and dwarf stars, in comparison with Harvard, must be taken into account. The determination given in Table 7 applies directly only to bright stars (magnitudes 9 and 10); in applying a similar correction to fainter stars we make the arbitrary assumptions that the systematic difference will persist to fainter

TABLE 13

ADOPTED SYSTEMATIC CORRECTION FOR POTSDAM SPECTRA OF GIANT STARS

Spectrum (PSD)	11^m	11^m-12^m	12^m-13^m
G2	+7.1:	+7.5:	+6.0:
G7	+2.3	+1.4	−3.3
K2	+0.5	−0.8	−6.6
K7	−2.9	−3.3:	−9.1:

magnitudes and that the so-called "d stars" will give the same average as all the stars, at fainter magnitudes. Thus, we use the last column of Table 7 as a differential correction to the equivalent Harvard spectra deduced from Table 5, and obtain the equivalent Harvard spectra for giant stars, as shown in Table 13.

The comparison of observed and expected colors is made in Table 14. The color excesses, in the last column but one of Table 14, furnish a measure of the assumption that the colors of stars in high latitude may be treated as normal, for comparison with those in low latitude. The mean errors, in the last column, are calculated from the dispersion of Harvard spectra on Potsdam (Table 6) and the uncertainty of one measure of color (m.e. = 0^m10 adopted). They take no account of the uncertainty of the luminosity equation, which becomes more and more important for the later classes, where giant stars are increasingly preponderant. The adopted luminosity equation (see Table 13) is greatest at G2, but there are also the fewest giant stars

[27] *Harvard Circ.*, No. 400, 1935. [28] *Zs. f. Ap.*, **10**, 161, 1935.

at this class. Therefore, all the mean errors are underestimates for classes from G2 onward; they are so indicated by the plus (+) sign. In class F, no allowance has been made for possible supergiants.

TABLE 14

COMPUTED AND OBSERVED COLOR IN HIGH GALACTIC LATITUDES

Spectral Class (PSD)	Equivalent Harvard Spectrum		Average Pg. Mag.	Adopted Percentage of Dwarfs	Computed Color	Observed Color	Color Excess	Mean Error (Estimated)
	Giant	Dwarf						
B7	.....	B8.2	11	100	−0m07	−0m13 (1)	−0m06	±0m05
A2	.....	A2.1	11	100	+0.12	−0.01 (18)	− .13	.02
		A3.4	11–12	100	+0.15	+0.17 (7)	+ .02	.04
A7	.....	A6.8	11	100	+0.22	+0.20 (20)	− .02	.03
		A9.6	11–12	100	+0.26	+0.22 (3)	− .04	.04
F2	.....	F3.3	11	100	+0.33	+0.45 (66)	+ .12	.02
		F4.2	11–12	100	+0.35	+0.42 (50)	+ .07	.02
		.....	12–13	100	.....	+0.79 (12)	.....	.06
F7	.....	F6.1	11	100	+0.41	+0.45 (48)	+ .07	.03
		F7.4	11–12	100	+0.45	+0.58 (106)	+ .13	.02
		.....	12–13	100	.....	+0.64 (54)	.....	.....
G2	G9.1:	F9.9	11	55	+0.90	+0.65 (50)	− .25	.03+
	G9.5:	G0.3	11–12	68	+0.86	+0.71 (168)	− .15	.02+
	G8.0:	F8.8	12–13	75	+0.72	+0.80 (102)	+ .08	.04+
G7	G9.3	G7.2	11	35	+1.27	+1.16 (90)	− .11	.03+
	G8.4	G6.3	11–12	44	+1.14	+1.09 (100)	− .05	.04+
	G3.7	G1.6	12–13	49	+0.89	+1.12 (36)	+ .23	.09+
K2	K2.5	K1.7	11	15	+1.57	+1.62 (65)	+ .05	.03+
	K1.2	K0.4	11–12	20	+1.45	+1.47 (110)	+ .02	.02+
	G5.6	G4.6	12–13	23	+1.11	+1.26 (25)	+ .15	.09+
K7	K4.1	K5.8	11	3	+2.06	+2.10 (8)	+ .04	.04+
	K3.7	K5.5	11–12	6	+1.75	+2.01 (2)	+ .26	.12+
	G7.9	K0.0	12–13	8	+1.30	+1.42 (3)	+0.12	±0.20+

which would, if present, cause a positive color excess, such as is, perhaps, shown at F7 for stars of magnitude 11–12. But supergiants are presumably scarce among faint stars in high latitudes.

There is no indication that the tabulated color excesses are significant. It should be noted that the agreement between observed and computed color is almost as good if the spectral classes are

uncorrected, except for classes G7, K2, and K7, and there especially for the faintest stars. We conclude that the colors of the stars in the high galactic latitudes can legitimately be treated as normal for the spectral classes and magnitudes concerned. This will facilitate the

TABLE 15

SELECTED AREAS IN LOW GALACTIC LATITUDE

Selected Area	Right Ascension	Declination	Galactic Latitude	Galactic Longitude	Number of Stars
191	$7^h22^m.8$	$-60°\ 18'$	$-19°$	239°	403
192	9 26.3	60 0	− 6	248	627
193	11 26.9	60 6	+ 1	261	771
194	12 56.7	60 12	+ 3	272	561
195	14 57.3	60 4	− 2	286	606
196	17 2.5	−59 58	−12	298	620
Total					3588

TABLE 16

COLORS AND SPECTRA IN SELECTED AREA 191 ($7^h22^m.8$, $-60°18'$)

Limits of Pg. Mag.	Spectral Class (Potsdam)									
	B5–B9	A0–A4	A5–A9	F0–F4	F5–F9	G0–G4	G5–G9	K0–K4	K5–K9	M0–M4
$9^m.0$– $9^m.9$	−0.04 (1)	−0.48 (15)	−0.44 (5)	−0.19 (16)	+0.04 (5)	+0.12 (5)	+0.78 (10)	+0.88 (6)	.....	.....
10.0–10.9	.....	−0.42 (14)	−0.20 (8)	−0.16 (11)	−0.18 (10)	+0.24 (15)	+0.64 (9)	+1.10 (14)	+2.00 (1)	.....
11.0–11.9	.....	−0.30 (7)	−0.34 (4)	+0.13 (27)	+0.14 (30)	+0.39 (40)	+0.78 (27)	+1.41 (20)	+2.10 (7)	.....
12.0–12.9	.....	+0.20 (1)	.....	+0.02 (6)	+0.30 (22)	+0.53 (36)	+0.88 (12)	+1.05 (15)	+1.28 (2)	+1.16 (2)

treatment of the low latitudes, since the Potsdam classes can now be used without reduction.

4. *Spectra and colors in low galactic latitudes.*—There are six Selected Areas, in declination −60°, that have galactic latitudes less than 20°. They are enumerated in Table 15.

The observed colors in the six low-latitude areas are given in Tables 16–21.

TABLE 17

COLORS AND SPECTRA IN SELECTED AREA 192 (9^h26^m3, $-60°0'$)

LIMITS OF PG. MAG.	SPECTRAL CLASS (POTSDAM)										
	Bo–B4	B5–B9	Ao–A4	A5–A9	Fo–F4	F5–F9	Go–G4	G5–G9	Ko–K4	K5–K9	Mo–M4
9^m0– 9^m9	−0.52 (1)	0.00 (22)	+0.20 (19)	+0.58 (2)	+0.59 (4)	+1.11 (3)	+0.80 (2)	+1.45 (6)	+1.56 (2)	.....	.....
10.0–10.9	+0.26 (1)	−0.12 (26)	0.00 (45)	+0.46 (6)	+0.53 (11)	+0.78 (7)	+1.07 (1)	+1.51 (23)	+2.00 (16)	+2.49 (1)	.....
11.0–11.9	−0.25 (1)	+0.12 (4)	+0.06 (79)	+0.32 (28)	+0.31 (36)	+0.54 (17)	+0.64 (27)	+1.44 (19)	+1.82 (41)	+2.47 (3)	+2.43 (2)
12.0–12.9	.....	.....	+0.37 (13)	+0.30 (11)	+0.47 (36)	+0.66 (32)	+0.98 (29)	+1.33 (11)	+1.53 (34)	+2.07 (4)	+1.86 (2)

TABLE 18

COLORS AND SPECTRA IN SELECTED AREA 193 (11^h26^m9, $-60°6'$)

LIMITS OF PG. MAG.	SPECTRAL CLASS (POTSDAM)										
	Bo–B4	B5–B9	Ao–A4	A5–A9	Fo–F4	F5–F9	Go–G4	G5–G9	Ko–K4	K5–K9	Mo–M4
9^m0– 9^m9	−0.18 (10)	−0.30 (20)	−0.14 (16)	+0.17 (1)	+1.08 (1)	+0.71 (1)	+1.35 (1)	+2.53 (1)	.....	+2.61 (1)	+2.79 (1)
10.0–10.9	−0.29 (15)	−0.26 (42)	−0.25 (63)	+0.09 (7)	+0.05 (17)	+0.31 (4)	+0.63 (2)	+1.63 (11)	+1.66 (4)	.....	.....
11.0–11.9	−0.42 (11)	−0.38 (45)	−0.33 (89)	−0.32 (43)	−0.11 (60)	+0.13 (11)	+0.64 (15)	+1.25 (12)	+1.55 (19)	+2.00 (2)	.....
12.0–12.9	−0.29 (4)	−0.28 (4)	−0.26 (23)	−0.20 (48)	−0.13 (78)	+0.05 (42)	+0.25 (15)	+0.26 (12)	+1.74 (16)	+2.05 (3)	+2.58 (1)

TABLE 19*a*

COLORS AND SPECTRA IN SELECTED AREA 194 (12^h56^m7, $-60°12'$)

LIMITS OF PG. MAG.	SPECTRAL CLASS (POTSDAM)										
	Bo–B4	B5–B9	Ao–A4	A5–A9	Fo–F4	F5–F9	Go–G4	G5–G9	Ko–K4	K5–K9	Mo–M4
9^m0– 9^m9	+0.17 (19)	−0.10 (23)	+0.04 (29)	+0.50 (3)	+0.29 (5)	+0.70 (2)	+0.42 (3)	+1.03 (2)	+2.02 (3)	+2.63 (1)	+2.21 (1)
10.0–10.9	−0.10 (10)	−0.22 (23)	−0.16 (42)	−0.04 (13)	+0.28 (14)	+0.50 (4)	+0.32 (1)	+1.51 (6)	+1.78 (8)	.....	.....
11.0–11.9	+0.18 (2)	+0.02 (9)	+0.13 (47)	+0.20 (34)	+0.30 (61)	+0.32 (31)	+0.76 (18)	+1.46 (10)	+1.66 (10)	+2.41 (3)	+2.57 (1)
12.0–12.9	.....	.....	+0.39 (3)	+0.78 (10)	+0.54 (16)	+0.54 (17)	+1.34 (9)	+0.98 (6)	+2.06 (1)	.....	.....

A comparison with the normal colors for the Potsdam classes (Table 9) leads to the average color excesses, which are summarized, in groups of equal apparent magnitude, for each Selected Area, in

TABLE 19*b*

COLORS AND SPECTRA IN SELECTED AREA 194 (STARS WITHIN COAL SACK)

LIMITS OF PG. MAG.	SPECTRAL CLASS (POTSDAM)								
	B0–B4	B5–B9	A0–A4	A5–A9	F0–F4	F5–F9	G0–G4	G5–G9	K0–K4
9^m0– 9^m9	+0.94 (4)	+0.53 (3)	+0.61 (4)	+0.41 (1)	+0.41 (1)	+0.55 (1)	+0.17 (1)	.....	+0.75 (1)
10.0–10.9	+0.10 (1)	+0.38 (6)	−0.12 (2)	+0.42 (6)	+0.37 (1)	+1.52 (2)	+0.47 (1)	.....	.....
11.0–11.9	+0.06 (1)	.....	+0.26 (3)	+0.86 (1)	+0.57 (7)	+0.58 (2)	+0.94 (2)	+2.18 (2)	+2.56 (2)
12.0–12.9	.....	.....	.....	.....	+0.56 (1)	.....	+0.59 (1)	+1.56 (2)	+2.40 (2)

TABLE 20

COLORS AND SPECTRA IN SELECTED AREA 195 (14^h57^m3, $-60°4'$)

LIMITS OF PG. MAG.	SPECTRAL CLASS (POTSDAM)									
	B0–B4	B5–B9	A0–A4	A5–A9	F0–F4	F5–F9	G0–G4	G5–G9	K0–K4	K5–K9
9^m0– 9^m9	+0.15 (1)	+0.35 (15)	+0.35 (26)	.....	+0.83 (10)	+0.74 (3)	.....	+1.32 (5)	+2.12 (4)	+2.64 (3)
10.0–10.9	.....	+0.24 (9)	+0.29 (58)	+0.74 (9)	+0.62 (14)	+0.64 (10)	+0.89 (9)	+1.44 (13)	+2.11 (19)	+2.72 (3)
11.0–11.9	.....	.....	+0.23 (32)	+0.48 (15)	+0.48 (60)	+0.57 (29)	+0.83 (42)	+1.35 (15)	+1.93 (40)	+2.54 (7)
12.0–12.9	.....	.....	+0.20 (1)	+0.46 (2)	+0.64 (29)	+0.67 (31)	+0.84 (55)	+1.22 (10)	+1.43 (24)	+0.85 (3)

Table 22. The last column gives an idea of the average "reddening" of the whole area. Selected Areas 192 and 195 seem to be redder than the average. Selected Area 191 looks as though it were significantly bluer. For this area, however, Becker states that his spectrum plate

was out of focus, and it is possible that the spectral classifications were systematically affected.

The last line of Table 22 shows a progression of color excess with apparent magnitude, which might at first be attributed to an error in

TABLE 21

COLORS AND SPECTRA IN SELECTED AREA 196 (17^h2^m5, $-59°58'$

LIMITS OF PG. MAG.	SPECTRAL CLASS (POTSDAM)										
	B0–B4	B5–B9	A0–A4	A5–A9	F0–F4	F5–F9	G0–G4	G5–G9	K0–K4	K5–K9	M0–M4
9^m0-9^m9	.....	−0.11 (8)	+0.04 (21)	+0.42 (9)	+0.88 (7)	+0.76 (2)	+1.06 (1)	+1.53 (8)	+1.67 (4)	+2.10 (1)	.....
10.0–10.9	.....	−0.09 (4)	−0.12 (46)	+0.07 (19)	+0.17 (23)	+0.24 (11)	+0.48 (13)	+0.90 (34)	+1.36 (32)	+2.05 (6)	+2.50 (2)
11.0–11.9	.....	.....	−0.10 (22)	+0.06 (18)	+0.26 (45)	+0.34 (58)	+0.52 (49)	+0.86 (48)	+1.12 (60)	+1.33 (5)	+1.62 (3)
12.0–12.9	.....	.....	+0.15 (1)	+0.26 (2)	+0.77 (8)	+0.69 (8)	+0.82 (14)	+1.09 (9)	+1.16 (14)	+1.49 (4)	+1.88 (1)

TABLE 22

COLOR EXCESS AND APPARENT MAGNITUDE IN LOW LATITUDES

Selected Area	9^m0-9^m9	10^m0-10^m9	11^m0-11^m9	12^m0-12^m9	All Magnitudes
191	-0^m69	-0^m43	-0^m30	-0^m34	-0^m44
192	+ .14	+ .32	+ .12	+ .17	+ .19
193	+ .18	− .02	− .23	− .30	− .09
194	+ .01	− .01	+ .07	+ .17	+ .06
195	+ .29	+ .39	+ .22	− .06	+ .21
196	+0.10	−0.14	−0.28	0.00	−0.08
Mean	0.00	+0.02	−0.07	−0.09	.....

the magnitudes (either blue or red). The same data are assembled in a different manner in Table 23, and it is seen that the reason cannot lie in the magnitude scales, since half the table shows color excesses affected in one way, half affected in the other way.

The bluening effect shown by the first half of Table 23 with increasing apparent magnitude is almost certainly a result of the inclusion of some B stars among the faint stars of class F. The slight reddening effect shown by faint stars in the lower half of the table is

probably produced by a greater number of low-latitude giant and supergiant stars in the spectral classes concerned, as compared with the high galactic latitudes where the normal colors were determined. The means in the last line of the table resemble those of the last line of Table 22, but it is now clear that they are the resultant of two oppositely directed tendencies and therefore cannot be ascribed to errors of magnitude scale.

TABLE 23

COLOR EXCESS, GROUPED BY SPECTRUM AND APPARENT MAGNITUDE

Spectrum (PSD)	$9^m.0$–$9^m.9$	$10^m.0$–$10^m.9$	$11^m.0$–$11^m.9$	$12^m.0$–$12^m.9$
B7	$-0^m.05$	.....	.....	.....
A2	+ .08	$-0^m.16$	$-0^m.22$	.....
A7	− .07	+ .04	.15	.....
F2	− .02	− .14	.19	$-0^m.41$
F7	+0.22	−0.07	−0.21	−0.16
Mean	+0.06	−0.08	−0.19	−0.28
G2	−0.02	−0.02	−0.08	−0.01
G7	+ .09	+ .18	+ .10	+ .16
K2	− .19	+ .12	+ .10	+ .24
K7	+0.24	+0.27	+0.13	+0.13
Mean	+0.03	+0.14	+0.06	+0.13
Mean of all	+0.02	+0.03	−0.06	−0.08

From Tables 22 and 23 it may be concluded that a comparison of colors in high and low latitudes for the same Potsdam classes does not lead to a clear picture concerning the color excesses. There are three reasons for this disappointing result: the stars of earliest spectral class, which (because of high luminosity and therefore great distance) should show the largest color excesses, are not represented in the high-latitude areas, and therefore no standards of comparison are available; the stars of spectral class B7–F7 are affected, in the low latitudes (but not in the high latitudes) by the error of confusing F and B stars, so that the normal colors cannot be legitimately compared; and for stars of later spectral class we cannot tell how the relative numbers of giant and dwarf stars, adopted for high latitudes, should be modified to be appropriate to low latitudes.

It therefore becomes necessary to make use of the reductions of Potsdam to Henry Draper classes, in order to utilize the high-luminosity stars of early type in estimating the color excesses. The relevant comparisons are made in Table 24.

TABLE 24

COLOR EXCESS AND DISTANCE MODULUS FOR EARLY-TYPE STARS

SPECTRUM		NORMAL COLOR	COLOR EXCESSES IN SELECTED AREAS						DISTANCE MODULUS	ABSOLUTE PG. MAG
PSD	HD		191	192	193	194	195	196		
B2—										
9^m0– 9^m9	B4^{m}5	−0.28	.....	−0.24	+0.10	+0.41	+0.43	.....	13.0	−3.52
10.0–10.9	.....	.....	.....	+ .54	− .01	+ .18	.....	.....	14.0	.....
11.0–11.9	.....	.....	.....	+ .03	− .14	+ .46	.....	.....	15.0	.....
12.0–12.9	.....	.....	.....	.....	− .01	.....	.....	.....	16.0	.....
B7—										
9.0– 9.9	B8.2	− .07	−0.87	+ .07	− .23	− .03	.42	−0.04	10.7	−1.18
10.0–10.9	.....	.....	.....	− .05	− .19	− .15	.31	.02	11.7	.....
11.0–11.9	.....	.....	.....	+ .19	− .31	+ .09	.....	.....	12.7	.....
12.0–12.9	.....	.....	.....	.....	− .21	.....	.....	.....	13.7	.....
A2—										
9.0– 9.9	A2.1	+ .12	− .60	+ .08	− .26	− .08	.23	.08	8.8	+0.72
10.0–10.9	A2.1	+ .12	− .54	− .12	− .37	− .28	.17	.24	9.8	+0.72
11.0–11.9	A3.4	+ .15	− .45	− .09	− .48	− .02	.08	.25	10.9	+1.05
12.0–12.9	A5:	+0.18	+0.02	+0.19	−0.44	+0.21	+0.02	−0.03	11.9	+2.0:

TABLE 25

COLOR EXCESS AND DISTANCE MODULUS

	AVERAGE MODULUS				
	9^m0	11^m0	13^m0	15^m0	16^m0
S.A. 193	$-0^m.32$	$-0^m.34$	$-0^m.18$	$-0^m.08$	$-0^m.01$
All others	− .14	− .02	+ .16	+0.30	.....
Coal Sack	+0.24	+0.39	+0.52	.....	.....

In all the studies of these Selected Areas it is clear that Selected Area 193 stands a little apart from the rest. The color excesses have been grouped according to modulus in Table 25, the values for Selected Area 193 being kept separate from the others.

The value of the absorption coefficient will be discussed after the frequency of colors has been used to derive a similar quantity. At present it will suffice to point out that the color excess increases with decreasing brightness in all three lines of Table 25. The Coal Sack gives the greatest reddening; Selected Area 193, the least.

The absolute values of the color excesses indicate that the whole system of assumed colors (Table 10) is probably too red for the present system of photo-red colors. These adopted colors have the same zero point as the Harvard photovisual system of colors, which, based as it is on the assumption that the average Ao star has a color index zero, is not consistent with the zero point of the colors at the North Pole, on which the photo-red magnitudes are based. The average color deficiency, −0.17, given by all the regions (Coal Sack excluded) is not far from the correction that must be applied to reduce the zero point of the North Polar Sequence to the adopted zero point of the Harvard Standard Regions ($-0.14 \times 1.15 = -0.16$).

5. *Frequency of colors.*—The difficulties and uncertainties involved in the study of the relationship between color and spectral class suggests that it may be profitable to study the colors by themselves. Although the classifications given in the Potsdam catalogue are not quite complete to any given magnitude limit (most of the bright stars being omitted, and also many faint ones, especially in crowded regions[29]), there is little reason to suppose that the incompleteness will affect conclusions that may be drawn from the *relative* frequency of the colors of the classified stars (these alone having been measured in the photometric program). Conclusions as to the frequency of colors per unit area of sky should, however, be drawn with caution.

[29] Becker has published reclassifications of stars in the Selected Areas at −60°. The second classification has been carried out on the same plates as the first, but only for a limited central area. A comparison of old and new classifications shows that on each occasion some stars have been omitted that were included in the other. The number of stars per square degree, given by Becker in the two catalogues that contain his first and second classification, refer only to the stars that have been classified on that occasion; the total number classified will be found to be greater than either and can be found only by identifying the stars common to the two classifications. In fact, for one area the number of stars per square degree given in the second catalogue is smaller than in the first. However, in an earlier discussion Becker considers that in S.A. 193 and 194 his classifications are complete down to 11^m5 (*Zs. f. Ap.*, **6**, 199, 1933). Further examination of his data makes this assumption appear to be doubtful.

The relative frequency of colors in each of the six low-latitude areas and in the sum of the six high-latitude areas is shown in Figure 1 for four intervals of apparent photographic magnitude. The principal features of the diagram are:

a) The six high-latitude areas all show a maximum frequency at about $+0^{m}.6$, which does not change appreciably with apparent magnitude.

b) The two low-latitude areas (S.A. 193 and 194) that lie north of the galactic plane show frequency distributions that are much alike, with a preponderance of stars at the blue end of the frequency distribution and scarcely any stars of moderate or large color index.[30] For Selected Area 193 there is little change of maximum frequency (-0.40) with magnitude; but Selected Area 194, which is in a region of recognized nebulosity, containing the "Coal Sack" (separately plotted in the figure), shows a shift of maximum frequency toward the red for fainter magnitudes.

c) The four other low-latitude areas (S.A. 191, 192, 195, and 196) show likewise a maximum frequency toward blue colors, shifted slightly toward the red for fainter magnitudes. Furthermore, all show a considerable number of stars of moderate and red color, which produce, in Selected Area 196, a pronounced secondary maximum in the frequency distribution. It should be noted that actual numbers of stars are plotted in Figure 1, so that the deficiency of red stars in Selected Areas 193 and 194 is a real and striking phenomenon.

6. *Frequency of spectra.*—The study of the frequency of spectra in the selected areas, for various intervals of magnitude, forms an instructive parallel to the frequency of the colors. Such studies have already been published by Becker[31] for two of the regions now studied, and by Becker[32] and Brück[33] for other regions in the Potsdam Selected Area survey. In his discussion of Selected Areas 193 and 194 Becker obtained results that are of great importance in the problem of galactic structure, especially in their bearing on the possible existence of negative density gradients in the direction of Carina[34] (S.A. 193). Our results do not lead to exact agreement with his, and therefore they will be analyzed in somewhat greater detail.

[30] Cf. Wilkens, *A.N.*, **266**, 349, 1938.

[31] *Op. cit.*, p. 198.

[32] *Zs. f. Ap.*, **5**, 274, 1932.

[33] *Zs. f. Ap.*, **13**, 266, 1937.

[34] Bok, *The Distribution of the Stars in Space*, pp. 107 and 109, 1937.

The data for the six high-latitude areas indicate no appreciable change in the frequency distribution of the colors with apparent

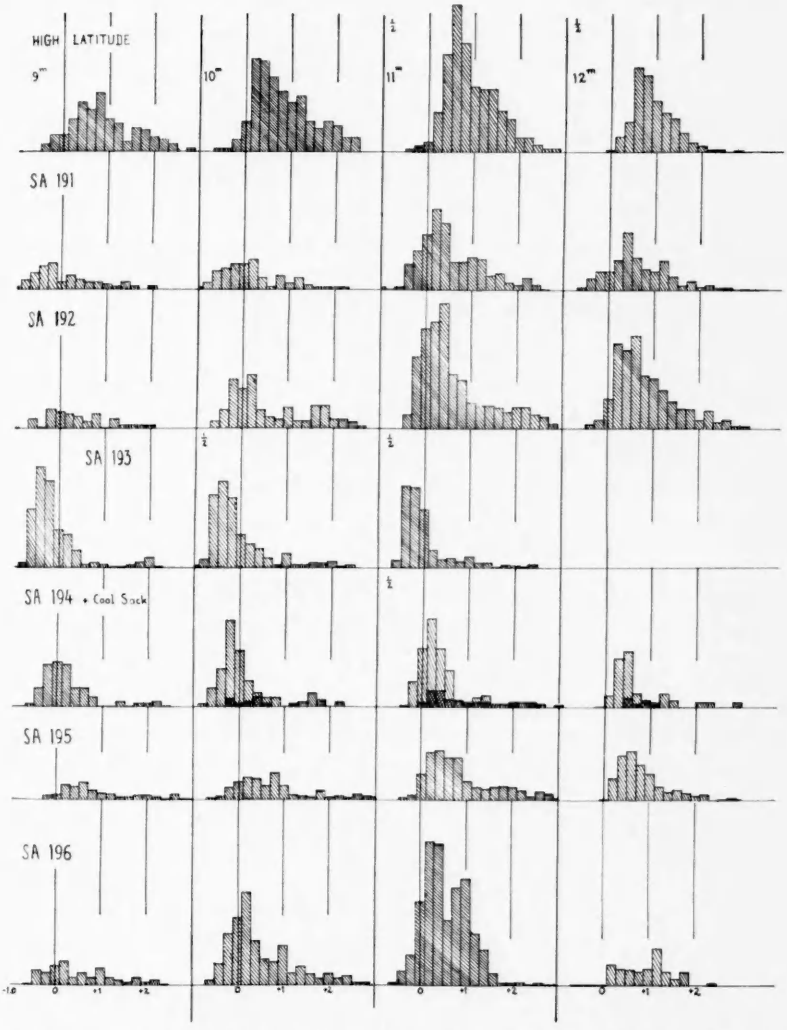

FIG. 1.—Frequency of colors. Ordinates, numbers of stars ($\frac{1}{2}$ indicates ordinates have been halved). Abscissae (*below*), red indices.

magnitude. Therefore, all the diagrams for different intervals of apparent magnitude in high latitudes were combined to form the frequency-distribution diagram of colors for high latitudes. In addition to the observed frequency of colors, the frequency of colors deduced

from the observed frequency of the spectra of the same stars was also plotted. In order to obtain comparable frequency plots from colors and spectra, the relative numbers of stars in successive spectral groups were multiplied by the reciprocals of the intervals of color index covered by the corresponding spectral classes. The areas under the resulting curves were arbitrarily adjusted so as to be equal to the areas under the curves for frequency of colors. The correspondence between the two frequency distributions was rather close. In other words, in high galactic latitudes the frequency of colors is exactly what would be expected from the observed frequency of spectra.

This is not, however, the case in Selected Area 193. The frequency of colors is approximately the same for all apparent magnitudes—there is a small shift of maximum frequency with apparent brightness, to be discussed later. The three frequency-curves have been combined to give the frequency of colors; the great number of blue stars and the almost complete absence of red ones are very striking.

The colors, deduced from the observed spectral frequencies of the same stars do not, however, duplicate the color-frequency curve; on the contrary, they are redder, on the average, by more than half a magnitude. Not only is the high maximum of color frequency, composed of the very blue stars, unrepresented in the spectral frequency, but there is also a maximum of spectral frequency with no maximum of color frequency to correspond to it. These improbabilities would be removed if it were to be assumed that the fainter stars, responsible for the second maximum of the color-curve predicted from the spectral frequency (classified as late A and early F stars), are actually B stars. The color-curve deduced from the spectral frequencies on this assumption approaches the observed color-curve in shape. We may regard it as evidence that many, if not most, of the faint stars classified A and (especially) F by Becker should really be of class B, at least in Selected Area 193.[35]

The difficulty of distinguishing faint F stars from faint B stars is well known. A direct comparison between the classifications made by Becker and by Miss Cannon for faint stars in low galactic latitudes has furnished a large number of examples where a star is placed by the two investigators in different categories. A similar difficulty

[35] Payne-Gaposchkin, *Harvard Ann.*, **105**, 393, 1936.

is pointed out by Humason[36] in connection with the classification of faint spectra[37] in Selected Area 98; he had originally placed in class B a number of stars which he later reclassified as F stars. The difference was discovered as a result of comparing the Mount Wilson and the Bergedorf[38] classifications of the same stars.

That the F and G stars should preponderate at the eleventh magnitude in Carina is not consistent with other data concerning the distribution of such stars. The apparently brighter F stars (7^m – $8^m.25$, and also all such stars brighter than $8^m.25$), in all galactic longitudes taken together, show little, if any, change in actual numbers per square degree with galactic latitude.[39] Their relative frequency is, if anything, less at low than at high latitudes.[40] Additional evidence is furnished by Miss Cannon's summary[41] of the frequency of spectral types as a function of right ascension (and therefore of galactic latitude) for the stars in the Gesellschaft Zone from $+50°$ to $+60°$. The stars classified for this zone are complete to the ninth magnitude and include many stars down to $9^m.5$. Table 26 summarizes the percentages of stars in the main spectral groups at various galactic latitudes; the data are derived directly from the tables in Miss Cannon's paper, just cited, by plotting against galactic latitude and interpolating. The relative frequency of F stars is seen to be practically constant. It is noteworthy that the percentage of B stars shown in Table 26 is greater for northern than for southern galactic latitudes, as was found also (for the opposite side of the sky) for the Selected Areas at $-60°$. We have here an additional effect of the northerly position of the sun relative to the galactic plane.

The last line of Table 26 shows, for comparison, the percentage frequency of spectra in the six high-latitude areas at $-60°$. Although the magnitude limit (about 12) is much fainter than for the Gesellschaft Zone spectra, there is no motion of the maximum of spectra frequency to later spectral classes, as Becker's work[42] led him

[36] *Mt. W. Contr.*, No. 560, 1935.

[37] *Ibid.*, No. 458, p. 35, 1932.

[38] *Ibid.*, No. 560, p. 4, 1936.

[39] Shapley and Cannon, *Harvard Rept.*, No. 6, Figs. 3*a* and 3*b*, 1924.

[40] *Ibid.*, Fig. 5, 1924.

[41] *Harvard Bull.*, No. 862, 1928.

[42] *Zs. f. Ap.*, **6**, 198, 1933.

to expect there would be. His spectral counts give a maximum at class G (which, according to Table 4, corresponds to a rather *earlier* Draper class), so that the shift of maximum is toward earlier, rather than later, spectral classes.[43] In the foregoing comparison it must not be forgotten that Miss Cannon's spectra are in declination +60°, so that her low-latitude regions are in galactic longitude 60°, and the two spectral frequencies now compared relate to different galactic

TABLE 26

PERCENTAGE OF SPECTRA IN VARIOUS GALACTIC LATITUDES

GALACTIC LATITUDE	PERCENTAGE OF STARS DOWN TO 9^m					
	B	A	F	G	K	M
− 5.....	7	39	7	14	23	10
0.....	5	35	10	14	24	12
+ 5.....	4	31	11	16	26	12
+10.....	2	28	11	17	29	13
+15.....	0	25	12	18	33	14
+20.....	0	20	12	18	36	14
+25.....	0	16	12	19	38	15
+30.....	0	11	13	20	40	16
>−30 (high lat.).....	0	2	13	46	38	1

quadrants, where important differences may be found. For example, the lack of G and K stars indicated in Carina is not evident in Table 26, where even in the lowest latitudes, about a quarter of the classified stars are of class K.

If our conclusions, based on the frequency of color and spectrum in Selected Area 193, are correct, it is easy to see how Becker derived a negative density gradient for the blue stars. In his diagram of density-distribution with distance,[44] we see the fall of the B8–A2 stars taking place just where the A5–G5 stars begin to increase. If the colors are to be trusted, many of these latter stars are actually B stars, and the negative density gradient may, therefore, not be real, especially if absorption is operating, as indicated by our results.

[43] Part of the difference may result from the unexplained fact that Miss Cannon has a fainter limit, apparently, for second-type stars, and Becker for blue stars.

[44] *Zs. f. Ap.*, **6**, 199, 1933.

The maximum of the frequency of colors for each Selected Area and its displacement with apparent magnitude may be used to derive a table of color excesses similar to that derived from a comparison of spectrum and color. Such a table is given in Table 27.

The data of Tables 24 and 27 provide two different sources for determining the obscuration per kiloparsec in the six low-latitude areas. The zero point of color excesses in Table 24 has been determined by the spectral discussions of section 1 of the present paper.

TABLE 27

MAXIMUM FREQUENCY OF COLOR AND APPARENT MAGNITUDE

Selected Area	$9^m.0-9^m.9$	$10^m.0-10^m.9$	$11^m.0-11^m.9$	$12^m.0-12^m.9$
191	$-0^m.25$	$+0^m.10$	$+0^m.25$	$+0^m.45$
192	− .10	+ .25	+ .35	.50
193	− .35	− .35	− .25	.....
194	− .25	− .05	+ .15	.45
195	+ .25	+ .30	+ .40	.55
196	+0.05	+0.15	+0.25	+0.45

The color excesses of Table 27, on the other hand, are relative. Their zero point has been adjusted, by using the data for the material common to Tables 24 and 27, to the zero point of Table 24.

The absorption per kiloparsec is calculated by means of the formula

$$M = m + 5 - 5 \log d - 3E ,$$

where M and m are the absolute and apparent magnitudes, d the distance, and E the color excess. The adopted values for M, corresponding to the various spectral classes (see Table 24), are taken from a recent compilation by S. Gaposchkin.[45] The results are given in Table 28.

The results given in Table 28 are clearly very sensitive to the adopted absolute magnitudes. The absolute magnitudes on which the table is based are those given in Table 24; they are near to the values presented by Stebbins[46] in his discussion of a similar group of material.

[45] *Unpublished.*

[46] Paper presented at the dedication of the McDonald Observatory, May, 1939.

To show the effect of adopting a different scale of absolute magnitudes, the obscurations have been recomputed with absolute magnitudes -2.5 and -1.2 for classes B2 and B7, respectively, the other

TABLE 28

OBSCURATION IN LOW-LATITUDE AREAS AT $-60°$
(MAGNITUDES PER KILOPARSEC)

SELECTED AREA	DISTANCE MODULUS $(m-M)$			
	$12^m.5$	$14^m.5$	$16^m.5$	Mean
191	$0^m.0$	$0^m.87$	$0^m.40$	$0^m.42$
192	1.9	.97	.....	1.45
193	0.12	.02	.18	0.11
194	1.8	.94	0.38	1.04
195	2.5	.....	.....	2.5
196	1.1	0.94	.....	1.0
Mean(excl. 193)	1.48	0.93	0.39	0.93

TABLE 29

OBSCURATION IN LOW-LATITUDE AREAS AT $-60°$

SELECTED AREA	DISTANCE MODULUS $(M-m)$				
	$9^m.0$	$11^m.0$	$13^m.0$	$15^m.0$	All
All but 193—					
Color excess	$0^m.0$	$+0^m.11$	$+0^m.39$	$+0^m.57$	.....
Obscuration (per kiloparsec)	.....	0.24	0.51	0.38	$0^m.38$
193—					
Color excess	.....	.....	+0.13	+0.17	.....
Obscuration (per kiloparsec)	.....	.....	0.11	0.06	0.08

absolute magnitudes remaining unchanged. Two effects are produced: the change of obscuration with distance is made smaller, and the total obscurations are diminished. The results are summarized in Table 29.

It can, therefore, be definitely stated that appreciable reddening and obscuration are present in all areas, though for Selected Area 193

they are very small. The actual amount of obscuration depends intimately on the absolute magnitudes and must at present be left uncertain.

There is one effect that has not been taken into account in deducing the results given in Tables 28 and 29. It has been assumed that the real maximum frequency of color is the same, in each Selected Area, without regard to magnitude (at least over the range of magnitudes now considered). Actually, there is a small but definite change of average spectrum with distance from the galactic plane. This is shown by the amount of the systematic correction that is required (see previous paragraphs) to reduce the color excesses derived from maxima of color frequency to the same zero point as those derived from the spectral classes and colors; it is greatest ($+0^m.27$) at low latitudes, falling to zero at latitude $-19°$. In other words, in the higher latitudes the bluer stars are really of slightly later spectral class, and so are the fainter stars in a given Selected Area (being more distant from the galactic plane than the brighter ones). The actual numbers of B2, B7, and A2 stars classified at different magnitudes show the same effect, the B7 and A2 stars predominating, respectively, at the eleventh and twelfth apparent magnitudes. The effect just described, if uncorrected, will cause the calculated absorptions to be rather too great for faint apparent magnitudes, and, therefore, for large distances. The obscurations at modulus 16.5 are, however, of small weight; and probably the mean absorptions are not much affected.

HARVARD COLLEGE OBSERVATORY

PROPER MOTIONS AND MEAN ABSOLUTE MAGNITUDES OF CLASS N STARS*

RALPH E. WILSON

ABSTRACT

The investigation is based upon the proper motions of 106 stars and upon the radial velocities of 145 stars. The mean parallax of the proper-motion stars obtained from the parallactic and peculiar motions is $\bar{\pi} = 0''.00166 \pm 16$. The mean absolute magnitude computed from this parallax agrees well with that derived by Sanford from the galactic rotation factor. The data are satisfactorily represented by Plaskett's value of the rotational constant, $A = 15.5$ km/sec kpc, and by an effective galactic absorption of visual light, $a = 0.2$ mag/kpc. The mean absolute magnitude of the stars is found to be $\bar{M} = -1.84 \pm 0.20$.

When the data are divided into groups according to spectral subtypes and character of light-variation, there appears to be comparatively little deviation in $\bar{M}$ from that given by all the data, except in the case of the emission stars, which appear to be about 2.5 mag. brighter than the stars in the other groups.

The first attempts to estimate the mean absolute magnitude of the class N stars were based upon Nörlund's proper motions[1] of stars supposedly of Secchi's type IV. In addition to the inherent weakness of these proper motions, owing to the lack of positional data, the list contained many stars which have since been found to belong to spectral classes other than N. Thus Kapteyn's first value, $\bar{M} = -2.6$, published in 1910,[2] was based upon 120 proper motions and his revised value in 1920,[3] $\bar{M} = -1.5$, upon 175; both values being derived from a comparison of the mean parallactic motion with the solar speed derived from stars of all types. Since with all the positional data added since 1910 through the stimulus of Nörlund's work we are even now able to collect fairly reliable proper motions for only 106 of these stars, it must be obvious that Kapteyn's estimates refer to a mixture of stars of late types rather than to class N alone. The estimate of Luplau-Janssen and Haarh,[4] $\bar{M} = -1.3$,

* *Contributions from the Mount Wilson Observatory, Carnegie Institution of Washington*, No. 615.

[1] *A.N.*, **189**, 19, 1911.

[2] *Ap. J.*, **32**, 91, 1910.

[3] *Gron. Pub.*, No. 30, 1920.

[4] *A.N.*, **214**, 388, 1921.

is subject to the same criticism, though to a lesser degree, since they used but 78, presumably the better, of Nörlund's motions and made some attempt to differentiate between stars of classes N and R.

The first estimate of mean absolute magnitude based on purely N-type stars, $\bar{M} = -1.5$, was made by Moore[5] in 1922 and depended upon but 25 radial velocities and 19 proper motions. In 1923 Wilson[6] published proper motions of 92 of these stars and, using Moore's solar speed, 17.1 km/sec, found $\bar{M} = -1.4$. The agreement between the four values derived in the period 1920–1923 appeared to be quite satisfactory.

In 1935, however, Sanford[7] published radial velocities of 145 class N stars and from them derived the solar speed, 23.2 km/sec, the mean peculiar motion, 20.4 km/sec, and the coefficient of galactic rotation, 13.4 km/sec. It then became possible to estimate the mean absolute magnitude not only through comparisons of better-determined parallactic motions but also from peculiar motions and from galactic rotation. Using Wilson's parallactic motion, Sanford found $\bar{M} = -2.1$, and from the galactic-rotation coefficient $\bar{M} = -1.4$ or -1.8, depending upon whether Joy's[8] (18.5) or Plaskett's[9] (15.5) value of the rotational constant was used. In more recent work on the Cepheid variables Joy[10] has found a new value (20.9), the use of which would reduce the value of $\bar{M}$ derived from galactic rotation to -1.1. In view of the large range in these values, it is desirable to compute the mean parallactic and peculiar motions from the best proper motions at present available and to redetermine the mean absolute magnitude.

DATA

The radial velocities and most of the results based upon them are taken directly from Sanford's paper. In Table 1 are listed the 106 proper motions of class N stars which have been determined with

[5] *Lick Obs. Bull.*, **10**, 168, 1923.

[6] *A.J.*, **34**, 191, 1922.

[7] *Mt. W. Contr.*, No. 525; *Ap. J.*, **82**, 357, 1935.

[8] *Pub. A.S.P.*, **45**, 202, 1933.

[9] *Pub. Dom. Ap. Obs.*, **5**, 167, 1933.

[10] *Mt. W. Contr.*, No. 607; *Ap. J.*, **89**, 356, 1939.

TABLE 1

PROPER MOTIONS OF CLASS N STARS

Star	α_{1900}	δ_{1900}	Vis. Mag. Max.	Vis. Mag. Min.	Spectra		μ_α		μ_δ		Authorities*	Period
ST Cas	0^h12^m2	+49°44′	7.5	9.0	Nb		+0″.035	± 10	+0″.003	± 10	W	Irr.?
VX And	14.6	+44 9	8.1	9.5	Nc	N7	− .008	6	− .013	6	W	367
AQ And	22.2	+35 2	7.8	8.0	Nb		+ .004	6	− .016	5	W	332
Z Psc	1 10.6	+25 14	7.4	8.1	Na	No	− .009	4	− .008	4	W	Irr.
R Scl	22.4	−33 4	6.2	8.8	Np	N3	− .020	7	− .026	7	B	376
UY And	2 32.1	+38 44	9.4	12.0	Nb	N3	+ .001	11	+ .012	10	W	Irr.
					Na		+ .010	3	+ .006	3	B	
−57°513	3 10.1	−57 41	8.4	10.2	Nb	N3e	− .002	10	− .026	10	W	254
Y Per	20.9	+43 50	6.9	9.0	Nb	N5	+ .017	7	+ .028	6	W	419
U Cam	33.2	+62 19		8.9		N2	+ .014	9	− .002	11	W	
+51°762	34.1	+51 11										Irr.
ST Cam	4 40.8	+67 59	7.0	8.3	Nb		+ .002	4	+ .010	3	B	
				9.0	Nb		+ .022	8	− .032	8	W	
+34°911	42.7	+34 49	6.1	7.7	Nb		− .016	13	+ .032	12	W	
T Cae	43.8	−36 23	8.1	8.8	Nb	N3	− .015	6	+ .007	6	W	166
TT Tau	45.2	+28 21		8.8		No	− .035	12	− .042	10	W	
+38°955	45.7	+38 20										
R Lep	4 55.0	−14 57	6.1	9.7	Np	N6e	+ .022	5	+ .022	6	B	443
				9.0	Nb		+ .036	9	− .006	12	W	
+50°1112	55.6	+50 29	5.9	7.7	Nb	N5	+ .013	3	− .005	3	W	200
W Ori	5 0.2	+ 1 2	8.5	9.2	Nb	N3	− .012	10	+ .031	8	W	330?
TX Aur	2.2	+38 52	8.0	9.6	Nb	No	− .012	8	+ .025	9	W	
SY Eri	4.9	− 5 38		9.1	Nb		− .004	8	+ .005	8	W	
+35°1046	5 12.5	+35 41	9.3	12	Nb	N3	− .041	7	− .007	7	W	591
S Aur	20.5	+34 4	7.5	8.5	Nb		− .060	7	+ .010	7	W	Irr.?
RT Ori	27.8	+ 7 4		7.9	Na		+ .032	13	+ .020	12	W	
−25°2539	31.7	−25 48	8.7	9.5	Nb	N2	+ .009	5	− .010	5	W	Irr.
TU Tau	39.1	+24 23										
Y Tau	5 39.7	+20 39	6.9	8.9	Nb	N2	+ .003	5	− .004	5	W	240
W Pic	40.4	−46 30	8.5	12.5	N		− .015	10	+ .004	9	B	
+30°1014	41.7	+30 26	9.0	9.3	Na	No	+ .012	8	+ .002	8	W	
TU Gem	6 4.7	+26 3	7.4	8.3	Na	N3	+ .008	4	− .007	3	W	Irr.?
BL Ori	19.8	+14 48	4.7	6.6	Nb		− .010	6	− .002	5	W	
UU Aur	6 29.7	+38 31	6.2	6.7	Na	N3	+ .005	3	− .029	2	W	Irr.
VW Gem	35.7	+31 33	8.6	8.8	Na		− .008	6	− .049	6	W	Irr.
−48°2818	51.2	−42 14		6.0	Na		+ .001	5	+ .022	3	B	
RV Mon	53.0	+ 6 18	7.0	8.2	Nb		− .027	9	− .004	7	W	225
RY Mon	7 2.1	− 7 24	7.7	9.1		N5	− .006	8	+ .010	8	W	466
W CMa	7 3.4	−11 46	6.9	7.5	Na		− .029	4	+ .010	4	W	
	20.3	− 2 57		9.1	Nb		− .003	12	− .042	13	W	
− 2°2101	53.5	−49 43		7.6	Nb		+ .041	13	− .028	12	W	
−49°3201	8 3.2	−22 37	6.8	9.0	Nb		− .011	10	− .035	12	W	Irr.
RU Pup	14.9	+ 3 5	8.3	9.6	Nbe		+ .007	7	− .007	7	W	535
RY Hya	8 16.4	+33 51	8.0	12.0		Noe	+ .020	7	+ .006	8	W	419
T Lyn	49.7	+17 37	6.1	6.6	Nb	N3	+ .004	3	+ .003	3	W	130
X Cnc	51.0	+20 14	8.0	10.2		N3	− .008	4	− .003	4	W	500
T Cnc	9 45.9	− 1 33	8.8	12.3	Nbe		− .006	10	+ .004	11	W	
W Sex	46.4	−22 32	6.5	8.0	Np	N3	− .017	10	− .004	9	B	Irr.
Y Hya	9 51.3	−41 7	6.9	9.2	Nb		− .010	11	− .036	9	B	Irr.
X Vel	56.7	−59 44	6.0	7.5	Nb		+ .016	10	+ .010	10	W	
SZ Car	10 7.5	−34 50		7.0	Na		+ .002	5	+ .001	5	B	
−34°6528	30.8	−39 3	5.7	6.7	Nb		− .031	5	− .007	4	B	168?
U Ant	32.6	−12 52	4.5	6.3	Nb	N2	+ .036	3	− .034	3	W	Irr.
U Hya	10 38.1	+67 56		6.3	Na		+ .005	6	− .003	6	W	
+68°617	46.8	−20 43	6.7	12.0		N6	− .008	9	− .018	9	W	505
V Hya	12 20.1	+ 1 20	7.2	9.0	Np		− .007	7	− .003	7	W	354
SS Vir	40.4	+45 58	4.8	6.0	Nb	N3	+ .004	2	+ .008	2	B	158
Y CVn	52.5	+66 32	6.1	7.1	Np	N4p	+ .009	5	− .021	6	W	Irr.
RY Dra												

* Authorities: B, Boss; K, Kapteyn and van Rhijn; W, Wilson.

TABLE 1—*Continued*

Star	α_{1900}	δ_{1900}	Vis. Mag. Max.	Vis. Mag. Min.	Spectra		μ_α	μ_δ	Authorities*	Period
T Mus	13^h13^m5	−73°55′	5.4	7.1	Np		+0″.019±13	−0″.027±14	K	
UX Cen	15.5	−63 42	6.4	7.9	Nb		− .043 15	− .009 13	W	
−55°5802	51.6	−55 51	7.8	8.5	Na		− .012 16	− .028 14	W	
−53°5915	14 7.4	−53 28	7.0	8.5	Nb		− .018 15	− .031 13	W	
X TrA	15 4.7	−69 42	5.9	7.7	Nb		+ .007 4	− .015 3	B	Irr.
V CrB	15 46.0	+39 52	7.2	12.0	Nb	N3e	+ .020 7	− .017 6	W	362
V Oph	16 21.2	−12 12	7.0	10.5	Nb	N3e	+ .001 7	− .010 7	W	301
V TrA	39.8	−67 36	6.6	7.5	Nb		+ .003 9	− .007 10	K	
T Ara	54.4	−54 55	7.3	8.4	Nb		− .029 14	− .008 14	K	
TW Oph	17 23.8	−19 24	7.8	8.7	Nb		− .021 5	− .002 6	W	
TT Sco	17 33.4	−41 34	8.1	10.8		N3	+ .022 13	− .013 13	B	
V Pav	34.7	−57 40	5.7	7.2	Nb		− .006 9	− .055 9	B	
SZ Sgr	39.1	−18 37	5.9	7.2	Nb		− .004 6	− .004 5	W	
SX Sco	40.8	−35 39	8.0	8.5	Nb		+ .015 11	+ .012 11	W	128?
T Lyr	18 28.9	+36 55	7.8	9.6		N3	− .002 9	− .008 7	W	Irr.
RX Sct	18 31.7	− 7 41	8.5	9.4	Np	N3	+ .012 12	+ .010 12	W	Irr.
+36°3243	39.4	+36 53	8.1		Nb		+ .016 8	+ .010 7	W	
S Sct	44.9	− 8 1	6.4	7.3	Nb	N3	+ .010 9	+ .006 8	W	144?
T Sct	50.0	− 8 19	8.8	9.3	Nb	N3	− .015 10	− .013 10	W	Irr.
UV Aql	54.0	+14 14	7.9	9.0	Nb	N4	+ .013 11	+ .005 9	W	355
V Aql	18 59.1	− 5 50	6.5	8.0	Np	N6	+ .013 4	− .003 5	W	Irr.
−16°5272	19 13.4	−16 5	7.2		Na	N2	+ .029 4	+ .003 4	W	
UX Dra	25.1	+76 23	6.1	7.1	Nb	No	− .010 2	+ .002 3	B	Irr.
AW Cyg	25.8	+45 50	8.0	10.2		N3	− .010 8	+ .056 8	W	Irr.
AQ Sgr	28.6	−16 35	6.6	7.6	Nb	N3	+ .001 4	− .001 4	W	Irr.
TT Cyg	19 37.1	+32 23	7.3	8.4	Nb	N3	− .022 6	− .002 6	W	118
UW Sgr	40.6	−18 24	6.4	8.2	Na		+ .034 7	− .021 6	W	
AX Cyg	54.0	+44 0	7.4	7.9	Nb		− .014 4	− .011 4	W	
+ 9°4369	56.3	+ 9 14	8.7		Nb		− .013 6	− .019 6	W	
+20°4390	58.0	+20 49	9.2		Nb		− .004 7	− .010 8	W	
X Sgr	20 0.7	+20 22	8.7	9.7	Nb		− .013 9	− .030 9	W	196
AY Cyg	6.3	+41 12	8.9	10.2	N		− .062 14	− .026 14	W	
SV Cyg	6.5	+47 35	8.1	9.4	Nb	N3	− .031 12	+ .034 12	W	Irr.
RS Cyg	9.8	+38 28	7.5	8.7	Nap	Noep	− .007 4	+ .001 4	W	Irr.
RT Cap	11.3	−21 38	6.4	7.8	Nb	N3	− .024 5	+ .011 6	W	Irr.
U Cyg	20 16.5	+47 35	6.1	11.8	Npe	R9	− .010 7	− .003 6	W	457
V Cyg	38.1	+47 47	6.8	13.8	Npe	N3e	− .016 6	− .019 5	W	416
T Ind	21 13.6	−45 26	5.2	6.9	Na		− .004 11	− .010 9	B	
Y Pav	15.2	−70 10	3.7	6.5	Na	No	+ .007 8	− .017 7	B	
YY Cyg	18.6	+41 58	8.5	9.5	Nc		− .021 8	+ .008 8	W	387
S Cep	21 36.5	+78 10	7.9	13.1	Nce	N8e	+ .003 4	− .013 5	W	482
DS Peg	37.8	+35 3	6.0	7.0	Nb	N1	+ .011 5	− .005 4	W	
RV Cyg	39.1	+37 34	7.1	9.3	Np	N5	− .002 5	+ .011 5	W	Irr.
LW Cyg	51.5	+50 1	9.3	10.2	Nc		+ .018 8	− .001 7	W	
RX Peg	51.7	+22 24	7.7	8.6	Nb	N3	− .009 5	.000 5	W	Irr.
+60°2342	22 40.4	+61 12	9.0		Nb		− .006 13	− .005 12	W	
TV Lac	51.9	+53 41	9.1	10.1	Nb		+ .004 10	.000 13	W	Irr.
+48°4051	23 22.2	+48 58	8.6		Nb		− .008 10	+ .009 5	W	
19 Psc	41.3	+ 2 56	5.3		Na	No	− .039 2	− .016 2	B	
WZ Cas	56.2	+59 48	6.9	8.5	Na	N1p	+ .010 5	− .002 4	W	193
SU And	59.4	+43 0	7.9	8.5	Nb		+0.025 7	+0.009 7	W	Irr.

probable errors not exceeding 0".015. These have been taken mainly from the *Boss General Catalogue* and Wilson's supplementary list;[11] three were added from Kapteyn's list.[3] In the various solutions and summations the following weights were used:

P.E.	Weight
0".001–0".005	1.5
0.006–0.010	1.0
0.011–0.012	0.7
0.013–0.015	0.5

The magnitudes, the spectra, and the information as to the character of variation and period are from Schneller's *Katalog und Ephemeriden veränderlicher Sterne für 1939*,[12] the Harvard classification when available being added wherever Schneller gives the decimal classification. Considerable uncertainty in the visual magnitude arises where the photographic magnitude alone has been measured. The color indices of the N stars have a wide range and the mean is rather indefinite. In order to reduce the magnitudes to one system, the following color indices were used:

	C.I.
Na	+2.0
Nb	2.6
Nc	+3.0

Where no subclass was recorded, the value +2.6 was used, following Sanford's example.

GROUP MOTION

Although the distribution of the N stars with known proper motions is highly unfavorable for a determination of the solar apex, it is desirable that the co-ordinates of the group motion be derived from the proper motions for comparison with those depending upon the radial velocities. The corrections to the Newcomb precessions derived by Wilson and Raymond[13] were accordingly applied to the

[11] *A.J.*, **48**, 41, 1939.

[12] *Kleinere Veröff. Universitäts-Stern. Berlin-Babelsberg*, No. 20, 1938.

[13] *A.J.*, **47**, 57, 1938.

proper motions, which were then transformed to motions relative to the galaxy and analyzed by means of the relations[14]

$$\mu_l \cos b = X \sin l - Y \cos l + Q \cos b + C \cos 2l \cos b + S \sin 2l \cos b ,$$

$$\mu_b = X \cos l \sin b + Y \sin l \sin b - Z \cos b - \frac{C}{2} \sin 2l \sin 2b + \frac{S}{2} \cos 2l \sin 2b .$$

The results of this analysis are given in Table 2.

TABLE 2

RESULTS FROM PROPER MOTIONS

	(Unit 0".01)		
X	+0.35±0.18	l_a	51°
Y	+ .44 .16	b_a	+ 40°
Z	+ .48 .13	A_0	240°
Q	− .31 .14	D_0	+ 56°
C	+ .19 .18	q	0".74±0".16
S	+0.19±0.18	l_0	22°
		P	0".27±0".18

From the radial velocities Sanford obtained for the directions of the apex of group motion and of the galactic center $A_0 = 257°$, $D_0 = +30°$, and $l_0 = 315°$. The differences between the values of these quantities derived from radial velocities and from proper motions are due partly to the small number of stars involved but much more to the effect of their unfavorable distribution on the proper-motion solution. Since this distribution is favorable from the standpoint of the radial velocities, the results based upon them must be regarded with considerably more confidence than those based upon the proper motions. In view of the uncertainties involved, the values derived from the two sets of data may be considered not unduly different from those of the apex referred to the stars in general and from the conventional value of the longitude of the galactic center. In the computations to follow, the values $A_0 = 270°$, $D_0 = +30°$, and $l_0 = 326°$ have therefore been adopted. It is interesting, if not

[14] For the significance of the symbols here used see R. E. Wilson, *Mt. W. Contr.*, No. 604; *Ap. J.*, **89**, 218, 1939.

particularly significant in view of the result for l_0, that the values here found for $Q(-0''.0031)$ and $P(+0''.0027)$ agree well with the more accurately determined values of the galactic rotation, $Q = -0''.0030$ and $P = +0''.0033$.

MEAN PARALLAX

In order to obtain the best results for mean parallax, especially when dealing with small proper motions and meager data, it is essential that the computations be made by several different methods. The three relations most convenient in application are

$$\pi_q = \frac{kq}{V_0} = \frac{k}{V_0} \frac{\sum v \sin \lambda}{\sum \sin^2 \lambda}, \tag{1}$$

$$\pi_q = \frac{\sum (A\mu_1 + B\mu_2)}{p \sum (A^2 + B^2)}, \tag{2}$$

and

$$\pi_\tau = \frac{k\tau_0}{\theta}. \tag{3}$$

Formulae (1) and (3) may each be used in two ways; the value of q may be determined from the solution for group motion or from the v components of the proper motions; and a value of τ_0 may be derived, when the data are sufficient, from the relation

$$\tau_0^2 = \tau_{\text{av}}^2 - \kappa \bar{\rho}^2, \tag{4}$$

in which $\bar{\rho}$ is the mean of the quoted probable errors, or from the relation

$$\tau_0^2 = \tau_{\text{av}}^2 - \eta^2, \tag{5}$$

in which η is the true average error. In formula (2) μ_1 and μ_2 are the proper motions in arc in right ascension and declination, respectively, and A and B are functions of V_0 and the position of the apex.[15]

Values of the mean magnitudes (maximum and minimum), total proper motions, their quoted probable errors, and various components are given in Table 3.

[15] G. Strömberg, *Mt. W. Contr.*, No. 558; *Ap. J.*, **84**, 555, 1936.

The true mean peculiar motion, τ_0, was derived through a least-squares solution based upon equation (4), from which it was found that

$$\tau_0 = 0''.0090 \pm 7 \quad \text{and} \quad \kappa = 2.28 .$$

The value of κ indicates that the true value of the mean probable error is $\rho_0 = 1.28\ \bar{\rho}$ or that the quoted probable errors are under-

TABLE 3

OBSERVED MEAN VALUES OF MAGNITUDES AND PROPER MOTIONS

$\bar{m}_{max}$	7.32	$100\bar{\tau}$	$+0''.09$
$\bar{m}_{min}$	8.66	$100\bar{v}$	$+0.37$
$100\bar{\mu}_{obs}$	$2''.21$	$100\tau_{av}$	1.40
$100\bar{\rho}$	0.77	100η	1.17
$100\rho_0$	0.99	$100q$	0.54

TABLE 4

DETERMINATIONS OF MEAN PARALLAX

Method	$\bar{\pi}$
(1) q from Table 2	0.00151 ± 33
(1) q from v—comp.	.00110 24
(2)	.00108 24
(3) τ_0 from Eq. (4)	.00209 16
(3) τ_0 from Eq. (5)	0.00179 ± 16
$\bar{\pi}_q$	0.00118 ± 15
$\bar{\pi}_\tau$	0.00194 ± 11

estimated by 28 per cent. Since η, the average error, is $1.18\ \rho_0$, equation (5) gives the value

$$\tau_0 = 0''.0077 \pm 7 .$$

From his analysis of the radial velocities Sanford finds

$$V_0 = 23.2 \text{ km/sec} \quad \text{and} \quad \theta = 20.4 \text{ km/sec} .$$

The five values of the mean parallax derived with the foregoing values are summarized in Table 4.

Inasmuch as the mean absolute magnitudes computed from $\bar{\pi}_q$ and $\bar{\pi}_r$ differ by a whole magnitude, the proper combination of the two values to obtain a representative mean is important. The relative weights computed from the probable errors are 1:1.77, while Russell's criterion[16] gives 1:1.66. Adopting the mean,

$$p_q : p_r :: 1 : 1.7 ,$$

one gets as the mean parallax of the 106 stars listed in Table 1

$$\bar{\pi} = 0''.00166 \pm 16 .$$

The probable error is the mean of three values based upon the results given in Table 4. One was computed from the five probable errors of the separate determinations of $\bar{\pi}$, a second from the range in the five values of $\bar{\pi}$, and a third from the difference between $\bar{\pi}_q$ and $\bar{\pi}_r$.

MEAN ABSOLUTE MAGNITUDE

The mean absolute magnitude may now be determined from two sets of data; one given in the preceding section,

$$\bar{m}_1 = 7.32 , \qquad \bar{\pi} = 0''.00166 \pm 16 ,$$

and the other from Sanford's discussion of the radial velocities,

$$\bar{m}_2 = 7.9 , \qquad \bar{r}A = 13.4 \pm 2.6 \text{ km/sec} .$$

The relations applying are

$$\bar{M}_\pi = \bar{m}_1 + 5 + 5 \log \bar{\pi} + 5C_1 - \frac{ac}{1000\bar{\pi}} , \tag{6}$$

$$\bar{M}_r = \bar{m}_2 + 5 - 5 \log \bar{r} - 5C_2 - \frac{a\bar{r}}{1000} , \tag{7}$$

in which $C_1 = \overline{\log \pi} - \log \bar{\pi}$, $C_2 = \overline{\log r} - \log \bar{r}$, $c = \bar{\pi} \cdot \bar{r}$, $\bar{r} = \bar{r}A/A$, and a is the galactic absorption per kiloparsec.

The fifth term involves the effective galactic absorption, which, owing to the strong concentration of the N stars toward the galactic plane, must considerably affect the apparent magnitudes. The best

[16] *Mt. W. Contr.*, No. 215; *Ap. J.*, **54**, 142, 1921.

determinations of the absorption of visual light give $a = 0.30$ mag/kpc in the region of the galaxy, and a reasonable estimate of the mean effective absorption for the N stars is $a = 0.20$ mag/kpc. With this value of a, one finds from (6) and (7)

$$M_\pi = \left\{ \begin{matrix} -1.58 \\ \pm 0.23 \end{matrix} \right\} + 5C_1 - \frac{0.2c}{1000\bar{\pi}}, \tag{8}$$

$$M_r = \left\{ \begin{matrix} -1.79 \\ \pm 0.43 \end{matrix} \right\} - 5C_2 - \frac{0.2\bar{r}}{1000}, \tag{9}$$

the value $A = 15.5$ km/sec kpc having been used to determine $\bar{r}$. The probable error of M_π was estimated from the probable error of $\bar{\pi}$, from the range in $\bar{M}$ based upon the various values of $\bar{\pi}$ in Table 4, and from the difference in the values of $\bar{M}$ derived from $\bar{\pi}_q$ and $\bar{\pi}_r$. That for M_r is based upon the probable error of $\bar{r}A$.

A rigorous determination of $\bar{M}$ requires knowledge of the values of C_1, C_2, and c. There are as yet no spectroscopic criteria of absolute magnitude for the N stars, and the direct measures of parallax are too few to give any information as to these values. However, approximations may be made on the assumption that M_π and M_r refer to representative groups of N stars, such that

$$\text{true } M_\pi = \text{true } M_r . \tag{10}$$

By definition, for any set of stars, whatever the distribution of $\log \pi$,

$$C = \overline{\log \pi} - \log \bar{\pi} ,$$

$$C' = \overline{\log r} - \log \bar{r} ,$$

$$c = \bar{\pi} \cdot \bar{r} ,$$

whence

$$\log c = -(C + C') . \tag{11}$$

Also, since $r = 1/\pi$ and we may write $\pi = \bar{\pi} + \epsilon$,

$$r = \frac{1}{\bar{\pi}\left(1 + \frac{\epsilon}{\bar{\pi}}\right)}$$

and

$$\bar{r} = \frac{1}{\bar{\pi}}\left(1 - \frac{\bar{\epsilon}}{\bar{\pi}} + \frac{\overline{\epsilon^2}}{\bar{\pi}^2} - \frac{\overline{\epsilon^3}}{\bar{\pi}^3} \cdots\right).$$

Since, by definition $\bar{\epsilon} = 0$ and $\overline{\epsilon^2} = \sigma_\pi^2$, σ_π being the dispersion in π,

$$c = \bar{\pi} \cdot \bar{r} = 1 + \frac{\sigma_\pi^2}{\bar{\pi}^2} - \frac{\overline{\epsilon^3}}{\bar{\pi}^3} \cdots.$$

and

$$\log c = \operatorname{Mod}\left(\frac{\sigma_\pi^2}{\bar{\pi}^2} - \frac{\overline{\epsilon^3}}{\bar{\pi}^3} \cdots\right). \tag{12}$$

Further,

$$\overline{\log \pi} = \overline{\log (\bar{\pi} + \epsilon)} = \log \bar{\pi} + \overline{\log\left(1 + \frac{\epsilon}{\bar{\pi}}\right)},$$

$$C = \overline{\log \pi} - \log \bar{\pi} = \overline{\log\left(1 + \frac{\epsilon}{\bar{\pi}}\right)}$$

$$= \operatorname{Mod}\left(\frac{\bar{\epsilon}}{\bar{\pi}} - \frac{\overline{\epsilon^2}}{2\bar{\pi}^2} + \frac{\overline{\epsilon^3}}{3\bar{\pi}^3} \cdots\right),$$

which reduces to

$$C = -\operatorname{Mod}\left(\frac{\sigma_\pi^2}{2\bar{\pi}^2} - \frac{\overline{\epsilon^3}}{3\bar{\pi}^3} \cdots\right). \tag{13}$$

From equation (11)

$$C' = -\operatorname{Mod}\left(\frac{\sigma_\pi^2}{2\bar{\pi}^2} - \frac{2\overline{\epsilon^3}}{3\bar{\pi}^3} \cdots\right),$$

whence

$$C - C' = \operatorname{Mod}\left(-\frac{\overline{\epsilon^3}}{3\bar{\pi}^3} \cdots\right). \tag{14}$$

All series are convergent for values of $\overline{\epsilon^2}/\bar{\pi}^2 < 1$. To powers of the second order inclusive, therefore,

$$C = C' ,$$

$$c = 1 + \frac{\sigma_\pi^2}{\bar{\pi}^2} ,$$

and

$$\log c = -2C .$$

In the first approximation for the solution of equations (8) and (9), then,

$$\left.\begin{aligned} -2C_1 &= \log c_1 , \\ -2C_2 &= \log c_2 . \end{aligned}\right\} \tag{15}$$

Neglecting the absorption terms, one finds from condition (10) and the difference between equations (8) and (9)

$$C_1 + C_2 = 2C_1 = -0.042$$

and from equations (15)

$$\log c_1 + \log c_2 = -0.084 ,$$

from which it follows that $C_1 = C_2$ with only a small percentage error. Then

$$\log c = \log c_1 = \log c_2 = 0.042$$

gives

$$c = 1.102 .$$

The values of the absorption terms may now be taken into account and the process repeated. The third approximation gives

$$c = 1.121 ,$$

a value differing only 0.001 from that given by the second. Since

$$5C_1 = 5C_2 = -2.5 \log c = -0.125 ,$$

equations (8) and (9) give on the third approximation

$$M_\pi = -1.58 - 0.125 - 0.135 = -1.84\,,$$

$$M_r = -1.79 + 0.125 - 0.173 = -1.84\,,$$

and

$$\bar{M} = -1.84 \pm 0.20\,.$$

If the distribution of $\log \pi$ is Gaussian, we have the rigorous relation

$$\log c = \frac{\sigma^2_{\log \pi}}{\text{Mod}}\,.$$

For $c = 1.12$ the corresponding value of the dispersion in $\log \pi$ is

$$\sigma_{\log \pi} = \pm 0.144\,.$$

Although the value of c appears reasonable, little confidence can be placed in it. Two assumptions have been made which may seriously influence the values of c and $C_1 = C_2$: first, that the values of $\bar{\pi}$ and $\bar{r}$ are observationally consistent, i.e., not affected by any important systematic errors; and, second, that both refer to representative groups of N stars, such that $M_\pi = M_r$. The value calculated for $C_1 = C_2$ is obviously sensitive to departures from either of these assumptions. On the other hand, the value of $\bar{M}$ is but little affected by the failure of either assumption, unless possible systematic errors in $\bar{\pi}$ and $\bar{r}$ make both M_π and M_r too large or too small. The most obvious possibility is an error in the rotational constant A. However, larger values of A connote smaller values of σ_π and c_1, which become 0 and 1, respectively, for $A = 17.2$ km/sec kpc.

TABLE 5

MEAN ABSOLUTE MAGNITUDES FROM APPARENT-MAGNITUDE GROUPS

No.	$\bar{m}$	$\bar{r}A$ km/sec	$\bar{r}$ kpc	$\bar{M}$
41	6.5	7.2	0.465	−1.81
48	8.2	16.3	1.050	.99
44	9.3	22.4	1.445	.67
133	7.9	13.4	0.865	−1.83

Sanford divides his radial velocity data into groups according to apparent magnitude and derives values of $\bar{r}A$ and $\bar{r}$. The internal agreement of the absolute magnitudes computed for each group with the constants resulting from the general solution, as shown in Table 5, serves as a partial check upon the values of the constants.

The conclusions are, therefore, that the data are well represented by the values

$$a = 0.2 \text{ mag/kpc} \qquad \text{and} \qquad A = 15.5 \text{ km/sec kpc}$$

and that the mean absolute magnitude of the class N stars with measured proper motions and radial velocities at maximum is

$$\bar{M} = -1.84 \pm 0.20 .$$

MEAN ABSOLUTE MAGNITUDES OF SUBTYPES

It is of interest to inquire whether the mean absolute magnitude derived above is representative of the various subtypes and of divisions made according to the character of the variability or nonvariability of the stars. For this purpose mean parallaxes were computed from means of the data in nine subgroups. The group motion was assumed to be the same for all subdivisions as that derived from the general solution. Values of the mean peculiar motions derived from the radial velocities are given in Table 6. As radial velocities up to 150 km/sec enter into the determination of these values, the scatter about the mean, $\theta = 20.2$ km/sec, is small enough to justify its use in the computation of π_r. The difference between this mean

TABLE 6

MEAN PECULIAR MOTIONS IN SUBGROUPS

Spectrum	No.	θ km/sec	Type	No.	θ km/sec
Na	38	16.1	Periodic	41	20.3
Nb	89	22.2	Irregular	34	19.1
Nc	7	16.3	All variable	93	20.6
Np	14	18.2	Nonvariable	52	19.1
Ne	19	21.0	All	145	20.2

TABLE 7

COMPUTATION OF $\bar{M}$ FOR SUBGROUPS

	Na	Nb	Nc	Np	Ne	Periodic	Irregular	Variable	Nonvariable
No.	22	72	7	12	11	33	29	87	19
Wt.	26.0	73.4	8.0	13.5	11.7	36.7	33.8	92.5	18.9
Max.	6.88	7.31	7.54	6.87	7.44	7.28	7.19	7.14	7.63
Min.	7.62	8.75	10.31	9.48	11.18	9.51	8.43	8.87	.....
100μ	2".24	2".26	2".00	1".71	1".81	1".96	2".02	2".25	2".44
$100\bar{p}$	0.66	0.78	0.66	0.68	0.70	0.67	0.68	0.76	0.81
$100\rho_0$	0.84	1.00	0.84	0.87	0.90	0.86	0.87	0.97	1.04
$100\bar{\tau}$	+0.50	−0.01	−0.21	−0.12	−0.02	+0.37	−0.58	+0.01	+0.47
$100\bar{v}$	+0.81	+0.28	+0.31	+0.03	−0.48	−0.23	+0.46	+0.34	+0.49
$100\tau_{av}$	1.39	1.41	1.49	1.35	1.26	1.31	1.43	1.37	1.54
100η	0.99	1.17	0.99	1.03	1.06	1.02	1.03	1.15	1.22
$100\tau_0$	0.98±14	0.79± 8	1.11±27	0.87±19	0.68±19	0.82±11	0.99±13	0.74± 7	0.94±18
$100q$	0.87±24	0.47±15	0.41±49	0.08±38	−0.51±42	−0.25±21	0.61±22	0.58±14	0.35±31
$100\pi_q$	0.18±4.9	0.10 ±3.1	0.08±10	0.02±7.8	−0.10±8.6	−0.05±4.3	0.12 ±4.5	0.12±2.7	0.07 ±6.3
$100\pi_s$	0.20±4.9	0.09 ±3.1	0.10±10	0.02±7.8	−0.24±8.6	−0.07±4.3	0.15 ±4.5	0.10±2.7	0.12 ±6.3
$100\bar{\pi}_q$	0.19±3.5	0.095±2.2	0.09± 7.0	0.02±5.5	−0.17±6.1	−0.06±3.0	0.135±3.2	0.11±2.0	0.105±4.5
$100\pi_{\tau}$	0.23±3.5	0.19 ±1.9	0.26± 6.3	0.20±4.4	0.16±4.4	0.19±2.6	0.23 ±3.0	0.17±1.6	0.22 ±4.2
p_τ/p_q	1.0	1.3	1.2	1.6	1.9	1.3	1.1	1.3	1.2
$100\bar{\pi}$	0".210±24	0".149±14	0".183±46	0".131±34	0".046±36	0".081±19	0".185±21	0".144±12	0".163±30
$\bar{M}_{max}$	−1.7±0.3	−2.1±0.3	−1.4±0.8	−2.8±0.8	−4.9±3.2	−3.6±0.7	−1.7±0.3	−2.4±0.3	−1.6±0.6
$\bar{M}_{med}$	−1.3	−1.4	(0.0)	−1.5	−3.0	−2.5	−1.1	−1.5	−1.6

and the 20.4 km/sec given by Sanford is due to the fact that he used only the 133 stars between galactic latitudes $\pm 40°$.

The mean $\overline{\pi}_q$ of the values of π_q determined by equations (1) and (2) was combined with π_r from equation (3) with weights based upon the computed probable errors. The mean absolute magnitudes corresponding to maximum and to median apparent magnitudes were computed by equation (6) with the values of σ and a given by the general solution. The details of the computations are given in Table 7.

There appears to be little evidence of any pronounced difference in mean absolute magnitude among the normal N stars, although the value for Nc is quite uncertain owing to the small number of stars involved. The outstanding group is that composed of the emission stars. These appear to be about 2.5 mag. brighter than the average. All are variable, nine are periodic, one is irregular, and for the other the type of variation is unknown. Their inclusion in the Np, periodic, and all-variable groups tends to make brighter the $\bar{M}$ computed for these groups. The Ne stars as a class also have the greatest range in magnitude variation; in fact, when an N star is found to have a large variation in apparent magnitude, the presence of emission in its spectrum may be predicted with a reasonable degree of certainty.

The variable stars at maximum appear to be somewhat brighter than those in which no light-variation has been noted, even when the Ne stars are left out. If, however, the values of $\bar{M}$ corresponding to median apparent magnitude are considered, the scatter in $\bar{M}$ appears to be very small. It has been customary to consider the maximum as the normal state of these stars along with the long-period variables of other spectral types. The foregoing results seem to indicate that possibly the median magnitude represents the normal state, as is the case with the Cepheids. Whichever state be considered as normal, the N stars may all be classified as giants, the emission stars possibly as supergiants. No dwarf star with this type of spectrum is yet known.

CARNEGIE INSTITUTION OF WASHINGTON
MOUNT WILSON OBSERVATORY
June 1939

INTENSITY CHANGES IN BRIGHT CHROMOSPHERIC DISTURBANCES*

R. S. RICHARDSON

ABSTRACT

Intensities are given for 18 bright chromospheric disturbances observed at Mount Wilson for which complete photographic records are available. The values are a combination of the measured areas of the flocculi and eye-estimates of their individual brightness.

On the assumption that the chromospheric emission in Lyman α is five times stronger than in $H\alpha$, radiation through the atmospheric "window" from λλ 1100–1300 during a bright chromospheric disturbance of intensity 2 or 3 should be about 60 per cent greater than normal.

I. INTRODUCTION

The most convincing evidence of a direct connection between the sudden appearance of very bright flocculi in the chromosphere and fade-outs in high-frequency radio signals is the simultaneity of their occurrence. The effect is especially striking when the flocculi are exceptionally bright and the time of commencement accurately known. For then it may be confidently asserted that a fade-out began within a few minutes of the solar disturbance,[1] which will almost invariably be confirmed by later reports.

The fade-outs have been satisfactorily explained as the result of an intense burst of ultraviolet light from the bright flocculi, capable of penetrating the atmosphere down to the D-layer, at a distance of only 100 km from the surface. The solar radiation produces numerous ions, which quickly absorb the radio wave-energy. But the high density also favors rapid recombination of ions and electrons, so that when the ultraviolet light begins to fail the percentage ionization soon returns to normal. The wave is now no

* *Contributions from the Mount Wilson Observatory, Carnegie Institution of Washington,* No. 616.

[1] Previously the sudden appearance of bright flocculi in the chromosphere was called an "eruption," on the tacit assumption that this was the only way such an effect could be produced. But, owing to the absence of high radial velocities in the intensely luminous flocculi, it seems safer to refer to them simply as "disturbances"—a term without the implications of "eruptions."

longer absorbed and passes through to the higher layers, where it is reflected as usual.

If the degree of ionization in the D-layer is as sensitive to the chromospheric emission as this theory implies, then a detailed comparison of solar and radio data should be of the greatest interest. Radio records suitable for this purpose are available, but the solar data are scanty and incomplete. Except for a few isolated cases, the only accounts that have been published are those in the Zürich bulletins, giving the time of beginning and end and an eye-estimate of the maximum intensity.

Starting in June, 1936, an automatic camera which runs almost continuously from sunrise to sunset has been used at Mount Wilson, taking spectroheliograms on motion-picture film about every three minutes. Although reports on the bright chromosphere disturbances photographed during this time have all been sent to Meudon, a detailed description of our best examples is made available here, since apparently no other continuous photographic observations have been taken.

II. OBSERVATIONAL MATERIAL

The observational material in Tables 1 and 2 includes all disturbances photographed on film from June, 1936, to April, 1939, for which we have a complete record from beginning to end. The only exception is the disturbance of January 20, 1938, the beginning of which was evidently missed by a few minutes. But since this is one of the longest and brightest disturbances recorded, it has been retained because of its extraordinary character.

The values called "Integrated Intensities" in the last column are a combination of measured areas of the flocculi and eye-estimates of their brightness on a scale of 1–5. They have been rounded off to two figures owing to the approximate nature of the data.

The areas were found by putting the film in a motion-picture machine, which enlarged the images from 2 to 25 cm, and by making an outline of the projected image on a sheet of squared paper.

It is customary to express the areas of sunspots in millionths of the sun's visible hemisphere by the formula

$$A = \frac{A' \, 10^6 \sec a}{2\pi R^2},$$

where A' is the measured area, R the radius of the disk, and α the angular distance of the spot from the center of the disk. A spot with an area of 1000 is considered "large" and is visible to the unaided eye when near the solar meridian. The areas given in Table 2 are in millionths of the sun's visible hemisphere, but have not been corrected for foreshortening. It is doubtful if such a correction is

TABLE 1

BRIGHT CHROMOSPHERIC DISTURBANCES FOR WHICH COMPLETE RECORDS EXIST

Mt. W. No.	Date	Position	Exposure Interval	First Seen	Projection Factor (sec α)
			min.	G.C.T.	
4921	1936 June 19	20° N, 30° E	3.61	19^h34^m4	1.23
5075	Oct. 14	14 S, 44 W	3.67	22 39.9	1.40
5172	Dec. 24	15 S, 38 E	4.35	22 31.0	1.36
5343	1937 Apr. 21	18 N, 37 E	4.21	14 50.8	1.38
5343	Apr. 21	18 N, 37 E	3.96	20 04.7	1.38
5409	June 20	12 N, 3 E	2.94	21 03.3	1.03
5412	June 20	11 N, 39 E	3.17	00 10.3	1.34
5453	July 11	13 N, 48 E	3.41	00 28.1	1.54
5453	July 11	12 N, 33 E	3.40	19 08.9	1.33
5455	July 16	15 S, 21 W	3.43	22 41.3	1.14
5578	Sept. 29	12 N, 64 E	4.13	19 49.6	2.06
5578	Oct. 4	10 N, 7 W	3.48	20 36.4	1.04
5578	Oct. 6	9 N, 33 W	3.39	20 17.2	1.20
5716	1938 Jan. 11	13 N, 65 W	3.26	19 31.0	2.11
5726*	Jan. 20	18 N, 30 W	3.25	18 19.7	1.32
5853	Apr. 23	13 S, 14 W	2.98	19 33.4	1.06
5883	May 11	26 S, 37 E	3.06	14 59.5	1.34

* This is the only disturbance for which the record is incomplete. The exposure called 0 was at 17^h57^m. The next exposure called 1 was at 18^h19^m7, after which they follow at regular intervals.

valid since we have no assurance that the flocculi are level with the solar surface. However, this correction may be applied if desired simply by multiplying the areas by sec α, the projection factor, given in Table 1.

The estimated brightness of each flocculus was written on the diagram when it was drawn. In making the table, the areas of flocculi of equal intensity on the successive exposures were added together and the sum multiplied by their intensity; the integrated result for all the flocculi is given in the last column.

The intensities thus derived show irregular variations from one

TABLE 2

AREAS AND ESTIMATED INTENSITIES OF BRIGHT CHROMOSPHERIC DISTURBANCES

Mt. W. No.	Expos. No.	Estimated Intensity	Area	Integrated Intensities	Mt. W. No.	Expos. No.	Estimated Intensity	Area	Integrated Intensities
4921	0	3	406	12	5343	12	1	568	6
	1	2	304	6		13	1	203	6
	2	2	304	6			2	203	
	3	1	507	5		14	1	609	6
	4	1	203	2		15			
	5	1	162	2		16			
						17	1	609	6
5075	0	1	122	1		18	1	508	5
	1	2	243	5		19	1	406	4
	2	2	243	5		20	1	508	5
	3	1	203	2		21			
	4	1	203	2		22	1	406	4
	5	1	203	2		23	1	41	5
							2	243	
5172	0	2	406	8		24	2	406	8
	1	2	406	8		25	2	406	8
	2	1	466	5		26	2	446	9
	3	1	406	4		27	2	446	9
						28	1	122	9
5343	0	1	446	4			2	406	
	1	2	487	10		29	3	162	14
	2	2	406	8			2	467	
	3	2	406	8		30	2	203	8
	4	2	508	10			1	406	
	5	1	284	3		31	1	183	6
	6	1	406	4			2	203	
	7	1	406	4		32	2	162	5
	8	1	446	4			1	203	
	9	1	406	4		33	1	102	5
5343	0	1	609	6			2	183	
	1	3	406	12		34	1	406	4
	2	3	406	12		35	1	162	2
	3	1	61	5		36	1	122	1
		2	203			27	1	102	1
	4	1	61	8					
		2	365		5409	0	1	203	2
	5	1	162	6		1	1	345	22
		2	203				3	609	
	6	2	508	10		2	3	345	10
	7	2	508	10		3	2	406	8
	8	1	609	6		4	1	325	3
	9	1	751	8		5	1	244	2
	10	1	771	8		6	1	162	2
	11	1	609	6		7	1	142	1

TABLE 2—*Continued*

Mt. W. No.	Expos. No.	Estimated Intensity	Area	Integrated Intensities
5412	0	1	122	1
	1	1	406	4
	2	1	731	7
	3	1	73	15
		2	710	
	4	3	914	27
	5	3	914	27
	6	3	1015	30
	7	3	1015	33
		2	122	
	8	3	1015	30
	9	3	812	24
	10	3	710	22
		1	81	
	11	2	914	20
		1	162	
	12	1	244	17
		2	710	
	13	2	426	8
	14	1	447	7
		2	122	
	15	1	183	5
		2	183	
	16	1	304	3
	17	1	122	1
5453	0	3	609	18
	1	3	629	19
	2	3	508	15
	3	2	508	10
	4	2	508	10
	5	2	345	7
	6			
	7	1	386	4
	8	1	426	4
	9	1	244	2
	10	1	244	2
5453	0	1	589	12
		2	323	
	1	1	304	23
		2	406	
		3	406	
	2	1	304	38
		2	508	
		4	609	
	3	1	162	28
		2	710	
		3	406	
	4	1	122	24
		2	203	
		3	609	
5453	5	1	203	34
		2	203	
		3	934	
	6	1	406	28
		2	609	
		3	406	
	7	1	771	15
		2	365	
	8	1	690	15
		2	406	
	9	1	650	13
		2	304	
	10	1	609	12
		2	304	
	11	1	812	8
	12	1	508	5
	13	1	508	5
	14	1	609	6
5455	0	1	122	1
	1	2	914	18
	2	1	304	33
		3	1015	
	3	1	244	36
		3	1116	
	4	1	162	50
		2	203	
		4	1116	
	5	1	244	52
		2	244	
		4	1116	
	6	2	406	45
		4	914	
	7	1	365	44
		3	142	
		4	914	
	8			
	9	1	304	53
		4	1259	
	10	1	406	43
		4	974	
		1	81	
	11	2	304	47
		4	1015	
	12	1	406	37
		2	142	
		3	1015	
	13	1	81	38
		2	162	
		3	1116	

TABLE 2—*Continued*

Mt. W. No.	Expos. No.	Estimated Intensity	Area	Integrated Intensities
5455	14	1	102	35
		2	102	
		3	1056	
	15	1	162	36
		2	203	
		3	1015	
	16	1	81	31
		2	162	
		3	914	
	17	1	102	35
		2	304	
		3	914	
	18	1	122	31
		2	284	
		3	812	
	19	1	142	36
		2	122	
		3	1076	
	20	1	122	34
		2	122	
		3	1015	
	21	1	304	35
		2	812	
		3	508	
	22	1	183	26
		2	609	
		3	406	
	23	1	244	22
		2	954	
	24	1	771	16
		2	406	
	25			
	26	1	690	15
		2	406	
	27	1	508	11
		2	304	
	28	1	304	3
5578	0	1	609	6
	1	1	609	6
	2	3	548	16
	3	3	710	21
	4	3	609	18
	5	2	893	18
	6	1	710	7
	7	1	609	6
	8	1	568	6
5578	0	1	406	4
	1	1	914	9
5578	2	2	406	12
		1	406	
	3	4	1644	66
	4	4	1218	48
	5	4	1563	62
	6	3	2314	69
	7	3	1807	54
	8	3	1462	44
	9	2	1705	34
	10	2	1259	25
	11			
	12	1	1320	13
	13	1	1116	11
	14	1	914	9
	15	1	914	9
	16	1	508	5
	17	1	508	5
	18	1	508	5
	19	1	508	5
	20	1	508	5
5578	0	1	508	5
	1	1	1076	11
	2	1	203	12
		2	508	
	3	1	203	17
		3	508	
	4	1	244	19
		3	568	
	5	1	244	19
		3	568	
	6	1	284	24
		3	710	
	7	1	244	13
		2	508	
	8	1	710	12
		2	244	
	9	1	853	9
	10	1	609	10
		2	203	
	11	1	914	9
	12	1	609	11
		2	244	
	13	2	914	18
	14	3	1177	35
	15	3	1015	30
	16	3	954	29
	17	3	995	30
	18	2	812	24
		3	244	

TABLE 2—*Continued*

Mt. W. No.	Expos. No.	Estimated Intensity	Area	Integrated Intensities
5578.....	19	2	508	19
		3	284	
	20	1	508	9
		2	203	
	21	1	508	9
		2	203	
	22	1	467	10
		2	284	
	23	1	853	9
	24	1	853	9
	25	1	974	10
	26	1	1015	10
	27	1	1015	10
	28	1	914	9
	29	1	771	8
5716.....	0	1	183	2
	1	3	244	7
	2	1	102	10
		3	284	
	3	2	244	5
	4	1	61	5
		2	244	
	5	1	61	5
		2	244	
	6	1	61	7
		2	304	
	7	1	284	3
	8	1	406	4
	9	1	406	4
5726.....	0	2	183	22
		3	609	
	1	2	162	28
		3	812	
	2	2	162	25
		3	710	
	3	1	203	18
		2	203	
		3	406	
	4	1	122	14
		2	162	
		3	304	
	5	2	223	22
		3	568	
	6	2	609	12
	7	2	812	16
	8	2	589	12
	9	2	771	15
	10	2	771	15
	11	2	710	14
5726	12	2	365	19
		3	406	
	13	3	690	21
	14	3	914	27
	15	3	629	27
		4	203	
	16	1	122	32
		3	203	
		4	609	
	17	1	122	37
		2	142	
		3	244	
		4	629	
	18	1	1522	40
		2	203	
		4	528	
	19	1	1624	45
		5	568	
	20	1	1218	55
		2	304	
		5	731	
	21	1	710	45
		2	508	
		5	548	
	22	1	812	43
		2	304	
		4	710	
	23	1	1218	50
		4	934	
	24	1	1015	59
		4	1218	
	25	1	609	60
		2	243	
		4	1218	
	26	1	81	50
		2	162	
		3	183	
		4	1015	
	27	1	406	56
		2	244	
		4	284	
		5	710	
	28	1	142	57
		2	142	
		3	203	
		4	406	
		5	609	
	29	3	954	89
		4	568	
		5	751	

TABLE 2—*Continued*

Mt. W. No.	Expos. No.	Estimated Intensity	Area	Integrated Intensities
5726.....	30	1	203	56
		2	243	
		3	548	
		4	812	
	31	1	609	53
		2	203	
		3	609	
		4	609	
	32	1	406	59
		3	1015	
		4	609	
	33	1	406	67
		3	1015	
		4	812	
	34	1	406	70
		2	203	
		3	1116	
		4	710	
	35	1	203	61
		2	812	
		3	609	
		4	609	
	36	1	914	56
		3	1563	
	37	1	812	39
		3	1015	
	38	1	710	41
		3	1116	
	39	1	812	35
		2	406	
		3	609	
	40	1	710	33
		2	304	
		3	650	
	41	1	609	29
		2	406	
		3	508	
	42	1	203	22
		2	365	
		3	406	
	43	1	244	29
		2	406	
		3	609	
	44	1	203	29
		2	609	
		3	487	
	45	1	710	18
		2	568	
5726.....	46	1	812	16
		2	406	
	47	1	771	16
		2	406	
	48	1	710	15
		2	406	
	49	1	284	9
		2	284	
	50			
	51			
	52	1	508	12
		2	365	
	53	1	508	13
		2	406	
	54	1	1116	19
		2	406	
	55	1	710	15
		2	406	
	56	1	609	14
		2	406	
	57	1	304	11
		2	406	
	58	1	812	8
	59	1	710	7
	60	1	609	6
	61	1	609	6
	62	1	609	6
	63	1	508	5
	64	1	710	7
	65	1	710	7
	66	1	812	8
	67	1	812	8
	68	1	710	7
	69	1	1116	11
	70	1	914	9
	71	1	914	9
	72	1	812	8
	73	1	914	9
5853.....	0	1	914	9
	1	1	508	21
		2	812	
	2	1	629	20
		2	710	
	3	1	406	22
		2	914	
	4	3	812	24

TABLE 2—*Continued*

Mt. W. No.	Expos. No.	Estimated Intensity	Area	Integrated Intensities	Mt. W. No.	Expos. No.	Estimated Intensity	Area	Integrated Intensities
5853	5	1	122	30	5883	3	1	122	8
		2	203				2	345	
		3	812			4	1	142	10
	6	1	162				2	406	
		2	203	30		5	1	244	11
		3	812				2	406	
	7	1	102	27		6	1	162	11
		2	1320				2	487	
	8	2	1218	24		7	1	203	12
	9	1	142	25			2	487	
		2	1157			8	2	609	12
	10	1	162	26		9	1	284	13
		2	1218				2	508	
	11	1	102	29		10	1	244	11
		2	1421				2	447	
	12	1	406	24		11	1	243	12
		2	1015				2	487	
	13	1	304	25		12	1	61	9
		2	1116				2	406	
	14	1	304	23		13	1	203	11
		2	1015				2	447	
	15	1	304	27		14	1	203	11
		2	1218				2	447	
	16	1	1320	13		15	1	873	9
	17	1	1259	13		16	1	690	7
	18	1	1116	11		17	1	1157	12
	19	1	914	9		18	1	1056	11
	20	1	812	8		19	1	914	9
						20	1	812	8
5883.....	0	1	142	1		21	1	508	5
	1	1	142	5					
		2	203						
	2	1	122	9					
		2	406						

exposure to the next, which in most cases simply represents the difficulty of outlining the flocculi. In comparing these values with the radio data, principal emphasis should be placed on their general trend rather than on the short fluctuations. Another feature that may be somewhat misleading is that frequently after a disturbance has run its course a large area may still remain slightly brighter than the average for several hours. This makes the final value for the integrated intensity appear rather high, as if some activity were

still going on. Quite often the end was fixed arbitrarily, when no change was perceptible in the form or in the brightness of the flocculi.

III. QUANTITY OF ULTRAVIOLET EMISSION

Since the bright flocculi are prominent in the Balmer series from $H\alpha$ to $H\epsilon$, the most probable source of ionizing radiation is the Lyman series with its first member at λ 1215.6. From consideration of the transition probabilities involved, a reasonable estimate for the minimum intensity of Lyman α would appear to be about five times that of $H\alpha$.[2] Examination of the spectra of a large number of bright chromospheric disturbances taken during a previous investigation[3] shows that those called 2 and 3 on the I.A.U. scale or 3, 4, and 5 on the scale used here are about equal in brightness to the continuous spectrum near by. Taking the width of $H\alpha$ as $2A$, and the temperature of the sun 5740° K, the intensity of emission at $H\alpha$ for a black body is 1.35×10^7 ergs, making a lower limit for the intensity of Lyman α 6.75×10^7 ergs.

The atmosphere happens to be fairly transparent from λλ 1100–1300, so that light from Lyman α can penetrate to a considerable depth, as others have already pointed out in this connection.[4] The normal radiation in this spectrum interval for a black body is 2.67×10^5 ergs. From the table the largest area covered by the bright flocculi is about 2500 millionths of the sun's visible hemisphere. Hence, on the basis of these assumptions, the total radiation through this atmospheric "window" during a disturbance of more than average brightness should be 60 per cent greater than normal.

CARNEGIE INSTITUTION OF WASHINGTON
MOUNT WILSON OBSERVATORY
May 1939

[2] Conversation with Dr. R. Minkowski.

[3] *Mt. W. Contr.*, No. 606; *Ap. J.*, **89**, 347, 1939.

[4] *Nature*, **140**, 603, 1937.

NEW IDENTIFICATIONS OF *Fe* III IN THE SPECTRA OF EARLY B STARS

P. SWINGS, B. EDLÉN, AND J. GRANDJEAN

ABSTRACT

Starting from their laboratory measurements, the authors are able to show that about one hundred lines observed in the spectra of early B-type stars are due to *Fe* III. The ionization potential of *Fe* III is 30.48 volts.

1. In a previous paper[1] several *Fe* III lines of the astronomical region were computed, beginning with a term analysis of the *Fe* III spectrum in the far ultraviolet region: these lines were found to be prominent in early B-type stars. We have now investigated the vacuum-spark spectrum of iron, with a large quartz spectrograph (Hilger E.1), from λ 2000 through the visible region. The spark was obtained by discharging 0.4 μF at about 60,000 volts through a spark gap of 1 mm, a few sparks being sufficient for an exposure. The spectrum is extremely rich in lines. After removing *Fe* I and *Fe* II from the measurements, some three thousand lines remain in the region above λ 2975. The very high stages of ionization were suppressed by means of a large induction coil, but *Fe* IV and, probably, *Fe* V are also excited in the spark. Considering the spectral structure of the various ions, however, it is not likely that stages higher than *Fe* III will be prominent in this region, and most of the lines measured in the astronomical region are certainly of *Fe* III origin.

Although the term analysis is not yet quite complete, the measured wave lengths enable us to identify with certainty many unexplained lines of early B-type stars. This identification work constitutes the main subject of the present paper.

We shall examine successively the identifications of absorption lines in the ultraviolet, the ordinary photographic, and the visual regions of the early B-type spectra. Next we shall consider the spectra of Be and P Cygni stars.

[1] Swings and Edlén, *Ap. J.*, **88**, 618, 1938.

2. *Ultraviolet region of the early B-type stars.*—A good list has been published by W. S. Adams and Theodore Dunham, Jr.,[2] covering the region between λ 3000 and λ 3600. It happens that strong *Fe* III lines appear in this region and give reliable identifications of fairly strong absorption lines, namely, the group of prominent unidentified lines at λλ 3266.9, 3276.2, and 3288.9; Adams and Dunham had

TABLE 1

Laboratory Wave Length and Intensity	Mean Stellar Wave Length	Intensity in—				Previous Identification	Notes
		βC Ma (cB1)	εC Ma (B1)	χ² Ori (cB1)	γ Peg (B2)		
3086.31 (6)	86.4	5	5	8	6	86.3 *Si* III	1
3136.43 (10)	36.5	1	2	.....	.....	.....	4
3174.09 (10)	74.1	1	2	.....	.....	.....	5
3176.00 (10)	76.0	2	1	2	.....	.....	5
3178.03 (10)	78.05	1	1	.....	.....	.....	5
3198.81 (5)	98.9	1	.....	1	.....	98.6 *Ne* II	
3218.34 (6)	18.2	1	.....	.....	.....	18.2 *Ne* II	
3266.88 (20)	66.95	3	2	4	3	.....	2, 3
3276.08 (15)	76.25	3	2	2	2	.....	2, 3
3280.58 (6)	80.5	.....	.....	1	.....	.....	3
3288.81 (15)	88.9	2	.....	2	.....	.....	2, 3
3305.22 (10)	05.2	2	2	2	.....	05.2 O II	3
3339.36 (10)	39.4	1	.....	1	.....	.....	3
3360.84 (6)	60.6	1	.....	.....	.....	60.7 *Ne* II	
3367.02 (6)	67.2	2	.....	1	.....	67.2 *S* III	
3586.12 (9)	86.05	1	.....	.....	1	.....	6
3600.93 (10)	00.9	1	.....	.....	.....	.....	6
3603.88 (9)	03.95	2	.....	1	.....	.....	6

1. *Fe* III minor contributor.
2. Group of prominent unidentified lines suggested, by W. S. Adams and Th. Dunham, to be due to the same element.
3. Multiplet $a^5F - z^5G^o$; low excitation potential, 10.3 volts.
4. Multiplet $a^3F - z^3D^o$; low excitation potential 11.2 volts.
5. Multiplet $a^3F - z^3G^o$.
6. Multiplet $a^3F - z^3F^o$.

actually suggested that these three lines are probably due to the same element. The identifications are summarized in Table 1. No very strong line of *Fe* III appears in the region λλ 3604–3964.

3. *Photographic region of the early B-type stars.*—For the region λ 3900 to λ 4700 we possess very good lists of wave lengths by O. Struve,[3] O. Struve and Theodore Dunham, Jr.[4] (τ Sco), R. K. Mar-

[2] *Ap. J.*, **87**, 102, 1938. [3] *Ap. J.*, **74**, 225, 1931. [4] *Ap. J.*, **77**, 321, 1933.

shall,[5] and, recently, H. Kühlborn.[6] The comparison of the laboratory data with the stellar wave lengths and intensities is based essentially on Kühlborn's extensive and excellent table. Of course, there appear many wave-length coincidences, several of which have a physical meaning. But for the weak laboratory lines the chance coincidences are very numerous. A detailed and complete discussion is not feasible before a more advanced term classification is performed. In fact, the general procedure here has been:

a) To examine first the lines of laboratory intensity greater than 5 (on our arbitrary scale). The corresponding identifications are probably certain.

b) Next, to examine the lines of laboratory intensity 5. It seems possible that a few identifications are somewhat doubtful. Within the region concerned, no vacuum-spark line of intensity greater than 5, and hardly any of intensity 5, are missing in Kühlborn's list.

c) To examine, finally, the lines of laboratory intensity 4 in γ Pegasi only (except when observed by Struve in γ Peg and not by Kühlborn in that star), in order to reduce the number of chance coincidences. Even so, there may still be a few purely chance coincidences.

No line of intensity weaker than 4 has been considered, although there seem to be good reasons to believe that several lines of laboratory intensity 3 or 2 are present in γ Peg. This part of the investigation will be performed later, when a more advanced term classification will be available.

Table 2 summarizes the results. The notations used are: column 3: K_1, from the list of lines in ζ Persei by Kühlborn; K_2, from the list of lines in γ Orionis; K_3, from the list of lines in ζ Cassiopeiae; S, from the list by Struve; SD, from the list by Struve and Dunham; M, from the list by Marshall; B, from the list by Baxandall;[7] column 4 (notations used by Kühlborn): a, major contributor (50–100 per cent); b, contributor from 20–50 per cent; c, contributor from 5–20 per cent; a?, major contributor unknown. The intensities are from γ Peg. References to the tables by H. H. Plaskett,[8] Pillans,[9] and

[5] *Pub. U. of Michigan Obs.*, **5**, 137, 1934.

[6] *Veröff. Babelsberg*, **12**, Heft 1, 1938.

[7] Solar Physics Committee, 1914.

[8] *Dom. Ap. Obs.*, **1**, 325, 1922.

[9] *Ap. J.*, **80**, 51, 1934.

TABLE 2

Laboratory Wave Length and Intensity	λ and Intensity in γ Peg, According to Kühlborn	Other Observations	Previous Identifications (in Kühlborn's Table)	Notes
3964.11 (5) 3964.44 (3)	64.24 (1–2)	.....	a?	
3968.78 (8)	68.78 (1–2)	M 68.41 (3)	a?; ? *C* II 8.63 (00)	
3975.13 (4)	75.17 (2–3)	K_1 75.29; ? M 74.58 (1)	a?; ? *Fe* II 5.03 (1)	
3978.43 (4)	.....	K_1 78.39; S 78.30 (1)	*P* III 8.27 (9)	
3979.42 (5)	.....	K_1 and K_2 79.58	*Ar* II 9.36 (7); *S* II 9.86 (3)	
3993.15 (5)	93.16 (1)	S 93.33 (1); M 93.61 (2 in δ Cet)	a?	
4000.83 (4)	00.86 (2–3)	K_1 and K_2 00.83	a?	
4002.36 (4)	02.40 (1)	K_2 02.38	a?; ? *Fe* II 2.55 (3)	
4003.41 (4)	03.51 (1–2)	K_2 03.40	a *Ca* III ? 3.35 (5); a *N* III 3.64 (4)	
4008.81 (5)	08.76 (2–3)	.....	a?	
4022.36 (4)	22.24 (3–4)	K_1 and K_2 22.35	a?	1
4035.54 (4)	35.384 (3–4)	K_1 35.52; S 35.12 (2)	a?; b *Ar* II 5.47 (6)	1, 2
4039.12 (3s)	39.03 (1–2)	K_1 and K_2 39.02; S 9.24 (1)	a?	3
4044.05 (4)	44.05 (3–4)	K_2 43.94	a?	1
4053.28 (5)	53.12 (4–5)	S 53.08 (1)	a?	1, 2
4057.51 (4)	57.46 (2)	.....	a *P* III 7.39 (4)	
4066.11 (4)	66.10 (1–2)	.....	a?	
4081.19 (7)	81.29 (1)	S 81.01 (1); SD 1.1 (1); M 1.38 (2 in δ Cet)	a?	2
4085.53 (4)	85.47 (3)	M 85.24	a?; ? *P* 5.55 (1)	
4103.15 (4)	03.02 (6)	.....	a *O* II; etc.	4
4109.95 (5?)	09.86 (2)	K_2 10.06	a *Ca* II 9.83 (1); a *N* I 9.98 (12)	
4113.23 (7) 4113.45 (7)	13.26 (1–2)	.....	a?	
4115.74 (4)	15.63 (2)	.....	a?	
4118.57 (8)	18.72 (3)	.....	a?; ? *P* II 8.96 (2)	
4120.02 (4)	20.18 (4–5)	K_1 and K_3 20.15	a *O* II 0.28 (5); b?	
4120.97 (8)	20.84 (3d)	.....	*He* I	4, 9
4121.31 (6)	21.51 (3)	.....	a *O* II 1.47 (4)	
4122.06 (8)	22.01 (2–3)	K_1 21.99	a *B* II 1.95 (7); a *C* III 2.05 (3)	5, 9
4122.98 (8)	22.84 (3–4)	S 22.75 (1); M 22.68 (2 in δ Cet)	a?	9
4136.95 (4) 4137.30 (2)	37.10 (1–2)	.....	a?	
4137.93 (8)	37.81 (4)	S 37.72 (2); M 37.50 (2 in δ Cet)	a?; ? *N* I 7.63 (7)	9
4139.37 (7)	39.37 (2–3)	? S 39.79 (1)	a?	9

TABLE 2—*Continued*

Laboratory Wave Length and Intensity	λ and Intensity in γ Peg, According to Kühlborn	Other Observations	Previous Identifications (in Kühlborn's Table)	Notes
4140.51 (6)	40.45 (1–2)	S 40.82 (1); M 40.48 (2 in βC Ma); SD 0.6 (1)	a?	9
4145.74 (5)	45.48 (1–2)	K_1 45.47; M 45.90 (2 in β Cep)	.....	
4146.82 (4)	46.94 (1)	K_1 and K_2 46.90	a *S* II 6.94 (3)	
4154.98 (8)	54.83 (1)	S 55.09 (1); B 4.8 (1)	a *N* II 5.0 (00*n*)	5
4161.39 (4)	61.28 (1–2)	.....	a?	
4164.79 (20)	64.76 (7)	K_1, K_2, and K_3 64.80; S 64.78 (3); SD 64.81 (3); M 64.71 (3 in δ Cet); B 64.8	a?; ? *S* III 4.96 (0)	6, 9
4166.86 (9)	66.82 (5–6)	S 66.90 (1); SD 6.70 (1); M 6.93 (1); etc.	a?; c *P* II 6.73 (3)	9
4168.41 (4)	68.43 (3)	K_1 68.30	a *S* II 8.41 (5); b *Al* II 8.42 (1); c *Al* II 8.51 (0.5)	9
4174.27 (10)	74.26 (2)	S 74.12 (1); M 74.06 (2 in δ Cet)	a *S* II 4.30 (6)	5
4176.79 (4)	76.80 (2)	K_1, K_2, and K_3 76.84	a?	
4179.25 (5)	.....	K_2 79.21 (1)	*Ar* II 9.31 (5)	
4182.02 (4)	82.11 (2)	K_1 and K_2 82.18; M 82.09 (1 in δ Cet)	a *S* III 2.14 (00); a?	
4184.09 (4)	84.23 (2)	K_1 and K_2 84.27	a *Ca* III ? 4.29 (8)	
4186.50 (4)	86.46 (1–2)	K_2 and K_3 86.46; S 86.83 (1); M 86.85	a?; b *K* II 6.23 (9)	
4189.10 (7)	89.21 (2)	S 88.74 (1)	a *P* III 9.08 (3); b?	
4193.98 (4)	93.96 (1–2)	K_1 93.95	a?	
4200.06 (6)	99.98 (2–3)	K_1 and K_3 99.86; M 00.21 (1 in β Cep)	a *N* III 0.02 (6); ? *He* II, *Ar* II, *Ti* III ?	
4200.38 (6)	00.37 (2)	K_2 00.47	a?	
4203.91 (5)	03.86 (1)	K_3 03.89	a?	
4210.87 (10)	10.74 (1–2)	K_2 10.77; ? S 11.36 (1)	a?; ? *P* 0.8 (0)	
4220.32 (5)	20.22 (3)	S 20.07 (1 in δ Cet); M 20.08 (1 in δ Cet)	a?; b *Ca* II 0.13	
4222.39 (8)	22.27 (2–3)	K_2 and K_3 22.19; S 22.36 (2); SD 22.04 (1)	a *P* III 2.15 (7); b?	
4230.52 (4)	30.62 (1)	S 30.76 (1)	a?	
4235.54 (10)	35.67 (2.3)	K_2 35.48	.....	
4238.78 (5)	38.55 (3)	K_2 38.46; S 38.83 (1)	a?	
4243.85 (8)	43.92 (1)	K_2 43.9; S 43.84 (1); M 44.09	a?; ? *Ne* II 4.17 (0)	

TABLE 2—*Continued*

Laboratory Wave Length and Intensity	λ and Intensity in γ Peg, According to Kühlborn	Other Observations	Previous Identification (in Kühlborn's Table)	Notes
4249.95 (7)	.....	K_1 and K_2 50.00; SD 9.83 (1)	*S* II 9.92; ?	
4253.62 (4)	53.63 (3–4)	S 53.66 (3); M 53.88 (2)	a *S* III 3.59 (9); a *O* II 3.74 (4)	4
4255.20 (5)	.....	K_1 and K_2 54.96	a?; *S* II 5.01 (0)	
4261.46 (4)	61.41 (2–3)	M 61.56	a?	
4263.52 (4)	63.52 (1)	S 63.81 (1 in δ Cet); M 63.67 (2)	a?; ? *K* II 3.31 (7)	
4263.94 (4)				
4271.47 (6)	71.63 (1–2)	S 71.78 (1); M 71.74 (2 in δ Cet)	a?; ? *P* III 1.85 (1); ? *Ca* III ? 1.87 (7)	
4273.43 (5)	.....	K_3 73.44 (3); S 73.35 (1 in γ Peg); M 73.19 (1 in γ Peg)	a?	
4286.13 (10)	86.2 (2)	S 86.24 (1)	a?; ? *C* II 5.96 (1)	
4291.11 (4)	91.26 (2)	? S 91.48 (2 in βC Ma)	a *O* II 1.22 (2); c *S* II 1.45 (1); c *P* III 1.1 (1)	
4296.86 (—)*	96.93 (3)	K_2 97.04; S 96.54 (1)	a?; b *Ne* II 6.96 (0)	
4304.81 (10)	04.79 (2–3)	K_1 and K_2 04.83	a?; a *K* II 4.94 (3)	5
4310.37 (12)	10.31 (1–2)	K_3 10.22; SD 10.39 (1); S 10.54 (1)	a?	
4352.70 (4)	52.48 (1–2)	S 52.47 (1)	a?; ? *Ar* II 2.23	8
4365.56 (3)	65.66 (1)	K_1 65.6	a *Ne* II 5.72 (2)	8
4372.41 (20)	72.404 (5)	K_1, K_2, and K_3 72.33; S 72.30 (2); SD 2.69 (1); M 2.30 (2)	a?; b *C* II 2.49 (4); ? *Si* 2.33	6
4372.88 (—)	72.85 (1–2)	.....	a?	
4395.78 (6)	95.80 (4)	K_2 95.85; S 95.88 (2); M 95.86 (2)	a *O* II 5.94 (4); a?	8
4419.59 (10)	19.601 (3)	K_2 19.55; S 19.62 ( ); M 19.67 (1 in βC Ma); SD 19.97 (1); B 9.4 (1–2); etc.	a?	8
4422.5 (5 bl.)†	22.33 (2)	K_2 22.31; M 22.53 (2 in δ Cet)	a?	
4430.95 (7)	31.08 (2)	S 31.03 (2); SD 30.99 (2)	a *Ar* II 1.02 (8); b *S* II 1.02 (1)	8
4447.86 (5 bl.)†	47.78 (2)	.....	a *Al* II 7.8 (3)	
4483.48 (4)	83.43 (2)	K_1 and K_2 83.38; S 83.24 (2)	a *S* II 3.42 (6); c *P* II 3.66 (4)	
4483.91 (4)	84.07 (2–3)	K_2 84.10; SD 83.93 (1)	a?	

* Part of blending with *Fe* II of total intensity 12.

† Part of blending with *Fe* I of intensity 5.

TABLE 2—*Continued*

Laboratory Wave Length and Intensity	λ and Intensity in γ Peg, According to Kühlborn	Other Observations	Previous Identifications (in Kühlborn's Table)	Notes
4535.50 (5)	35.88 (1–2)	.....	a?; a *S* IV 5.69 (4); ? *S* II 5.7 (00)	7
4545.16 (4)	45.21 (1)	SD 44.9 (1)	a *Ar* II 5.08 (10); b *P* III 4.97 (3)	
4559.09 (6)	59.25 (1–2)	K_2 59.3; B 59.3 (2); M 58.77 (2 in βC Ma)	a?	
4570.34 (4)	70.24 (2)	.....	a?	
4573.14 (5)	72.84 (3–4)	K_2 73.0 (1); SD 73.05 (1)	a?	
4581.58 (4)	81.66 (3)	K_2 81.7 (2)	a *P* II 1.76 (5); b?	
4591.84 (4)	91.98 (2)	K_2 91.9 (1); SD 92.19 (1); S 92.27 (2)	a?	
4694.57 (4)	94.67 (1–2)	K_2 94.4; S 94.67 (1)	a *N* II 4.55 (3)	

1. *Fe* III is probably not the only contributor.
2. Multiplet $5p^7P^o-6s^7S$; low excitation potential, 20.5 volts.
3. Sharp line (impurity?).
4. *Fe* III minor contributor.
5. *Fe* III important contributor.
6. The two strongest unidentified lines in the early B-type stars.
7. Doubtful identification.
8. Previously published; predicted $a^5P-4p^5P^o$ multiplet; low excitation potential, 8.2 volts.
9. Multiplet $5p^7P^o-5d^7D$.

Losh[10] seemed superfluous in connection with the present work and have therefore been omitted.

4. *Visual region of the early B-type stars.*—The lists of stellar absorption lines in the visual region of the early B-type stars[11] are still of a rather preliminary character. It is not impossible that the two lines measured by Marshall in γ Ori at 5001.36 (5) and 5127.51 (4) are actually the *Fe* III lines at 5002.02 (8) and 5127.32 (6), but these identifications are only provisional. In the vacuum spark a large number of fairly strong *Fe* III lines appear from λ 5000 to λ 6200, including the multiplets $a^5D - 4p^5P^o$, $4d^7D - 5p^7P^o$, $5s^7S - 5p^7P^o$, and, probably also, $4d^5D - 5p^5P^o$ and $5s^5S - 5p^5P^o$, which should all be found in suitable stellar spectra.

[10] *Pub. U. of Michigan Obs.*, **4**, 1, 1932.

[11] Marshall, *Ap. J.*, **82**, 97, 1935.

TABLE 3

Be STARS

Laboratory Wave Length and Intensity	Wave Length and Intensity in—		Previous Identifications	Notes
	γ Cass (Baldwin)	BD+11°4673 (Merrill)		
4352.7 (4)	.....	52.7 (0)	52.80 [*Fe* II]	1
4372.40 (20)	72.55 (0.3)	72.1 (0)	? 72.46 [*Fe* II]	
4382.5 (comp.)	82.63 (0.3)	.....	.....	1, 2
4395.78 (6)	95.60 (0)	96.0 (0)	.....	2
4419.59 (10)	19.57 (1)	19.8	.....	2
4430.95 (7)	.....	30.94 (0)	.....	
5157.85 (4)	.....	58.1 (0)	? 58.05 [*Fe* II]	1

1. Identification rather doubtful.
2. Previously published.

TABLE 4

P CYGNI

Laboratory Wave Length and Intensity	Absorption Line	Emission Line	Notes
3600.93 (10)	99.56 (3)	00.88 (3)	
3603.88 (9)	02.51	03.49 (2)	
4039.12 (3 s)	37.13 (2)	38.74 (1)	
4164.79 (20)	.....	64.07 (3)	
4352.7 (4)	.....	52.07 (2)	2
4372.41 (20)	72.66 (1)	.....	
4382.5 (comp.)	82 (1)	83.07 (3)	2
4419.59 (10)	17.42 (7)	19.24 (5)	2
4430.95 (7)	29.04 (4)	30.91 (3)	2
4940.46 (4)	38.01	.....	1
5073.78 (3)	71 (1)	.....	2
5100.7 (10)	97 (1)	.....	
5127.32 (6)	25 (2)	27 (2)	2
5155.97 (4)	54 (3)	56 (3)	1
5193.90 (4) / 5194.43 (4)	92.3 (1–2)	.....	3

1. Identification rather doubtful.
2. Previously published.
3. Observed by E. K. Kharadse, *Zs. f. Ap.*, 11, 304, 1936.

5. *Fe* III *lines in the spectra of Be and P Cygni stars.*—The lists of wave lengths considered are due to P. W. Merrill (BD+11°4673)[12] and R. B. Baldwin (γ Cass)[13] for Be stars and to O. Struve[14] (for P Cygni). Our results are summarized in Tables 3 and 4.

In connection with this question it may be noticed that *Fe* III offers a typical example of absorption lines starting from both metastable and non-metastable lower levels. This may be of interest in discussions concerning extended atmospheres.[15]

6. *The ionization potential of Fe* III.—The septet and quintet systems are now connected by intercombination lines. From three members of the ns^{7}S series a Ritz formula gives the ionization potential of *Fe* III as 30.48 volts, which is in close agreement with our previous estimate,[1] 30.3 volts.

DEPARTMENT OF ASTROPHYSICS, UNIVERSITY OF LIÉGE
AND
DEPARTMENT OF PHYSICS, UNIVERSITY OF UPSALA

May 1939

[12] *Ap. J.*, **69**, 330, 1929. [13] *Ap. J.*, **87**, 573, 1938. [14] *Ap. J.*, **81**, 73, 1935.

[15] See Struve, *Astronomical Symposium of Western Reserve Academy*, p. 52, Hudson, Ohio, 1938.

MAGNITUDES AND COLORS IN THE GLOBULAR CLUSTER MESSIER 4

JESSE L. GREENSTEIN

ABSTRACT

Magnitude sequences have been established in the giant-poor globular cluster, M 4, in both the photographic- and the red-magnitude systems. Each sequence involves two completely independent determinations. The magnitudes and colors of 660 stars in the cluster, to absolute magnitude (red) +1.4, have been measured and are given in Table 12. The cluster is found to be reddened by +0.8 mag. by the dark nebulosity in Scorpio-Ophiuchus. After correction for absorption the distance of the cluster is 1900 parsecs, the closest to the sun of the globular clusters. The color-magnitude array for the cluster stars, given in Figure 1, is similar to those found by Shapley. There is a peculiar group of blue stars near absolute-magnitude zero, distinguishing the cluster from galactic clusters and from field stars in the galaxy. Subgiants are very abundant, but bright main-sequence stars are completely absent. The cluster-type variables are similar to those in the galactic field; two longer-period variables are found to be very red. The frequency function of the magnitudes is analyzed, and various statistical properties are derived. The space distribution of fainter cluster stars is investigated by means of star counts. The expected velocity dispersion is found to be near 11 km/sec.

Messier 4, NGC 6121 ($\alpha = 16^h18$, $\delta = -26^\circ.3$), is one of the largest and most open of the globular clusters. It is also one of the small giant-poor class; the relatively small number of bright cluster stars makes it especially suitable for an investigation of the magnitudes and for statistical studies. Fast modern panchromatic plates lend themselves to the determination of color indices of faint stars. The work of Dr. Harlow Shapley on color-magnitude diagrams[1] for the brighter cluster stars can now be extended by using the Harvard photored-magnitude system established by C. Payne Gaposchkin.[2] The present investigation involves a determination of the magnitudes and colors of all cluster stars to absolute magnitude +1.0. It is hoped to extend the magnitude scales to fainter stars and to supplement the present data with determinations of the spectral types and radial velocities of the brighter stars.

OBSERVATIONAL TECHNIQUE

The fundamental standards for the magnitudes of faint stars are in the northern sky; the cluster M 4 is too far south for accurate

[1] See *Star Clusters*, Cambridge, 1930, for all detailed references to original publications of Shapley and collaborators.

[2] *Harvard Ann.*, **89**, No. 5, 1935; No. 8, 1937.

work in the northern observatories. As a result, it was necessary to establish blue- and red-magnitude sequences in the cluster in several steps, which will be briefly outlined. A total of seven series comparisons of the cluster with Harvard standard regions, available in the Harvard Observatory plate collection, were used to determine magnitudes of 77 cluster stars. These magnitudes are accurate to $14^{m}.0$ and are required as confirmation of the zero point of the photographic scale. Three direct comparisons of M 4 with the North Polar Sequence were also available. These plates were taken with the 60-inch reflector at Mount Wilson by Dr. Shapley and are used in this work with his kind permission. Because of the great zenith distance of the cluster these plates are used only to determine the scale from $14^{m}.0$ to $16^{m}.8$. The material is insufficient beyond $16^{m}.0$. Precaution was taken to remove the effect of color and the distance correction from the Harvard refractor material. The distance correction of the reflector plates was investigated and was found to be similar to that given by Seares.[3] The final photographic-magnitude sequence contained 71 stars from $10^{m}.9$ to $16^{m}.8$; some fainter stars were added subsequently.

The photographic magnitudes of a total of 866 stars were then determined. All stars to $15^{m}.6$, photographic within $13'.5$ from the center of the cluster, were measured, as well as fainter stars, complete to $16^{m}.3$ in two ring zones at $2'.2$ and $4'.5$ from the center. Magnitudes for the brighter stars were measured on four 60-inch Mount Wilson reflector plates taken by Dr. Shapley and on four plates taken with the 24-inch Bruce refractor at Arequipa. Magnitudes for fainter stars in the crowded central zones were also measured on two plates taken by Dr. Duncan with the 100-inch reflector at Mount Wilson and very kindly lent to Dr. Shapley and the author. Measures were made with a graduated scale of stellar images, the quality and definition of which matched the images on the plate. All magnitudes were combined with equal weight in the formation of a preliminary catalogue; the number of measures varied from three to ten per star, with an average of six. The sequence stars were measured in the course of the systematic *Durchmusterung* of each plate, and their magnitudes were rederived to ascertain whether the meas-

[3] *Mt. Wilson Contr.*, No. 80, 1914.

ures did, in fact, yield magnitudes on the same system as the original sequence. The mean residuals are found to be satisfactorily small, and no dependence on distance was found, so that the measured magnitudes are essentially on the same scale as the sequence stars. The mean error of a magnitude for one plate is ± 0.09 mag.; the average mean error of a final magnitude is not far from ± 0.04 mag.

A complete independent redetermination of the photographic-magnitude scale was made with the 36-inch reflector at the Steward Observatory of the University of Arizona. Eleven series comparisons of M 4 with Selected Areas 133, 135, and 136 were obtained. The magnitudes of 102 stars were thus determined on an average of seven plates and were then compared with the preliminary catalogue magnitudes. It was found that a scale difference existed which amounted to $+0.2$ mag. at $12^m.5$ and to -0.2 mag. at 17^m. The result is not unexpected, since only one Mount Wilson polar comparison goes beyond 16^m. The Steward Observatory material is not as dependable as the Harvard refractor material for the brighter stars. After proper weighting, a set of systematic corrections to the catalogue was derived, and has been included in the final photographic magnitudes given in Table 12.

The red-magnitude scale is based on the Harvard photored magnitudes[2] which have been established to $11^m.5$ at the North Pole and in Harvard standard regions. The Eastman I-C Special plates were used, in combination with a Wratten No. 28 filter; the effective wave length is close to λ 6300. The scale in Harvard standard region C12 (23^h, $+15°$) has been extended to 15^m by means of grating plates taken with the 24-inch reflector at Oak Ridge. The grating constant (2.42 ± 0.06 mag.) was determined by means of known red magnitudes in the Pleiades[4] and in the Harvard standard regions and by the method of disappearing orders. Eight plates were used to give the red scale to $13^m.5$, and five in the range to $14^m.5$; the scale is poor beyond that point. A sequence of 33 stars was established, with accidental errors of ± 0.05 mag.; the total uncertainty at $15^m.0$ arising from the grating constant should be of the order of ± 0.15 mag. This sequence was used to establish red magnitudes of the se-

[4] C. P. Gaposchkin, *Harvard Ann.*, **89**, No. 2, 1932.

quence stars in the cluster by means of eight series comparisons taken by Dr. Paraskevopoulos with the 60-inch reflector at Bloemfontein. The zero point could also be checked by four series comparisons with the 24-inch reflector at Oak Ridge, using Harvard standard regions C6, C9, C10, and C11. A red-magnitude sequence was established in the cluster over the range 9^m6–14^m7 and was used as a basis for the systematic *Durchmusterung* of the cluster stars. The measurement was carried through as before for 866 stars in the catalogue, on seven reflector plates (taken at Bloemfontein) and two 24-inch Bruce refractor plates. The number of measures varies from two to eleven per star, with an average of five. The mean errors are nearly the same as in the case of the photographic magnitudes; they average ± 0.05 mag. for a final determination on the red scale.

A complete rederivation of the red-magnitude scale was made by means of plates taken with the 36-inch reflector at the Steward Observatory. The zero point was redetermined by means of five series comparisons with Harvard standard regions C7, C9, and C10, using stars to 12^m0; the correction was found to be small, i.e., $+0.06 \pm 0.02$ mag. Eight direct exposures on Harvard standard regions (red) and Selected Areas (blue) were used to determine the grating constant of an objective grating built by L. Stoddard. Three long-exposure grating plates were then obtained to extend the red scale from 12^m0 to 14^m4. The magnitudes of 72 stars were thus determined and compared with the catalogue magnitudes. This yielded, finally, a systematic correction which ranged from $+0.06$ to $+0.20$ mag. The corrections have been applied to the red magnitudes given in Table 12. Because of the lack of sufficient data for stars fainter than 14^m4, they have been omitted from the catalogue and the discussions. It is hoped to extend this investigation to fainter stars. The catalogue contains 660 stars for which the magnitude scales and the measured magnitudes are of high weight.

The variable stars discovered by Miss Sawyer[5] were included in the regular measurement of the cluster. Their mean magnitudes are given in the catalogue. Several stars were suspected of variability because of large residuals. An unfortunate distribution in time of the plates measured makes it undesirable to use the residuals in a

[5] *Harvard Circ.*, No. 366, 1931.

search for new variables. The number of undiscovered variables is probably small, and no indication of variation was found for any star fainter than the cluster-type variables.

THE CORRECTION FOR SPACE REDDENING

Before discussing the color-magnitude diagram of the cluster, correction must be made for the effect of interstellar absorption on the magnitudes and colors of the cluster stars. Space reddening will result in a shift of the zero point of the relation between color and spectral type. The cluster lies behind a region of irregular clouds of obscuring material connected with the dark nebula in Scorpio-Ophiu-

TABLE 1

STAR COUNTS NEAR M 4

m_{pg}	log A_m	
	Normal Region	Cluster
10.5	0.95	0.53
11.5	1.27	0.65
12.5	1.62	1.03
13.5	1.91	1.26

chus. The surface density of stars varies sharply across the region of the cluster, and consequently the use of star counts for the determination of the total absorption in the dark nebula is subject to some uncertainty.

Star counts were made to various magnitude limits in fields surrounding the cluster in which no dark nebulae could be detected. A total area of 3 square degrees was counted. These fields were at a mean galactic latitude of $+11°$, and the counts were transformed to hypothetical counts at the latitude of the cluster. An area of 2 square degrees outside of, and immediately surrounding, the cluster was counted. The final adopted counts, A_m, in the normal and the obscured areas are given in Table 1, in terms of the number per square degree between $m+0.5$ and $m-0.5$. It is possible that the counts at $13^m.5$ are affected by the cluster stars at considerable distances from the center.

The absorption is large at the tenth magnitude, so that the dark nebula is probably less than 150 parsecs distant. The run of the counted numbers in the obscured area approximately parallels that in the normal area and corresponds to a photographic absorption of about 2 mag. The star counts in the normal region are probably affected by the general absorption covering the Scorpio-Ophiuchus region, as shown in the star counts of Lindsay and Bok.[6] We may estimate that the total obscuration in front of the cluster is at least 2.5 ± 0.5 mag., if we assume that there is no absorbing material beyond the Ophiuchus dark nebula. If the interstellar extinction coefficient varies as λ^{-1}, then this photographic absorption corresponds to a reddening of 0.75 mag. on the red index scale.

A measure of the reddening of the integrated light of the cluster is available in the data of Stebbins and Whitford.[7] The mean intrinsic photoelectric color of the three giant-poor clusters, NGC 4147, 5466, and 7492, is -0.17 ± 0.04 mag., when corrected for the general reddening given by the cosecant relation. M 4 has a color of +0.05 mag., so that the reddening is $+0.22 \pm 0.05$ mag. After conversion to the red index scale, we obtain a reddening of $+0.78 \pm 0.18$ mag. A similar estimate can be obtained from the color indices of globular clusters given by Vyssotsky and Williams.[8] No measures of unreddened giant-poor clusters are included, but their data indicate that the color excess is at least $+0.7 \pm 0.1$ mag.

An indirect estimate of the reddening may be obtained from the color of the bluest stars in the cluster field. If any field stars behind the dark nebula have been measured in the course of the survey of the cluster, we may obtain an upper limit to the reddening by assuming that the stars are intrinsically very blue—for example, B stars with true red indices of the order of −0.4 mag. The two bluest stars that occur in regions of the color-magnitude diagram in which cluster stars are infrequent are found to have colors of +0.57 (at 11^m1) and +0.53 (at 14^m4). The maximum reddening may consequently be assumed to be +1.0 mag.

Another estimate of the reddening can be obtained from the colors of the cluster-type variables in M 4. The difference between the

[6] *Harvard Ann.*, **105**, No. 14, 1937.

[7] *Ap. J.*, **84**, 132, 1936.

[8] *Ap. J.*, **77**, 301, 1933.

red and the blue median magnitudes of 28 cluster-type variables is $+0.93 \pm 0.06$ mag. There is no available series of measures of the true red colors of the galactic cluster-type variables. If we adopt a median spectral type[1] of A7, we obtain a predicted red index of $+0.12$ mag. Shapley has measured the median yellow index[1] of the variables in M 3, M 5, and M 15, which he gives as $+0.33$; this is equivalent to $+0.14$ on the red scale. The reddening of the variables in M 4 may be estimated as $+0.80$ mag., with an uncertainty of ± 0.1 mag.

The results of these very different methods of estimating the reddening of the cluster stars are essentially accordant. We shall arbitrarily adopt the value of $+0.8$ mag., obtained after weighting the various values, as the reddening of the cluster. The error should not be larger than ± 0.1 mag., a quantity of the same order as the total photometric uncertainty of the zero point of the measured colors. To a certain extent this correction for space reddening will contain possible errors of the zero point, and by applying such a correction to the measured colors we shall be able to interpret them in terms of spectral type. We shall also assume that the median photographic magnitude of the cluster-type variables is 0.0 mag.; the median red absolute magnitude is, then, -0.13 mag. The adopted reddening of $+0.8 \pm 0.1$ mag. corresponds to a photographic absorption of 2.6 ± 0.3 mag. The apparent photographic modulus is 13.97; the true modulus becomes 11.4, and the distance is 1900 ± 200 parsecs. The cluster is probably the nearest to the sun of the globular clusters.

COLORS AND MAGNITUDES OF CLUSTER STARS

The color-magnitude arrays for stars inside and outside a circle of radius $4'.5$ were first investigated. No significant difference between these two diagrams was found, except that in the outer zones considerable scatter is introduced by the greater percentage of field stars and the larger photometric accidental errors. No systematic photometric errors seem to exist as a function of distance from the center. The color-magnitude array for all 660 measured stars brighter than $14^m.4$ is given in Table 2 and in Figure 1. The stars are grouped in the table in intervals of 0.2 mag. in red index and 0.4 mag. in red magnitude. The probable intrinsic red indices, C'_r, are given

in the second row, the absolute red magnitude in the second column. The survey is incomplete at $15^m.6$, photographic; all counted numbers in the region of incompleteness are given in italics. The number of variable stars at a point in the array is given as (n), to be added to the number of nonvariables. Table 3 gives the color-magnitude array for 117 stars in the two rings at $2'.2$ and $4'.5$ from the center of the cluster. Except for stars fainter than $14^m.0$ with red indices greater than +2.2 mag., there is no incompleteness. The stars are

TABLE 2

COLOR-MAGNITUDE ARRAY—ALL STARS

m_{HPr}	M_{Hpr}	0.5 −0.3	0.7 −0.1	0.9 +0.1	1.1 +0.3	1.3 +0.5	1.5 +0.7	1.7 +0.9	1.9 +1.1	2.1 +1.3	2.3 +1.5	2.5 +1.7	C_r C'_r
<10.0	<−3.0	.....	.....	.....	.....	.....	.....	.....	1	.....	(1)	.....	1(1)
10.2	−2.8	.....	.....	1	.....	.....	.....	.....	.....	.....	.....	1	2
10.6	−2.4	.....	.....	.....	.....	.....	.....	.....	1(1)	1	3	.....	5(1)
11.0	−2.0	1	.....	1	.....	.....	.....	.....	2	1	1	.....	6
11.4	−1.6	.....	.....	2	.....	1	2	3	8	6	.....	.....	22
11.8	−1.2	.....	.....	1	.....	.....	1	9	6	1	.....	.....	18
12.2	−0.8	.....	.....	1	1	.....	5	14	9	1	.....	.....	31
12.6	−0.4	.....	1	1(2)	1	3	5	15(1)	8	1	.....	1	36(3)
13.0	0.0	10	11(5)	9(11)	19(4)	27(2)	21(4)	44	16	4	3	.....	164(26)
13.4	+0.4	6	18(1)	2(1)	1(1)	10	10	39	7	3	*1*	.....	*97*(3)
13.8	+0.8	.....	.....	2	1	16	39	47	*6*	*1*	.....	.....	*112*
14.2	+1.2	1	.....	.....	7	*48*	*71*	*5*	.....	.....	.....	.....	*132*
Sums	.....	18	30(6)	20(14)	30(5)	*105*(2)	*154*(4)	*176*(1)	*64*(1)	*19*	*8*(1)	*2*	*626*(34)

all plotted in Figure 1, without distinction as to photometric quality.

Table 2 is incomplete, but by the use of the data of Table 3, which is essentially complete, we may obtain the frequency distribution of the colors of all stars brighter than $14^m.4$, m_{HPr}. Corrections for the presence of field stars were first applied, and the hypothetical frequency function derived, which is given in Table 4. Except for the abnormal group of blue stars near absolute-magnitude zero, there exists only a small dispersion of intrinsic color about the value +0.8 mag. The dispersion in spectral type must be correspondingly small for the brighter stars.

The essential features of these diagrams are the same as in the yellow-index–magnitude diagrams of Shapley.[1] A nearly vertical supergiant branch reaches the absolute magnitude (red) of −3.0 mag. There is a very small dispersion in color in this supergiant region; the mean color decreases toward the fainter stars. Among the

supergiants probably only a small range of spectral type exists. A very striking feature is the group of stars with absolute magnitudes between −0.4 and +0.4 mag. At this range a group of blue stars

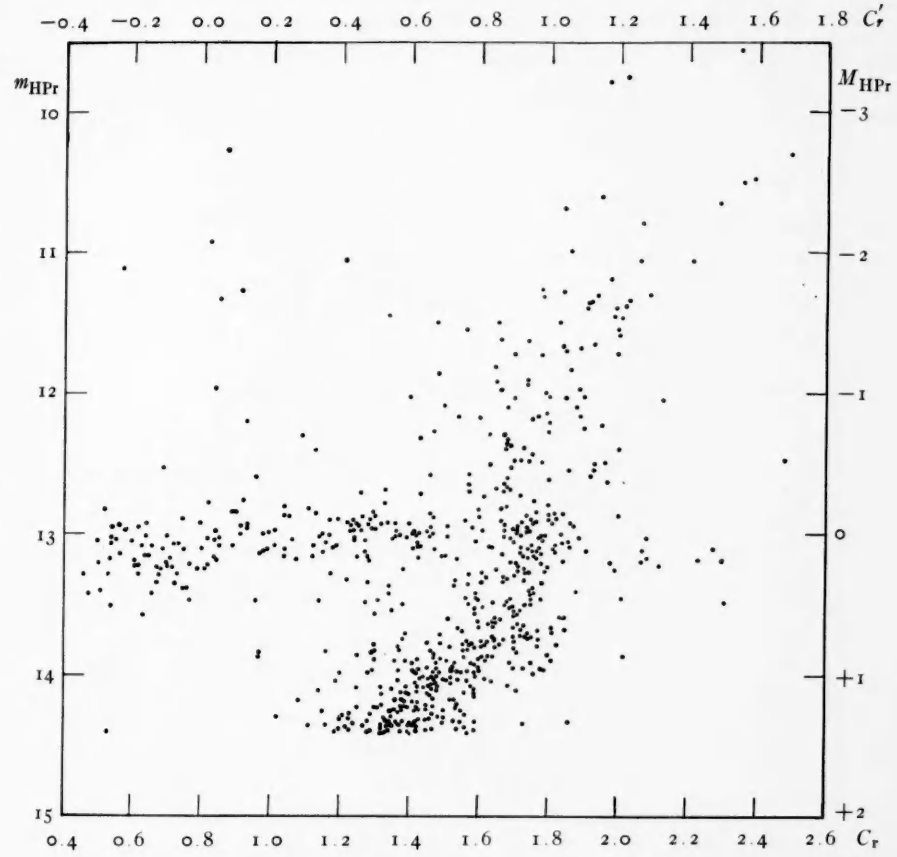

FIG. 1.—The color-magnitude diagram in M 4. C_r is the observed red index and C_r' the index after correction for space reddening. m_{HPr} is the apparent red magnitude and M_{HPr} the absolute red magnitude.

occurs, with small dispersion in absolute magnitude and with a very wide range in color (C_r' from −0.3 to +0.8 mag.). Below this magnitude the supergiant group seems to be continued toward the subgiants with a tendency for increasing blueness. The subgiants are very numerous. There are considerable regions of the diagram

which are essentially empty—for example, main-sequence stars of types B and A brighter than $M_{HPr} = +1$ are definitely absent. There are few, if any, supergiants in the A and F region, or later than $K5$. Normal giants in late K and M classes are probably also absent. There are ten stars in Table 2 brighter than $12^m.4$, with observed colors between 0.4 and 1.4 mag.; the expected number of field stars

TABLE 3

COLOR-MAGNITUDE ARRAY, INNER ZONES

m_{HPr}	M_{HPr}	0.5 −0.3	0.7 −0.1	0.9 +0.1	1.1 +0.3	1.3 +0.5	1.5 +0.7	1.7 +0.9	1.9 +1.1	2.1 +1.3	C_r C'_r
10.6	−2.4	.....	.....	.....	.....	.....	.....	.....	(1)	.....	(1)
11.0	−2.0	.....	.....	.....	.....	.....	.....	.....	1	.....	1
11.4	−1.6	.....	.....	.....	.....	.....	.....	.....	2	2	4
11.8	−1.2	.....	.....	.....	.....	.....	.....	2	.....	.....	2
12.2	−0.8	.....	.....	.....	.....	.....	.....	5	3	.....	8
12.6	−0.4	.....	.....	.....	.....	1	1	4	2	.....	8
13.0	0.0	.....	2	2(3)	4	5	4	7	6	.....	30(3)
13.4	+0.4	1	1	1	(1)	.....	1	9	.....	.....	13(1)
13.8	+0.8	.....	.....	.....	.....	.....	6	6	1	.....	13
14.2	+1.2	.....	.....	.....	1	5	25	1	1	.....	33
Sums	.....	1	3	3(3)	5(1)	11	37	34	16(1)	2	112(5)

TABLE 4

FREQUENCY OF RED INDICES

C_r	0.5	0.7	0.9	1.1	1.3	1.5	1.7	1.9	2.1
C'_r	−0.3	−0.1	+0.1	+0.3	+0.5	+0.7	+0.9	+1.1	+1.3
Percent	2	4	3	3	11	32	29	14	2

in an equal area of the sky is six. It is probable that all the bright blue stars are field stars; in Table 3, where the number of field stars is small, that region of the diagram is entirely vacant.

The point in the diagram at $M_{HPr} = 0$ and $C'_r = +0.8$ mag. is of particular interest as the common point for two very different groups of stars. In one group, stars of a nearly constant luminosity near that of the cluster-type variables show a wide range of possible temperatures and, therefore, of radii. In the other group, the luminosity and radius both vary, with the surface temperature remaining al-

most constant. The surface temperatures of the group of stars at $M_{HPr} = 0$ may be estimated, from the colors, to range from 15,000° to 6000°. This implies, for a constant luminosity, a sixfold variation of radius; a very selective process must be responsible for the existence of the group. At the crossing-point of the two groups a star with a uniquely determined radius, luminosity, and presumably a unique mass is capable of "evolving" in two different directions. The behavior of a two-parameter family of stars, differing in mass and in mean molecular weight, does not seem sufficient to describe the features of the globular-cluster, color-magnitude diagram. In galactic clusters such an interpretation meets with considerable success.[9] It should be remarked that the general appearance of the color-magnitude diagram in M 4 is almost completely different from that of any galactic cluster—the brighter stars fill those regions of the diagram avoided by stars in the galactic clusters. The color-magnitude diagrams of Shapley for M 3, a cluster rich in variables, is hardly different from that of M 13, which is remarkably poor in variables. They both resemble M 4, which has a peculiar deficiency only in the number of supergiants. The globular clusters seem to form a very homogeneous class, as far as the constitution of the brighter stars, at least, is concerned. This homogeneity is, in a sense, another significant difference from the galactic clusters.

THE FREQUENCY FUNCTION OF CLUSTER STARS

Perhaps the most striking feature of the frequency function of cluster stars is the group of stars at absolute-magnitude zero, and we shall first investigate them more closely. We shall arbitrarily divide the stars into two groups with observed colors smaller or larger than +1.40 mag. The numbers of blue stars, N_b, and of red stars, N_r, in intervals of 0.1 mag. in m_{HPr}, are given in Table 5. Thirty of the blue stars and five of the red stars are cluster-type variables. Six field stars may be expected in the magnitude range covered by the table. The blue stars show a remarkably sharp concentration about 13^m05, m_{HPr}. The mean magnitude is 13.06 ± 0.01 mag., 0.02 ± 0.03 mag. fainter than the cluster-type variables. The computed dispersion of the magnitudes about the mean is ± 0.20 mag. The dis-

[9] Kuiper, *Harvard Bull.*, No. 903, 1936; *Ap. J.*, **86**, 176, 1937.

persion includes the errors introduced by grouping, the variability of the 30 variables, the measuring error, and the presence of field stars. When we exclude as field stars those brighter than 12^m60, and the group at 13^m45 as belonging to the subgiants, we leave 127 stars. The total dispersion of the blue stars is then ± 0.12 mag.; the intrinsic dispersion may be less than ± 0.09 mag. The red stars also show a maximum near 13^m05, but the distribution curve is much flatter. This group of blue stars, close to the median magnitude of the cluster-type variables, produces the preliminary maximum in the frequency curves of the stars in globular clusters discussed by Shapley. Furthermore, the globular clusters are sharply distinguished from galactic clusters and field stars in the galaxy, by this group.

TABLE 5

FREQUENCY FUNCTION OF STARS NEAR $m_{HPr} = 0$

m_{HPr}	N_b	N_r	m_{HPr}	N_b	N_r
12.25	1	7	12.95	30	28
12.35	1	6	13.05	32	26
12.45	1	9	13.15	22	27
12.55	2	8	13.25	20	18
12.65	1	10	13.35	6	12
12.75	4	5	13.45	10	15
12.85	12	13			

The general frequency function of the photographic magnitudes is given in Figure 2, as the number of stars between $m - 0.1$ and $m + 0.1$. It is obtained from the catalogue, with the addition of 200 stars for which red magnitudes were uncertain. Since incompleteness exists for stars fainter than 15^m6 in the *Durchmusterung* of the cluster, the frequency of the fainter stars was derived from that given by the survey in the inner ring zones. The assumption that the frequency function does not vary strongly with distance from the center of the cluster is supported by the relative frequencies in the ring zones and in the entire cluster.

To supplement these counts based on the actual survey of the cluster, counts to various limiting photographic magnitudes have been made on a one-hour exposure taken with the 60-inch reflector at Bloemfontein. The counts cover an area of 0.11 square degree

centered on the cluster. The magnitude scale is subject to considerable uncertainty for the fainter stars and is affected by the dense background fog near the center of the cluster. The resultant fre-

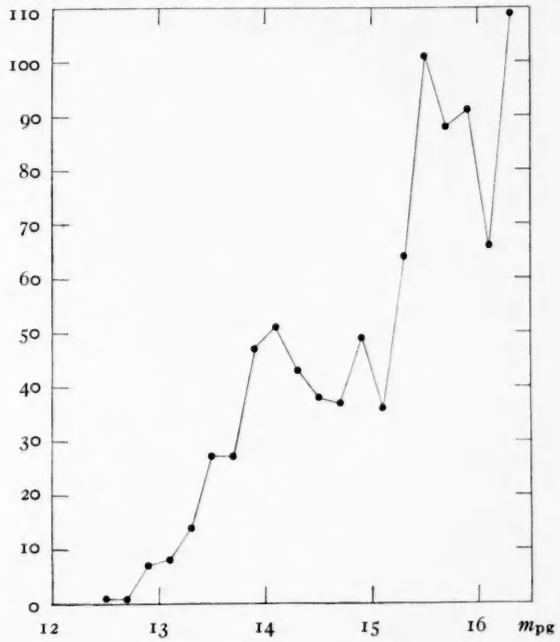

FIG. 2.—The frequenty function of cluster stars. The number of stars is given with magnitudes between $m_{pg} + 0.1$, and $m_{pg} - 0.1$.

TABLE 6

FREQUENCY FUNCTION OF CLUSTER STARS

M_{pg}	log A_m	log $\Phi(M)$	M_{pg}	log A_m	log $\Phi(M)$
−1.....	1.63	1.53	+3.....	3.32	3.31
0.....	2.23	2.01	4.....	3.58	3.56
+1.....	2.44	2.62	+5.....	3.92	3.78
+2.....	2.85	3.14			

quency function, fitted smoothly to that of the brighter stars, should be viewed as only approximate. It has been smoothed, corrected for the presence of field stars, and is given in Table 6 as the number of stars, A_m, between $m + 0.5$ and $m - 0.5$. The luminosity function of

stars in the galaxy, $\Phi(M)$, according to van Rhijn,[10] adjusted in zero point, is given in the third column. The differences show clearly the excess of cluster stars at $M_{pg} = -1, 0$; the deficiency at $M_{pg} = +1$, $+2$ probably arises from the absence of bright main-sequence stars in the cluster. The actual number of stars counted was $\approx 10^4$, and the estimated total population of the cluster, based on the van Rhijn luminosity function to $M_{pg} = +13$, is 10^5. If we adopt Luyten's values for the frequency of intrinsically fainter stars,[11] the total population is 3×10^5 stars.

In considering the population of the cluster, we must not forget that M 4 is a dwarfish cluster compared to other clusters in the galaxy. We lack extensive surveys of the richer clusters, but most of the clusters investigated contain a larger number of giant stars. Only 210 stars brighter than $M_{pg} = +0.5$ are found in M 4. In M 3 there are 600, and in M 13, 1000 stars brighter than this limit. The absolute photographic magnitude of M 4 can be obtained from an integration of the light of the catalogued stars, extrapolated by the counts of the fainter stars. For the objects in the catalogue the integrated absolute photographic magnitude is -6; including the stars counted to $M_{pg} = +5$, the result is -7.2. The integrated color cannot be obtained because of the unknown color of the fainter stars. For the catalogue stars the integrated color is $+1.56$ mag. on the red index scale, corresponding to gK7. The observed photoelectric color class[7] is gG4, and gG7 according to Vyssotsky and Williams.[8] The difference can be explained on the assumption that the cluster stars fainter than $M_{HPr} = +1$ are considerably bluer than the brighter stars.

The asymmetric nature of the luminosity function of the cluster stars leads to a statistical error which may be of some general interest. The observed differences between the median magnitudes of the cluster-type variables and of various typical stars in the cluster field have been determined. Shapley[1] has used extensively the difference between the median magnitude of the variable, m_v, and the mean magnitude of the 25 brightest stars in the cluster, m_{25}, the sixth brightest star, m_6, and the thirtieth brightest star, m_{30}. The observed values of these differences are given in Table 7

[10] *Groningen Pub.*, No. 38, 1925. [11] *M.N.*, **98**, 677, 1938.

for the whole area of the cluster and for the two inner ring zones. For comparison the table contains in the fourth column the values adopted by Shapley for giant-poor clusters in his homogeneous survey. The essential features of the discrepancy are present if we use the catalogues of stars in M 3 and M 13. The frequency function of cluster stars is responsible—the smaller the area surveyed, the smaller will become the difference between the magnitude of the brightest stars and the fixed median magnitude of the cluster-type variables. The effect is clearly visible in Table 7, where the adopted values

TABLE 7

	Δm Whole Cluster	Δm Inner Zone	Δm Shapley
$m_v - m_{25}$	$+0^{M}86$	$+0^{M}10$	$+0^{M}44$
$m_v - m_6$	1.37	+ .47	.94
$m_v - m_{30}$	+0.67	−0.20	+0.03

used by Shapley are intermediate between the value for the whole cluster and that for the smaller ring zones. In a survey of all clusters with a uniform technique such difficulties may be minimized.

VARIABLES IN THE CLUSTER

Miss Sawyer[5] lists 33 variables in M 4. Variables No. 4 and No. 13 of her list are bright, longer-period variables; No. 17 does not vary appreciably, and Nos. 20 and 33 were not measured. The colors of the two longer-period variables are not accurate, since the time-mean magnitude over only part of the light-cycle is available. Variable No. 4 has a red index of +2.35 mag., one of the largest in the cluster. If the variable is actually associated with the cluster, it may be a normal, long-period variable with the rather small intrinsic color of +1.4 mag. The observed photographic range is only 0.8 mag.,[12] and

[12] Dr. Helen S. Hogg (formerly Miss Sawyer) has been good enough to inform me, in advance of publication, of the results of her investigation of Variable No. 4. She states that the star is a semiregular variable of moderate range. The periods of variation range from fifty to seventy-five days, and the star may be similar to UU Herculis. Miss Cannon has classified the star as K2, in excellent agreement with the color class observed in the present investigation.

the star may be a peculiar object like the bright non-Cepheid variables in other clusters (e.g., No. 95 in M 3).[13] Variable No. 13 also has a small observed range on these plates and a color of +1.86 mag. Both the variables seem to lie close to the supergiant branch of the cluster. Their spectra should be of considerable interest.

The data for the cluster-type variables do not establish any dependence of their magnitude or mean color on their period. The observed mean of the photographic median magnitudes is 13.97 ± 0.05—yielding a total dispersion of ± 0.27 mag. In the red the mean median magnitude is 13.04 ± 0.03 mag., and the total dispersion is ± 0.18 mag. The largest part of this dispersion arises from the variability of the stars. The mean observed range is 0.93 mag. in the photographic and 0.55 mag. in the red. These ranges, of course, are not the total ranges of the variation. They indicate, however, that the change of temperature during a light-cycle is not a small one. If the stars radiate like black bodies at all times, the change in gradient is of the order of 0.5 during a cycle. For blue stars this involves a variation in temperature of the order of 5000°. Such behavior is similar to that found for galactic cluster-type variables.[14]

The known cluster-type variables are 35 in number. While others may exist, it seems improbable that their number is large. We should investigate the possibility that the large excess in the frequency of stars near $M_{\mathrm{HPr}} = 0$ may be caused by the presence of large numbers of variables of small range. In Table 5 we find 116 blue stars and 112 red stars between $12^{m}80$ and $13^{m}30$, m_{HPr}—an excess of about 150 stars over the smooth frequency-distribution. Variables of normal range cannot possibly account for more than 45 of the blue stars—leaving perhaps 100 stars as possible variables of very small range. An investigation of the residuals of the measured magnitudes on various plates, from the mean magnitude of each star in the suspected region, is not conclusive as to the reality of the variations. Four 60-inch plates were used, and 25 stars were selected at random from the catalogue in each of the tabulated groups. The average deviations from the mean are given, as well as the sampling error and the mean magnitude for each group, in Table 8.

[13] Greenstein, *Harvard Bull.*, No. 901, 1935.

[14] Norman, *Pub. A.A.S.*, **9**, 162, 1938.

In the photographic magnitudes the accidental error seems to be generally larger for the brighter stars, but no significant increase of the mean residual is apparent for the blue stars at $M_{pg} = 0$. In the red the situation is actually reversed, so that we may conclude that no significant excess variation can be proved to exist for the blue stars at the magnitude of the cluster-type variables. A more conclusive investigation of this possible explanation of the peculiar form of the color-magnitude diagram is to be desired.

TABLE 8

MEAN RESIDUALS, PHOTOGRAPHIC

Range of Mag.	C_r	$\lvert\bar{v}\rvert_{pg}$	$\bar{m}_{pg}$
13.75–14.25.....	<1.2	0.096±0.007	13.82
13.75–14.25.....	>1.4	.098 .008	13.82
<12.75, >14.25..	>1.4	.092 .007	13.78
>14.25.....	>1.4	0.068 0.005	14.73

MEAN RESIDUALS, RED

Range of Mag.	C_r	$\lvert\bar{v}\rvert_{HPr}$	$\bar{m}_{HPr}$
12.90–13.25.....	<1.2	0.075±0.004	13.06
12.50–13.50.....	>1.4	.080 .005	13.08
<12.75, >13.25..	>1.4	0.092 0.006	13.07

SPACE DISTRIBUTION OF CLUSTER STARS

Star counts on 100-inch reflector plates were made near the center of the cluster to determine the centroid of the cluster and its ellipticity. However, 1205 stars to $m_{pg} = 17.5$ showed no definite evidence of ellipticity. Counts were made on the long-exposure, 60-inch Bloemfontein reflector plate for the areal density of the cluster stars. The counts, reaching $m_{pg} = 19.3$, were made in *réseau* squares over a radius of 12′ from the center of the cluster, and they are approximately free from distance correction as far as 7′ from the center. The total counted number is 10,300. The counts, tabulated by *réseau* squares, have first been summed over twelve sectors, with $0.7' < r < 6'$; the total number of stars involved is 5925. The counted num-

ber for each 30° sector, $N(\theta)$, is given as a function of position angle in Table 9. A least-squares solution yields

$$N(\theta) = 494 + 40 \sin (2\theta - 52^\circ),$$

with residuals given in the last row of the table. The position angle of the major axis is 71°, and the ellipticity is 0.85, in good agreement with estimates made by Shapley.[1]

The comparison of the areal density (AD) of the stars, for the inner rings, with those found from the counts on the 100-inch reflector plates shows that the 60-inch counts are not complete to $19^m.3$ in the

TABLE 9

COUNTS FOR ELLIPTICITY

θ	15°	45°	75°	105°	135°	165°	195°	225°	255°	285°	315°	345°
$N(\theta)$	497	497	563	515	478	455	487	492	543	482	472	444
O−C	+18	−22	+29	+06	+09	+01	+08	−27	+09	−27	+03	−10

TABLE 10

AREAL AND SPACE DENSITIES, RING COUNTS

r	AD/mm²	D/mm³	r	AD/mm²	D/mm³
0.8′	59	25::	5.2′	5.3	0.35
1.6	27	5.4	6.1	4.6	0.35
2.4	17	2.4	7.0	3.4	0.28
3.4	11	1.2	7.9	2.9	0.13
4.3	8.2	0.95	8.8	0.41	0.44 ::

center. The ratio of the areal densities for zones in which both the 60-inch and the 100-inch counts are trustworthy yields a correction factor to be applied to the inner zones of the 60-inch counts. The areal density, so corrected, is given in Table 10 for ten concentric ring zones up to a distance of 9′ from the center of the cluster. The densities are given as the number of stars per square millimeter on the plate. The total counted number is 8714 stars; the corrections applied to the inner zones involved 400 stars. Corrections for the field stars were applied, and then the space density, D, per cubic millimeter, was determined by the method used by Wallenquist.[15] These densities are inaccurate for the central and for the outermost

[15] Bosscha, *Obs. Ann.*, **4**, No. 5, 1933.

zone. In the latter case an error arises because the counts do not reach the outer boundary of the cluster; the derived value of the density for the outer zone is too high, since no correction for stars projected upon it from more distant zones has been made. The actual radius of the cluster is at least 15′, or nearly twice that involved in the counts.

A better determination of the space density in this case can be made by the method suggested by Plummer.[16] A total of 8100 stars was counted in vertical and horizontal strips across the cluster. These counts were averaged on the assumption of spherical symmetry and

TABLE 11

SPACE DENSITIES FROM STRIP COUNTS

r	D/mm³, Strip	D/mm³, Mean	D/psc³	r in Parsecs
0.22′	28.6::	33::	2100::	0.12
0.66	7.7	12	770	0.36
1.1	4.6	5.8	370	0.63
1.6	2.6	3.2	210	0.87
2.0	1.4	1.8	120	1.1
2.5	1.1	1.4	90	1.4
2.9	0.9	1.0	64	1.6
3.4	0.8	0.8	52	1.9
3.8	0.6	0.7	46	2.1
4.3	0.3	0.6	42	2.4
4.8	0.3	0.5	31	2.6
5.2	0.2	0.3	16	2.9
5.6	0.13	0.2	10	3.1

smoothed. The space-density distribution in the second column of Table 11 was then obtained. The shape of this function is similar to that in Table 11, but the number of stars involved is different. On normalizing the two density distributions and taking means, we obtain the final adopted space density per cubic millimeter in the third column of Table 11. This has been transformed to the number of stars per cubic parsec in the fourth column; the fifth column gives the distance, in parsecs, from the center. The form of the density-curve differs from those found by Plummer for the brighter stars in other clusters. In M4 the density is too high at the center, and it also falls off more slowly in the outer portions of the cluster.

Too much weight may not be attached to the detailed form of the space-density distribution. It permits us, however, to estimate the

[16] *M.N.*, **71**, 460, 1911; **76**, 107, 1915.

gravitational potential as a function of the distance from the center. We can assume that the stars counted (to $M_{pg} = +5$) have a mean mass of $2\odot$ and represent about one-third of the total mass of the cluster, as they do in the galaxy.[11] A numerical summation then gives the course of the potential as a function of distance. The potential varies rather slowly in the central regions of the cluster, from 6.5 at the center to 3.1 at 2.5 parsecs (in arbitrary units). Within the distance of 2.5 parsecs, 50 per cent of the cluster stars will be found. We may take the mean value of the potential to be about 4 for the body of cluster stars, or about 1.2×10^{12} in c.g.s. units. If we assume that the mean kinetic energy of the cluster stars is half the mean potential energy, we obtain a value for the root mean-square peculiar velocity of the cluster stars. This value is 11 km/sec, the order of magnitude of the velocity dispersion to be expected in the cluster.

Stars 1–271 of Table 12 are identified on the chart in Plate IV. The identifying numbers are placed immediately to the right of the star referred to. Stars 272–662 are identified on Plate V for the outer regions of the cluster. Table 12 contains first the catalogue number of the star, then the photographic magnitude *minus* 10, with the decimal point omitted; the red magnitude *minus* 10 follows in the third column, similarly. (In the few cases where the apparent magnitude is less than 10, the magnitude itself is given.) The fourth column contains the red index, which is always positive. The last column contains remarks as to the quality of the magnitudes and colors. Stars with five or more measures in each color are quality "a"; those with three or four in each are quality "b"; those with two or less are quality "c." The mean errors for each quality class are given as shown in the accompanying tabulation. Stars whose image is some-

Quality	m.e. of Mag.	m.e. of Color
a	$\pm 0^m.038$	$\pm 0^m.054$
b	.048	.068
c	± 0.057	± 0.081

times blended with that of another fainter star are identified by the symbol "d"; those for which the blending is particularly large are

PLATE IV

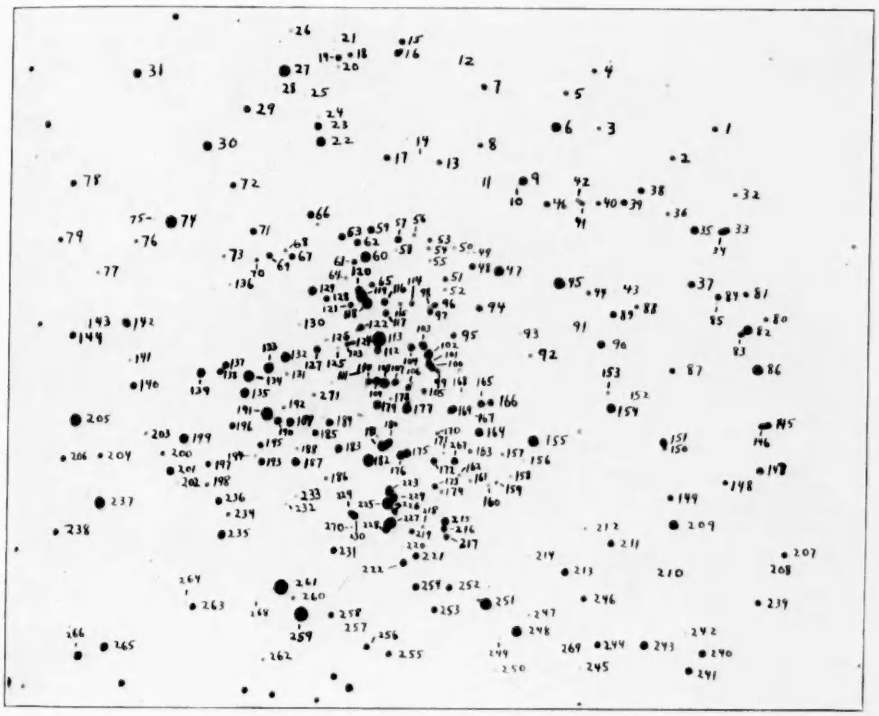

INNER REGION OF MESSIER 4. STARS 1–271, ON RED PLATE, SCALE 3″.8/MM

PLATE V

N

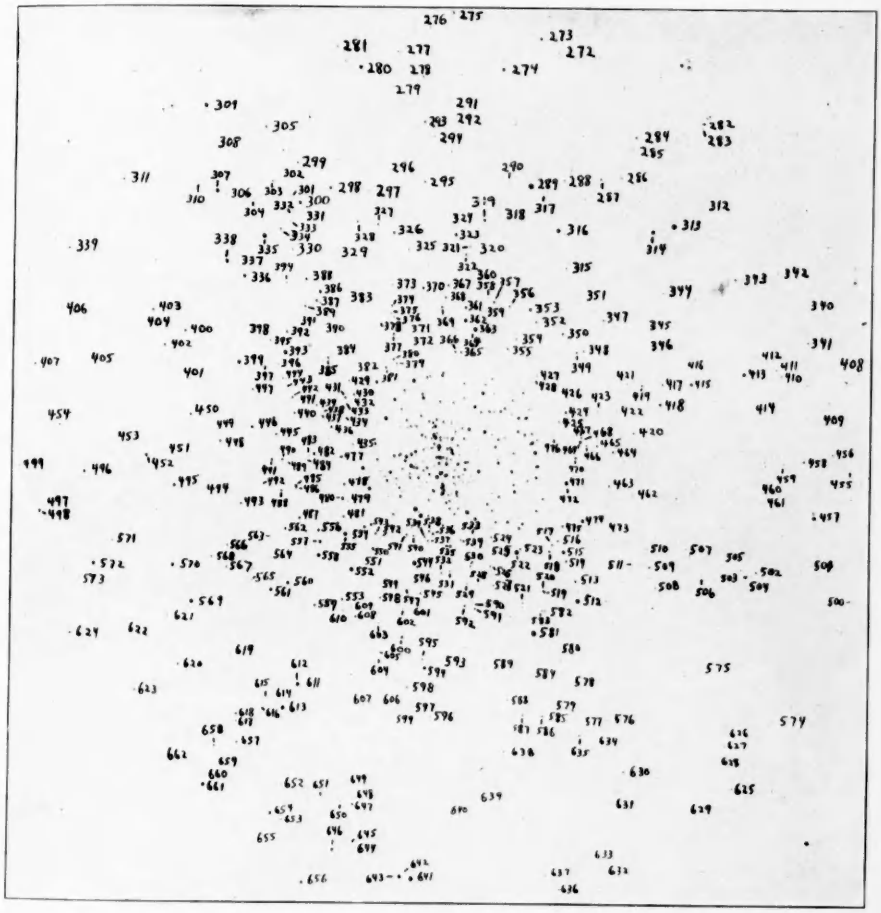

OUTER REGION OF MESSIER 4. STARS 272–662, ON RED PLATE, SCALE 15″.2/MM

TABLE 12

MAGNITUDES AND COLORS OF CLUSTER STARS

Star	m_{pg}	m_{HPr}	C_r	Notes	Star	m_{pg}	m_{HPr}	C_r	Notes
1	439	298	141	a	55	522	403	119	a
2	490	316	174	a	56	534	387	147	c
3	527	361	166	a	57	419	294	125	a
4	393	323	070	a	58	557	405	152	c
5	390	299	091	V10	59	398	285	113	a
6	364	190	174	a	60	356	171	185	a
7	379	315	064	a	61	500	332	168	a
8	500	330	170	a	62	398	300	098	V22
9	378	218	160	da	63	364	289	075	a
10	573	439	134	db	64	553	409	144	c
11	607	434	173	a	65	404	325	079	na
12	576	436	140	a	66	432	292	140	a
13	500	327	173	a	67	389	304	085	dV25
14	581	439	142	db	68	540	389	151	c
15	441	302	139	da	69	390	320	070	a
16	380	308	072	da	70	539	375	164	a
17	399	298	101	a	71	473	309	164	a
18	514	339	175	a	72	491	310	181	a
19	472	303	169	da	73	548	400	148	a
20	526	397	129	db	74	330	139	191	a
21	560	414	146	da	75	583	438	145	b
22	356	191	165	a	76	538	375	163	a
23	452	276	176	da	77	559	400	159	da
24	574	427	147	da	78	480	301	179	a
25	564	429	135	a	79	391	342	049	a
26	553	402	151	a	80	499	332	167	a
27	327	135	192	a	81	487	312	175	a
28	575	425	150	a	82	370	216	154	db
29	429	305	124	a	83	485	313	172	da
30	396	229	167	a	84	467	297	170	da
31	339	230	109	a	85	574	396	178	db
32	522	352	170	a	86	334	151	183	a
33	438	303	135	ddb	87	488	315	173	a
34	428	313	115	ddb	88	506	346	160	a
35	406	238	168	a	89	461	285	176	a
36	515	346	169	a	90	434	273	161	a
37	385	281	104	a	91	569	433	136	a
38	366	306	060	V8	92	543	373	170	b
39	442	317	125	V9	93	568	412	156	da
40	405	351	054	a	94	391	311	080	a
41	414	338	076	dda	95	542	319	223	na
42	549	386	163	da	96	506	349	157	dna
43	567	425	142	a	97	492	335	157	dna
44	517	341	176	a	98	584	431	153	ddc
45	340	138	202	a	99	544	370	174	ddnc
46	385	303	082	a	100	503	323	180	ddnc
47	383	203	180	a	101	472	298	174	ddnc
48	414	288	126	V16	102	435	268	167	dnV17
49	563	430	133	dc	103	373	293	080	na
50	483	386	097	da	104	444	299	145	ndV18
51	506	333	173	a	105	513	335	178	ddnb
52	543	377	166	a	106	408	342	066	dna
53	526	362	164	a	107	481	314	167	na
54	538	382	156	a	108	406	237	169	dna

TABLE 12—*Continued*

Star	m_{pg}	m_{HPr}	C_r	Notes	Star	m_{pg}	m_{HPr}	C_r	Notes
109	492	321	171	dna	163	527	357	170	na
110	407	335	072	dna	164	392	229	163	na
111	569	435	134	dnc	165	441	295	146	dna
112	471	317	154	dna	166	410	311	099	dna
113	286	079	207	nb	167	589	434	155	c
114	527	356	171	dna	168	559	418	141	nb
115	541	374	167	na	169	415	252	163	ddnb
116	468	292	176	na	170	550	408	142	dnc
117	361	305	056	na	171	581	410	171	dnc
118	313	220	093	ddnb	172	381	308	073	dna
119	342	172	170	dnb	173	395	323	072	dna
120	444	316	128	dna	174	554	383	171	dc
121	393	342	051	na	175	450	308	142	dna
122	384	322	062	ddnb	176	466	295	171	dna
123	548	367	181	ddnc	177	374	231	143	dna
124	565	385	180	ddnc	178	546	393	153	nc
125	551	431	120	dnc	179	359	277	082	nV21
126	575	399	176	dnc	180	464	305	159	dna
127	482	304	178	na	181	440	240	200	dnb
128	409	308	101	V24	182	327	135	192	na
129	427	249	178	a	183	369	277	092	dnV23
130	559	413	146	dnb	184	448	301	147	dna
131	533	386	147	dc	185	519	321	198	na
132	393	218	175	na	186	526	397	129	dna
133	387	198	189	na	187	458	278	180	na
134	359	166	193	a	188	548	409	139	c
135	402	222	180	a	189	402	269	133	na
136	552	397	155	da	190	417	287	130	na
137	483	308	175	da	191	337	134	203	na
138	391	324	067	da	192	548	402	146	c
139	375	228	147	a	193	445	294	151	na
140	366	302	064	a	194	558	438	120	c
141	552	406	146	a	195	501	327	174	na
142	471	289	182	ddb	196	379	318	061	a
143	555	417	138	da	197	499	332	167	a
144	468	297	171	a	198	539	377	162	a
145	469	302	167	da	199	400	232	168	a
146	475	305	170	da	200	521	367	154	a
147	403	257	146	a	201	396	270	126	a
148	382	321	061	a	202	569	424	145	b
149	415	300	115	a	203	540	392	148	a
150	535	377	158	ddb	204	524	349	175	a
151	443	250	193	da	205	311	127	184	a
152	567	422	145	da	206	374	328	046	a
153	538	365	173	a	207	473	301	172	a
154	393	203	190	a	208	554	394	160	da
155	351	167	184	a	209	379	200	179	a
156	562	427	135	a	210	578	440	138	a
157	548	390	158	na	211	448	282	166	a
158	548	388	160	a	212	549	379	170	b
159	540	398	142	c	213	438	269	169	a
160	547	398	149	nb	214	552	402	150	c
161	556	396	160	ddc	215	460	263	197	dna
162	555	378	177	ddnc	216	488	311	177	dna

TABLE 12—*Continued*

Star	m_{pg}	m_{HPr}	C_r	Notes	Star	m_{pg}	m_{HPr}	C_r	Notes
217	497	311	186	dna	271	555	407	148	dnc
218	538	395	143	c	272	477	343	134	fb
219	396	328	068	nV	273	418	248	170	fb
220	540	408	132	c	274	417	204	213	fb
221	481	303	178	a	275	427	297	130	fb
222	421	298	123	a	276	554	412	142	fb
223	445	273	172	dna	277	504	320	184	fb
224	499	321	178	dna	278	564	394	170	fb
225	337	161	176	dna	279	531	379	152	fb
226	402	329	073	dna	280	218	133	085	fb
227	372	172	200	dnb	281	371	314	057	fb
228	398	299	099	dnV20	282	565	403	162	fb
229	506	327	179	dnb	283	463	349	114	fb
230	492	314	178	dnb	284	356	302	054	fb
231	453	302	151	a	285	545	373	172	fb
232	592	436	156	nb	286	476	342	134	fb
233	570	417	153	a	287	446	300	146	fa
234	543	387	156	a	288	425	348	077	fa
235	431	285	146	V26	289	177:	.....	.....	fc
236	416	293	123	a	290	535	378	157	fb
237	359	159	200	a	291	526	392	134	fb
238	492	316	176	a	292	567	392	175	fb
239	415	301	114	V5	293	435	299	136	fb
240	441	261	180	a	294	503	347	156	fb
241	433	268	165	a	295	473	299	174	fda
242	548	374	174	a	296	564	417	147	fb
243	408	228	180	a	297	530	384	146	b
244	465	290	175	a	298	322	253	069	fa
245	551	374	177	a	299	398	309	089	fV29
246	425	318	107	a	300	333	185	148	fa
247	574	420	154	a	301	554	423	131	fb
248	350	172	178	a	302	539	382	157	fb
249	550	391	159	a	303	389	296	093	fa
250	567	408	159	da	304	509	379	130	fb
251	325	131	194	a	305	459	298	161	fb
252	424	298	126	a	306	521	372	149	fb
253	480	303	177	a	307	169	112	057	fc
254	471	291	180	a	308	568	395	173	fb
255	449	307	142	a	309	279	145	134	fb
256	491	305	186	a	310	527	391	136	fb
257	576	430	146	a	311	415	272	143	fb
258	422	306	116	a	312	568	421	147	fb
259	286	050	236	b	313	176	979	197	fa
260	535	364	171	a	314	338	139	199	fa
261	287	048	239	b	315	526	356	170	b
262	551	387	164	a	316	327	106	221	a
263	495	313	182	da	317	527	411	116	b
264	574	415	159	da	318	553	421	132	b
265	419	244	175	a	319	441	255	186	b
266	422	253	169	a	320	545	401	144	b
267	418	293	125	na	321	419	315	104	V15
268	592	438	154	db	322	473	293	180	b
269	597	438	159	db	323	415	225	190	a
270	570	435	135	c	324	567	435	132	b

TABLE 12—*Continued*

Star	m_{pg}	m_{HPr}	C_r	Notes	Star	m_{pg}	m_{HPr}	C_r	Notes
325	546	414	132	b	379	524	325	199	a
326	355	259	096	a	380	464	297	167	a
327	357	295	062	a	381	354	296	058	a
328	538	311	227	a	382	531	429	102	a
329	545	398	147	b	383	567	438	129	b
330	491	326	165	b	384	550	412	138	b
331	561	379	182	fb	385	464	292	172	b
332	549	426	123	fb	386	359	209	150	a
333	551	370	181	fb	387	487	287	200	b
334	492	303	189	b	388	392	281	111	a
335	256	061	195	fb	389	350	296	054	a
336	280	196	084	a	390	578	438	140	b
337	542	358	184	fb	391	553	430	123	b
338	298	150	148	fb	392	374	285	089	b
339	562	420	142	fc	393	285	099	186	a
340	588	386	202	fb	394	513	352	161	b
341	496	325	171	fb	395	526	318	208	b
342	488	353	135	fb	396	516	357	159	b
343	425	296	129	fb	397	563	436	127	b
344	577	436	141	fb	398	554	424	130	b
345	561	426	135	b	399	340	131	209	b
346	569	435	134	b	400	447	287	160	fb
347	489	320	169	b	401	544	359	185	fb
348	393	325	068	b	402	446	290	156	fb
349	383	299	084	b	403	442	299	143	fb
350	421	298	123	b	404	512	383	129	fb
351	548	387	161	b	405	502	343	159	fb
352	473	297	176	b	406	488	327	161	fb
353	394	217	177	b	407	448	280	168	fb
354	463	335	128	a	408	551	397	154	fb
355	446	329	117	V7	409	528	389	139	fb
356	393	308	085	V6	410	413	338	075	db
357	407	290	117	b	411	462	324	138	db
358	567	425	142	b	412	479	348	131	db
359	537	373	164	b	413	369	183	186	db
360	538	397	141	b	414	560	432	128	fb
361	434	267	167	b	415	404	236	168	a
362	217	126	091	a	416	561	438	123	b
363	254	070	184	V13	417	401	317	084	a
364	618	432	186	b	418	445	252	193	a
365	414	310	104	a	419	445	317	128	a
366	484	310	174	a	420	411	314	097	V
367	381	312	069	V19	421	537	381	156	a
368	421	309	112	b	422	547	400	147	b
369	435	301	134	b	423	526	362	164	b
370	428	260	168	b	424	432	265	167	a
371	585	429	156	a	425	489	336	153	a
372	580	425	155	a	426	560	422	138	a
373	512	361	151	b	427	522	377	145	a
374	511	303	208	b	428	583	433	150	b
375	524	346	178	b	429	494	332	162	a
376	513	349	164	b	430	472	309	163	a
377	385	294	091	V27	431	456	290	166	a
378	585	438	147	b	432	558	404	154	b

TABLE 12—*Continued*

Star	m_{pg}	m_{HPr}	C_r	Notes	Star	m_{pg}	m_{HPr}	C_r	Notes
433	578	436	142	a	487	409	290	119	db
434	573	440	133	a	488	374	308	066	V_{30}
435	525	360	165	a	489	563	426	137	b
436	401	287	114	a	490	350	294	056	b
437	385	292	093	V_{28}	491	459	292	167	db
438	558	436	122	a	492	575	433	142	b
439	495	334	161	a	493	482	310	172	b
440	453	295	158	b	494	550	388	162	b
441	537	388	149	b	495	422	265	157	fa
442	359	304	055	b	496	392	287	105	fV_{32}
443	518	398	120	b	497	550	411	139	fb
444	404	322	082	b	498	496	248	248	fb
445	374	285	089	V_{31}	499	575	421	154	fc
446	422	248	174	b	500	526	418	108	fb
447	353	303	050	a	501	421	358	063	fb
448	357	293	064	a	502	482	295	187	fb
449	551	435	116	b	503	532	376	156	fb
450	414	290	124	b	504	550	397	153	fb
451	544	396	148	b	505	566	424	142	fb
452	403	214	189	fa	506	532	390	142	fb
453	533	408	125	fb	507	545	368	177	b
454	516	379	137	fb	508	514	339	175	a
455	545	372	173	fb	509	470	299	171	b
456	497	324	173	fb	510	521	346	175	b
457	314	149	165	fb	511	562	425	137	b
458	443	283	160	fb	512	294	065	229	a
459	519	344	175	fb	513	410	277	133	b
460	561	404	157	fb	514	409	303	106	V_2
461	499	383	116	fb	515	311	155	156	b
462	526	377	149	b	516	417	295	122	a
463	492	308	184	b	517	492	316	176	a
464	432	305	127	b	518	428	292	136	a
465	485	301	184	b	519	428	316	112	ddb
466	388	317	071	V_1	520	463	315	148	ddV?
467	382	317	065	a	521	487	357	130	b
468	576	431	145	b	522	280	031	249	b
469	378	210	168	a	523	444	302	142	a
470	414	285	129	a	524	459	316	143	a
471	316	118	198	a	525	561	404	157	a
472	553	413	140	a	526	402	335	067	a
473	547	436	111	b	527	516	348	168	a
474	337	163	174	a	528	580	430	150	a
475	418	301	117	a	529	444	348	096	V_{14}
476	560	424	136	a	530	466	317	149	V_{12}
477	552	405	147	a	531	398	321	077	a
478	407	287	180	a	532	452	311	141	a
479	523	368	155	a	533	592	433	159	db
480	342	202	140	a	534	458	311	147	a
481	427	308	119	a	535	418	223	195	a
482	425	268	157	a	536	451	259	192	a
483	558	410	148	da	537	437	300	137	a
484	552	405	147	a	538	470	286	184	a
485	388	203	185	db	539	405	324	081	a
486	520	351	169	db	540	411	313	098	a

TABLE 12—*Continued*

Star	m_{pg}	m_{HPr}	C_r	Notes	Star	m_{pg}	m_{HPr}	C_r	Notes
541	426	302	124	a	595	527	320	207	b
542	554	397	157	a	596	514	355	159	b
543	479	293	186	a	597	552	367	185	b
544	114	027	087	b	598	467	285	182	b
545	491	309	182	a	599	511	386	125	b
546	559	390	169	a	600	420	248	172	b
547	509	417	152	a	601	557	398	159	a
548	439	298	141	a	602	571	390	181	a
549	556	409	147	a	603	540	368	172	b
550	553	417	136	a	604	545	380	165	b
551	564	406	158	a	605	545	403	142	b
552	.....	.....	.....	dd	606	537	376	161	b
553	335	283	052	a	607	525	353	172	b
554	552	382	170	a	608	425	293	132	a
555	313	107	206	a	609	536	366	170	a
556	411	238	173	a	610	564	431	133	b
557	373	203	170	a	611	552	401	151	b
558	309	131	178	a	612	346	147	199	b
559	420	291	129	b	613	304	126	178	fa
560	398	210	188	b	614	510	371	139	ddb
561	394	215	179	b	615	523	350	173	fa
562	422	294	128	b	616	573	431	142	fb
563	558	419	139	b	617	490	313	177	fb
564	549	428	121	b	618	571	434	137	fb
565	540	381	159	b	619	545	392	153	fb
566	494	323	171	b	620	427	309	118	fb
567	371	321	050	a	621	529	341	188	fb
568	381	328	053	a	622	540	395	145	fb
569	347	146	201	fa	623	503	312	191	fb
570	366	192	174	fa	624	547	422	125	fc
571	488	350	138	fb	625	451	309	142	fa
572	364	198	166	fb	626	518	350	168	fb
573	578	429	149	fc	627	535	372	163	fb
574	456	334	122	fb	628	540	403	137	fb
575	516	378	138	fb	629	575	406	169	fc
576	521	361	160	fa	630	387	312	075	fa
577	562	423	139	fb	631	548	373	175	fb
578	534	397	137	b	632	460	287	173	fb
579	558	434	124	b	633	533	392	141	fb
580	555	426	129	b	634	568	436	132	fb
581	192	957	235	V4	635	371	317	054	fa
582	579	348	231	db	636	572	413	159	fc
583	391	329	062	b	637	549	319	230	fb
584	433	287	146	b	638	548	347	201	fb
585	512	382	130	b	639	476	349	127	fb
586	371	308	063	V3	640	520	383	137	fb
587	372	302	070	a	641	176	094	082	fb
588	504	345	159	a	642	567	403	164	fc
589	573	433	140	b	643	357	157	200	fa
590	561	422	139	a	644	519	389	130	fb
591	388	303	085	V11	645	544	409	135	fb
592	467	292	175	a	646	415	258	157	fb
593	537	376	161	b	647	481	384	097	fb
594	344	180	164	b	648	493	440	053	fc

TABLE 12—*Continued*

Star	m_{pg}	m_{HPr}	C_r	Notes	Star	m_{pg}	m_{HPr}	C_r	Notes
649.....	526	366	160	fb	656.....	353	240	113	fa
650.....	485	328	157	fb	657.....	520	313	207	fa
651.....	540	425	115	fc	658.....	440	313	127	fa
652.....	487	334	153	fb	659.....	559	440	119	fb
653.....	575	396	179	fb	660.....	529	365	164	fb
654.....	445	249	196	fc	661.....	357	168	189	fb
655.....	544	401	143	fb	662.....	535	323	212	fb

identified by "dd." Stars whose magnitude might possibly be affected by the background fog at the center of the cluster are called "n"; those so distant from the center that the uncertainty of the distance correction might be serious are "f." The variable stars are given by the symbol "V" followed by the number assigned to them by Miss Sawyer.[5] Suspected variables are merely identified with "V." The star 552 is a very close double, each component of which seems to be a red supergiant. No measures are given, because of their uncertainty, for the bright star 289.

This investigation, begun at the Harvard College Observatory, has been completed at the Yerkes Observatory during my tenure as National Research Fellow. I am deeply indebted to Dr. Shapley for his encouragement and advice and for his kind permission to use the plates he obtained at the Mount Wilson Observatory. I also wish to express my gratitude to Dr. Duncan for the use of plates taken by him at Mount Wilson and to Dr. Paraskevopoulos for the plates taken for me at the Harvard College Observatory at Bloemfontein. I am indebted to Dr. Carpenter for the use of the 36-inch reflector at the Steward Observatory.

YERKES OBSERVATORY
February 1939

TRANSITION PROBABILITIES FOR *He* I

LEO GOLDBERG

ABSTRACT

Simple, screening-type wave functions have been utilized to derive general expressions for the line strengths in the 2s−np and 2p−nd series of *He* I. The resulting strengths calculated for these series compare favorably with those computed by Hylleraas for the transitions up to $n = 6$. A computation of the radiational damping constants shows that the *He* I triplet damping factors are of the order of one hundred times smaller than the singlet values, a result that arises from the metastability of the lowest triplet level and from the short wave length of the fundamental singlet line.

The expressions for the discrete f-values have been extended to the continuum by the device of letting $n \rightarrow i\kappa$, where κ is a continuous quantum number, according to the method outlined by Menzel and Pekeris. The resulting expressions provide for the determination of the absorption coefficients for bound-free transitions from the 2s and 2p levels.

The f-sum rule of Kuhn and Thomas-Reiche predicts that the sum of the f-values of all transitions from a singly excited level of *He* I should equal unity. The rule appears to be satisfactorily obeyed for all but the $2\ ^3S$ level, for which the sum is 0.849.

The theoretical prediction of the absolute strengths of spectral lines requires a knowledge of the approximate wave functions of the upper and lower levels involved in each electronic transition. In compiling tables for the intensities of *He* I lines, Hylleraas[1] expressed each radial function as a linear combination of Laguerre polynomials with variationally determined coefficients. Calculations of this type are exceedingly laborious and must be performed separately for each transition. For astrophysical purposes the derivation of simple, general expressions which may readily be extended to include the continuum is highly desirable.

Recent investigations[2] have shown that relatively simple variational wave functions are sufficiently accurate to reproduce satisfactorily the observed energies of many of the excited levels of *He* I For example, the singlet p- and both the singlet and triplet d-eigenfunctions may be represented by hydrogenic functions, the former with effective charge 0.97 and the latter with charge unity. In this paper simple, screening-type wave functions will be employed to de-

[1] *Zs. f. Phys.*, **106**, 395, 1937.

[2] Morse, Young, and Haurwitz, *Phys. Rev.*, **48**, 952, 1936; Goldberg and Clogston, *Phys. Rev.*, vol. 56, no. 7, 1939.

velop general formulae for the absolute strengths in the diffuse and subordinate series of neutral helium.

The strength of a line or multiplet is defined as the sum of the absolute squares of the matrix components joining the two sets of states comprising the levels or the terms between which a transition takes place:

$$S = \sum [\int \psi (r_1 + r_2) \psi' d\tau]^2 , \tag{1}$$

where ψ and ψ' are the normalized wave functions of the atom in the initial and final states, respectively, $d\tau$ is the volume element, and

$$r = \left\{ \begin{matrix} r \cos \theta \\ r \sin \theta \cos \varphi \\ r \sin \theta \sin \varphi \end{matrix} \right\} \tag{2}$$

representing the components of electric moment in the x, y, and z directions. The summation in equation (1) is taken over all possible pairs of states.

If we adopt the Slater[3] approximation of expressing ψ as a determinant of one-electron wave functions, we may write, in the case of helium:

$$\psi_{1snl} = \frac{1}{\sqrt{2}} [u_1(1s) u_2(nl) \pm u_2(1s) u_1(nl)] , \tag{3}$$

where the subscripts refer to the electron co-ordinates, and the plus and minus signs to the singlet and triplet states, respectively. The u's are taken to be normalized to unity and mutually orthogonal, and, being solutions of Schrödinger's equation for an electron moving in a central field, they are separable into functions of the angular, distance, and spin variables:

$$u = \Phi(\theta,\varphi) R(r) \chi(\alpha) , \tag{4}$$

where Φ depends only upon θ and φ, R is a function of r alone, and χ is the spin wave function. If we make the further assumption that the wave function of the stationary $1s$-electron is unchanged

[3] *Phys. Rev.*, **34**, 1293, 1929.

when the outer electron is excited, the strength of a transition between two terms of *He* I is given by[4]

$$S(1snl^{2S+1}L \rightarrow 1sn'l'^{2S+1}L') = (2S+1)(2L+1)(l)(2l-1)\sigma^2 , \quad (5)$$

when $l' = l - 1$, where

$$\sigma^2 = \frac{a_0^2\epsilon^2}{4l^2-1}\left[\int_0^\infty r^3 R(nl)R(n', l-1)dr\right]^2 . \quad (6)$$

$R(nl)$ and $R(n', l-1)$ are the normalized radial wave functions, in atomic units, of the transition electron in the initial and the final configurations, a_0 is the radius of the first Bohr orbit, and ϵ is the electronic charge.

Separable wave functions of the type represented by equation (3) have been computed variationally by Morse, Young, and Haurwitz[5] for the terms $2\,{}^3S$, $2\,{}^1P^o$, and $2\,{}^3P^o$, and by Goldberg and Clogston for the $3\,{}^1P^o$, $3\,{}^3P^o$, n ${}^1D$ and n ${}^3D$ levels. The following radial functions have been obtained:

$$R(2s) = 0.356(re^{-0.610r} - 2.93e^{-1.57r}) , \qquad (2\,{}^3S) ; \quad (7)$$

$$R(2p) = 0.259re^{-0.550r} , \qquad (2\,{}^3P^o) ; \quad (8)$$

$$= 0.189re^{-0.485r} , \qquad (2\,{}^1P^o) ; \quad (9)$$

$$R(3p) = 0.00990r(14.2e^{-0.490r} - re^{-0.318r}) , \qquad (3\,{}^3P^o) ; \quad (10)$$

$$= 0.0184re^{-0.325r}(6.137 - r) , \qquad (3\,{}^1P^o) ; \quad (11)$$

$$R(nd) = \sqrt{\frac{2^6}{n^8}\frac{(n+2)!}{(n-3)!(5!)^2}}\, r^2 e^{-r/n} F\left(-n+3, 6, \frac{2r}{n}\right), \quad (n\,{}^3D, n\,{}^1D). \quad (12)$$

The 1*s*-functions associated with the above excited functions are all hydrogenic, with effective nuclear charge 2.00, i.e., the screening of the inner 1*s*-electron by the outer excited electron is in every case negligible. The ${}^1P^o$ functions (9) and (11) are similar to those for hydrogen, except that the hydrogenic charge of unity is replaced by

[4] Cf. Shortley, *Phys. Rev.*, **47**, 295, 1935. [5] *Op. cit.*

an effective charge of 0.97. The function (12) is exactly similar to the hydrogenic ^{2}D function. F is the confluent hypergeometric function:

$$F(\alpha, \gamma, x) = 1 + \frac{\alpha}{1!\gamma} x + \frac{\alpha(\alpha+1)}{2!\gamma(\gamma+1)} x^2 + \cdots . \qquad (13)$$

In deriving suitable approximations to the *He* I line strengths, we first consider the 2p—nd, or diffuse, series. The functions (8) and (9) may be represented by

$$R(2p) = \sqrt{\frac{4s^5}{3}}\, re^{-sr}, \qquad (14)$$

where $s(2\ ^3P^o) = 0.55$, and $s(2\ ^1P^o) = 0.485$. If we substitute equations (14) and (12) in equation (5) and integrate, we obtain for the square of the integral in (5), which we designate by ρ^2,

$$\rho^2 = 3^{-1}2^{10}s^5(3s-1)^2n^9(n^2-1)(n^2-4)\frac{(ns-1)^{2n-8}}{(ns+1)^{2n+8}}. \qquad (15)$$

If we set $s = \frac{1}{2}$, (15) becomes equivalent to the hydrogenic expression. Values of ρ^2 computed up to $n = 10$ are given in Table 1, where

TABLE 1

VALUES OF ρ^2 FOR 2p—nd SERIES OF He I
(Hylleraas' values in parentheses)

n	$2\ ^1P^o$—n ^1D		$2\ ^3P^o$—n ^3D	
3	24.9	(24.3)	16.1	(19.0)
4	2.87	(3.20)	2.84	(1.75)
5	0.897	(0.935)	1.02	(0.984)
6	0.407	(0.414)	0.491	(0.353)
7	0.222		0.279	
8	0.136		0.174	
9	0.0900		0.117	
10	0.0631		0.0824	

they may be compared with the Hylleraas values, recorded in parentheses.

We next consider the strengths in the 2s—np, or subordinate, series of *He* I. The effective nuclear charges derived for the $2\ ^1P^o$ and $3\ ^1P^o$ functions are so close to unity that we may reasonably employ the

hydrogenic np-functions in calculating the strengths in the $2\ ^1S - n\ ^1P^o$ series. For this purpose, the best available wave function for the $2\ ^1S$ level is that obtained by Coolidge and James,[6] who employ an expression of the form:

$$\psi_{1s2s} = \sum_{ab} C_{ab}[ab]\,, \tag{16}$$

where

$$[ab] = \frac{\kappa^3}{4\pi}\left[(\kappa r_1)^a e^{-\nu\kappa r_1}(\kappa r_2)^b e^{-\delta\kappa r_2} + (\kappa r_2)^a e^{-\nu\kappa r_2}(\kappa r_1)^b e^{-\delta\kappa r_2}\right]. \tag{17}$$

In equation (17), κ is a scale constant, equal to 1.05, while ν and δ are parameters, the latter being always equal to 2. The expression

TABLE 2

CONSTANTS IN COOLIDGE-JAMES $1s2s$ WAVE FUNCTION

	ab	C_{ab}
$\nu=0.55$	00	4.88925
	10	−0.02948
	01	−0.85415
	11	0.23488
	20	0.09866
	02	0.03271
$\nu=1.00$	00	−7.17757
	10	−2.26128
	01	1.39627

for ψ contains nine terms; for the first six, $\nu = 0.55$, corresponding to a two-quantum orbital with effective charge 1.10, while in the last three terms $\nu = 1$, corresponding to the part of the $2s$-orbit where the electron makes a close approach to the nucleus. The values of the constants in equations (16) and (17) are tabulated in Table 2.

Since equation (16) is not readily separable into one-electron wave functions, we employ equation (1) directly to calculate the strengths of the $2\ ^1S - n\ ^1P^o$ transitions. For the $n\ ^1P^o$ levels, we use the functions

$$\psi_{1snp} = \frac{1}{\sqrt{2}}\left[u_1(1s)u_2(np) + u_2(1s)u_1(np)\right], \tag{18}$$

[6] *Phys. Rev.*, **49**, 676, 1936.

where $u(1s)$ is the wave function of an electron moving in the field of the bare helium nucleus, and $u(np)$ refers to the hydrogenic np-eigenfunctions:

$$u(1s) = \sqrt{\frac{8}{\pi}}\, e^{-2r}\,; \tag{19}$$

$$u(np) = \sqrt{\frac{2^3(n+1)!Z^5}{n^6(n-2)!3!4\pi}} \cos\theta r e^{-Zr/n} F\left(-n+2,\, 4,\, \frac{2Zr}{n}\right), \tag{20}$$

where $Z = 1$.

For a $^1S - {}^1P^o$ transition, the strengths of the three separate line components are equal. Hence, we calculate the strength of the z-matrix component and multiply by three to obtain the total line strength:

$$\boldsymbol{S}(2\,{}^1S - n\,{}^1P^o) = 3\left[\sum_{ab} C_{ab}\int [ab](r_1\cos\theta_1 + r_2\cos\theta_2)\psi_{1snp}\,d\tau\right]^2. \tag{21}$$

The evaluation of equation (21) is straightforward, although somewhat tedious. We obtain, in units of $a_0^2\,\epsilon^2$,

$$\left.\begin{aligned}
&\boldsymbol{S}(2\,{}^1S - n\,{}^1P^o) \\
&\quad = 38.10n^7(n^2-1)\left\{0.2299\,\frac{(0.5775n-1)^{n-3}}{(0.5775n+1)^{n+3}}\right. \\
&\qquad\qquad \left[1 + 0.4803(1 - 0.2200n^2)\,\frac{(0.5775n-1)^{-1}}{(0.5775n+1)}\right. \\
&\quad + 1.119n^2(1 - 0.2459n^2)\,\frac{(0.5775n-1)^{-2}}{(0.5775n+1)^2}\Bigg] \\
&\quad - 2.338\,\frac{(1.050n-1)^{n-3}}{(1.050n+1)^{n+3}}\left[1 + 0.7072(1 + 1.262n^2)\right. \\
&\qquad\qquad \left.\left.\left.\frac{(1.050n-1)^{-1}}{(1.050n+1)}\right]\right\}^2.
\end{aligned}\right\} \tag{22}$$

If we evaluate equation (22) for $n = 2$ and $n = 3$, we obtain

$$\boldsymbol{S}(2\,{}^1S - 2\,{}^1P^o) = 25.6\,;$$

$$\boldsymbol{S}(2\,{}^1S - 3\,{}^1P^o) = 1.94\,.$$

The strengths for these transitions may also be computed directly from equation (21), if we employ equations (9) and (11) in place of the hydrogenic functions. The resulting values 26.4 and 2.60 compare favorably with those computed from equation (22). Values of the strengths computed for the $2\ ^1S - n\ ^1P^o$ series are shown in Table 3. The Hylleraas values are again given in parentheses and are in excellent agreement with the present values.

Although the variational $^1P^o$ functions (9) and (11) justify the use of hydrogenic p-functions to represent the $n\ ^1P^o$ levels, the results

TABLE 3

LINE STRENGTHS IN $2\ ^1S - n\ ^1P^o$ SERIES

n	$2\ ^1S - n\ ^1P^o$	
2	26.4	(26.5)
3	2.60	(2.48)
4	0.744	(0.806)
5	0.300	(0.292)
6	0.154	(0.139)
7	0.0897	
8	0.0573	
9	0.0396	
10	0.0279	

for $2\ ^3P^o$ and $3\ ^3P^o$ indicate that such an approximation is invalid for the triplet levels. As a second approximation, however, we may adopt the functions (20) and employ an effective value of Z, the nuclear charge that will take account of the screening of the nucleus by the inner $1s$-electron. The effective value of Z for the $2p$-electron is 1.10, and, although the screening may well vary with the total quantum number, it will be interesting to compare the strengths in the $2\ ^3S - n\ ^3P^o$ series, derived on the assumption of $Z = 1.10$ for the $n\ ^3P^o$ levels, with the Hylleraas values. If we substitute equations (7) and (20) with $Z = 1.10$ in equation (5), and integrate, we find for the square of the radial quantum integral:

$$\rho^2 = 52.3n^7(n^2 - 1)\left\{\frac{(0.610n - 1.10)^{n-4}}{(0.610n + 1.10)^{n+4}}(1.21 - 0.284n^2) - 2.99\frac{(1.57n - 1.10)^{n-3}}{(1.57n + 1.10)^{n+3}}\right\}^2. \tag{23}$$

If we evaluate ρ^2 for the first two lines of the series, we find, respectively, 19.3 and 1.06. The latter value compares favorably with the value 0.918, obtained by employing the variational function (10) in place of the less accurate hydrogenic function. Table 4 contains values of ρ^2 computed up to $n = 10$. The good agreement with Hylleraas' values is gratifying, in view of the highly approximate nature of the np-functions.

Damping constants for He I. The material of the preceding section may now be utilized to derive radiation damping constants for the

TABLE 4

VALUES OF ρ^2 FOR $2\ ^3S - n\ ^3P^o$ SERIES

n	$2\ ^3S - n\ ^3P^o$	
2	19.3	(19.9)
3	0.918	(0.666)
4	0.284	(0.322)
5	0.119	(0.125)
6	0.0621	(0.0621)
7	0.0368	
8	0.0237	
9	0.0161	
10	0.0116	

helium lines. The radiation damping constant for a spectral line is equal to the sum of the reciprocal mean lives of the two levels involved in the atomic transition:

$$\Gamma_{nn'} = \frac{1}{T_n} + \frac{1}{T_{n'}}. \tag{24}$$

In the absence of collisions, the reciprocal mean lifetime of a level is simply

$$\frac{1}{T_n} = \sum_{n'} A_{nn'}, \tag{25}$$

where $A_{nn'}$ is the Einstein probability of spontaneous transition from level n to level n'. In terms of the strength of a line,

$$A_{nn'} = \frac{64\pi^4}{3\lambda^3 h} \frac{\mathbf{S}_{nn'}}{\bar{\omega}_n}, \tag{26}$$

where $\bar{\omega}_n$ is the statistical weight of the upper of the two levels. For a degenerate term,

$$\bar{\omega}_n = (2S + 1)(2L + 1)\,, \tag{27}$$

corresponding to the number of individual states comprising the term. The classical analogue of $\Gamma_{nn'}$ is $1/\tau$, where τ is the time taken for the amplitude of an oscillating dipole to fall to 1-eth of its maximum value. For radiation damping alone,

$$\tau = \frac{3mc^3}{8\pi^2\epsilon^2\nu^2} = 4.52\lambda^2\,. \tag{28}$$

At λ 5000 the classical damping factor has the value 8.85×10^7. Empirical determinations[7] of the damping constant from solar curves of growth have pointed toward a value about nine times the classical one for metallic lines, while quantum-mechanical calculations[8] for hydrogen have yielded similar results. Empirically determined damping factors will naturally include the effects of collisionally induced, as well as spontaneous, transitions. Theoretical determinations of the radiational constant will, therefore, contribute to the study of collisional processes in stellar atmospheres.

The computation of radiational damping constants for the singlet lines of helium requires a knowledge of the Einstein A's for the principal series. For this series, the results given by Vinti[9] and checked by the writer have been employed. The occurrence of the inverse λ^3 term in the expression for $A_{nn'}$ is fortunate. The procedure involved in calculating the damping constant for a transition between levels n and n' is, then, simply the following. To the Einstein A for the transition n–n', we add the corresponding A's for the transitions from levels n and n' to the lowest level of the same multiplicity. The contributions from all other transitions become negligible because of the λ^3 factor, even though the strengths themselves may be quite large.

[7] Minnaert and Mulders, *Zs. f. Ap.*, **2**, 165, 1931; Allen, *Mem. Comm. Solar Obs.*, **1**, No. 5, 1934; Menzel, Baker, and Goldberg, *Ap. J.*, **87**, 81, 1938.

[8] Menzel, *Lick Obs. Bull.*, **17**, 234, 1931.

[9] *Phys. Rev.*, **42**, 632, 1932.

The results for most of the important lines of *He* I are collected in Table 5. On the average, the damping constants for the singlet lines are of the order of one hundred times greater than those for the triplets. This result arises, of course, from the metastability of the lowest triplet level and also from the very short wave length of the singlet resonance line. There is little doubt of the metastability of both the $2\ ^3S$ and $2\ ^1S$ levels, in so far as spontaneous transitions

TABLE 5

DAMPING CONSTANTS FOR He I LINES

Transition	λ	$A_{nn'}\times10^{-6}$	$\Gamma\times10^{-9}$	$\Gamma/\nu\times10^{6}$
$1\ ^1S$ — $2\ ^1P^o$	584	2340.	2.34	0.456
$2\ ^1S$ — $2\ ^1P^o$	20582	2.05	2.34	16.0
— $3\ ^1P^o$	5016	14.0	0.575	0.961
— $4\ ^1P^o$	3965	8.13	0.239	0.316
$2\ ^1P^o$ — $3\ ^1D$	6678	68.3	2.41	5.36
— $4\ ^1D$	4922	19.7	2.36	3.87
— $5\ ^1D$	4388	8.67	2.35	3.44
— $6\ ^1D$	4144	4.67	2.34	3.23
— $7\ ^1D$	4009	2.82	2.34	3.13
— $8\ ^1D$	3927	1.83	2.34	3.06
— $9\ ^1D$	3872	1.27	2.34	3.02
—$10\ ^1D$	3834	0.915	2.34	2.99
$2\ ^3S$ — $2\ ^3P^o$	10830	10.3	0.0103	0.0372
— $3\ ^3P^o$	3889	10.6	0.0106	0.0137
$2\ ^3P^o$ — $3\ ^3D$	5876	64.7	0.0753	0.147
— $4\ ^3D$	4472	25.9	0.0362	0.0540
— $5\ ^3D$	4026	12.8	0.0231	0.0310
— $6\ ^3D$	3820	7.19	0.0175	0.0223
— $7\ ^3D$	3705	4.48	0.0148	0.0183
— $8\ ^3D$	3634	2.96	0.0133	0.0161
— $9\ ^3D$	3587	2.07	0.0124	0.0148
—$10\ ^3D$	3555	1.50	0.0118	0.0140

to the ground state are concerned. Such transitions are zero for electric and magnetic dipole, and for electric quadrupole, radiation. Consequently, in the absence of external influences, the mean lives of the $2s$-levels should be infinite.

f-Values for the continuum. Vinti[10] has derived a general formula giving the f-value or ionization probability from the ground state of helium to any point in the continuum. Similar formulae may now be derived for the absorption probabilities from the $2\ ^1S$, $2\ ^3S$, $2\ ^1P^o$,

[10] *Ibid.*, **44**, 524, 1933.

and 2 $^3P^o$ levels. The f-value for a line is given in terms of the strength, by

$$f_{n'n} = \frac{8\pi^2 \nu_{nn'} m}{3e^2 h} \frac{S_{nn'}}{\bar{\omega}_{n'}} . \tag{29}$$

Following Menzel and Pekeris,[11] we introduce a continuous quantum number κ, which is defined by the relation

$$\chi_\kappa = \frac{1}{\kappa^2} , \tag{30}$$

where χ_κ is the energy in atomic units of any point in the continuum, measured from the series limit. The frequency of a bound-free transition becomes

$$\nu_{n'\kappa} = R\left(\chi_{n'} + \frac{1}{\kappa^2}\right) , \tag{31}$$

where $\chi_{n'}$ is the energy of the discrete level n'. If we substitute equation (4) in equation (29) and employ equation (16), we obtain for the 2p—nd series

$$\left.\begin{aligned} &f(2\text{p} - \text{nd}) \\ &\quad = \frac{2^{14}\pi^2 a_0^2 \nu m}{27h} s^5(3s - 1)^2 n^9 (n^2 - 1)(n^2 - 4) \frac{(ns - 1)^{2n-8}}{(ns + 1)^{2n+8}} . \end{aligned}\right\} \tag{32}$$

Menzel and Pekeris[12] have shown that the general expression for the f-values of discrete transitions in hydrogen may be extended to include bound-free transitions by letting $n \to i\kappa$ and by taking the absolute value of the resulting expression. If we apply the same procedure to equation (32), we find for the continuous f-values:

$$\left.\begin{aligned} f(2\text{p} - \kappa\text{d}) &= D \frac{2^{14}\pi^2 a_0^2 \nu m}{27h} \\ &\quad s^5(3s - 1)^2 \kappa^9 (\kappa^2 + 1)(\kappa^2 + 4)(1 + s^2\kappa^2)^{-8} e^{-4\kappa \tan^{-1}(1/s\kappa)} . \end{aligned}\right\} \tag{33}$$

[11] *M.N.*, **96**, 77, 1935. [12] *Ibid.*

The factor D is inserted to take account of the normalization of the continuous wave functions.[13] For bound-free transitions,

$$D = (1 - e^{-2\pi\kappa})^{-1}. \tag{34}$$

D becomes appreciable only at very small values of κ, for which the ionization probabilities are relatively insignificant.

We find similarly for the $2s - \kappa p$ series

$$\left.\begin{aligned} &f(2\,{}^1S - \kappa\,{}^1P^0) \\ &\quad = D\,\frac{8\pi^2\nu m a_0^2}{3h} \times 12.70\kappa^7(\kappa^2+1)\{0.2299 \\ &(1+0.3335\kappa^2)^{-3} e^{-2\kappa\tan^{-1}(1.73/\kappa)}[1 - 0.4803(1+0.2200\kappa^2) \\ &(1+0.3335\kappa^2)^{-1} - 1.119\kappa^2(1+0.2459\kappa^2)(1+0.3335\kappa^2)^{-2}] \\ &\quad - 2.338(1+1.102\kappa^2)^{-3} e^{-2\kappa\tan^{-1}(0.952/\kappa)}[1 - 0.7072 \\ &(1-1.262\kappa^2)(1+1.102\kappa^2)^{-1}]\}^2 \end{aligned}\right\} \tag{35}$$

and

$$\left.\begin{aligned} f(2\,{}^3S - \kappa\,{}^3P^0) &= D\,\frac{8\pi^2\nu m a_0^2}{3h} \\ &\quad \times 52.3\kappa^7(\kappa^2+1)\{(1.21+0.372\kappa^2)^{-4} \\ &(1.21+0.284\kappa^2) e^{-2\kappa\tan^{-1}(1.10/0.610\kappa)} \\ &\quad + 2.99(1.21+2.46\kappa^2)^{-3} e^{-2\kappa\tan^{-1}(1.10/1.57\kappa)}\}^2. \end{aligned}\right\} \tag{36}$$

The expressions (33), (35), and (36) may be employed to derive the absorption coefficients beyond the limits of the various series. The atomic absorption coefficient for the continuum is

$$a_\nu = \frac{\pi\epsilon^2}{mc}\frac{df}{d\nu}, \tag{37}$$

where, by definition,

$$df = f d\kappa. \tag{38}$$

[13] *Ibid.*

Differentiating expression (31) with respect to κ, we obtain

$$\frac{d\nu}{d\kappa} = -\,2R\kappa^{-3}\,, \tag{39}$$

and

$$a_\nu = -\,\frac{\kappa^3}{2R}\,\frac{\pi\epsilon^2}{mc}\,f\,. \tag{40}$$

The variations of the absorption coefficients for the diffuse and subordinate series are shown in Figure 1, where the logarithm of the absorption coefficient has been plotted against the logarithm of the frequency in Rydberg units. Close to the series limit, where κ is very large, expressions (33), (35), and (36) may be expanded in powers of $1/\kappa^2$. We find, numerically,

$$\left.\begin{aligned} f(2\mathrm{p} - \kappa\mathrm{d}) &\sim 2.31 \\ &\times 10^{-14}s^{-11}(3s-1)^2 e^{-4/s}\nu\kappa^{-3}\left[1 + \frac{1}{\kappa^2}\left(\frac{4}{3s^3} - \frac{8}{s^2} + 5\right)\right]; \end{aligned}\right\} \tag{41}$$

$$f(2\,{}^1\mathrm{S} - \kappa\,{}^1\mathrm{P}^0) \sim 8.63 \times 10^{-16}\nu\kappa^{-3}\left(1 - \frac{9.12}{\kappa^2}\right); \tag{42}$$

$$f(2\,{}^3\mathrm{S} - \kappa\,{}^3\mathrm{P}^0) \sim 1.08 \times 10^{-15}\nu\kappa^{-3}\left(1 - \frac{7.90}{\kappa^2}\right). \tag{43}$$

Hence, by expressions (30), (38), and the binomial law,

$$a_\nu(2\,{}^3\mathrm{P}^0 - \kappa\,{}^3\mathrm{D}) \propto \nu^{-2.6}\,; \tag{44}$$

$$a_\nu(2\,{}^1\mathrm{P}^0 - \kappa\,{}^1\mathrm{D}) \propto \nu^{-3.2}\,; \tag{45}$$

$$a_\nu(2\,{}^1\mathrm{S} - \kappa\,{}^1\mathrm{P}^0) \propto \nu^{-1.7}\,; \tag{46}$$

$$a_\nu(2\,{}^3\mathrm{S} - \kappa\,{}^3\mathrm{P}^0) \propto \nu^{-1.8}\,. \tag{47}$$

The f-sum rule. According to the sum rule of Kuhn and Thomas-Reiche,[14] the sum of the f-values of all lines originating from a given level in an atom is equal to z, the so-called number of "optical electrons." The summation includes both the absorption and the emis-

[14] Cf. Unsöld, *Sternatmosphären*, p. 190.

sion from each level. If n' designates the level from which transitions are occurring, the f-sum rule may be written as

$$\sum_n f_{n'n} + \int_0^\infty f_{n'\kappa} d\kappa - \sum_n \frac{\bar{\omega}_n}{\bar{\omega}_{n'}} f_{nn'} = z \,, \tag{48}$$

where the $\bar{\omega}$'s are statistical weight factors. The first term represents the line absorption from level n', the third term accounts for

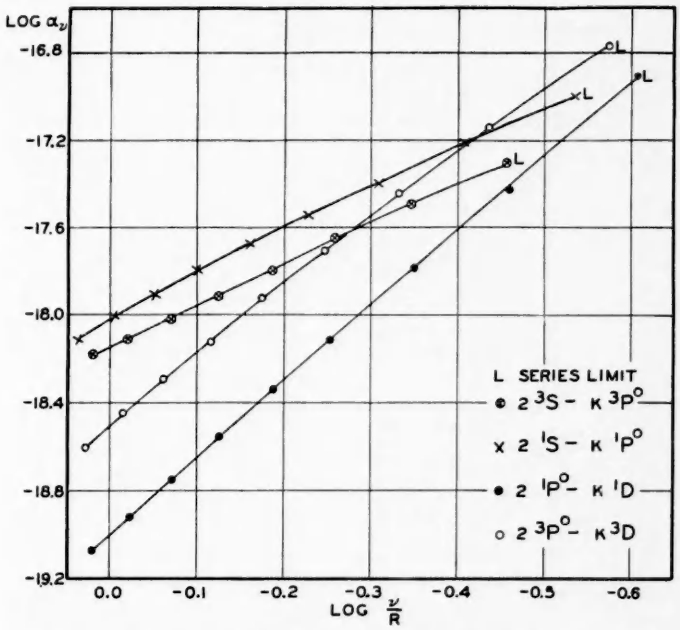

FIG. 1.—Variation of *He* I ionization probabilities with frequency

the downward transitions from n', while the second term represents the contribution to the sum from bound-free transitions. Care must be exercised in choosing the proper value of z for *He* I. For the principal series, $z = 2$, since either of the two 1*s*-electrons may jump during a transition from the ground state. Vinti[10] has obtained the value 2.13 for the sum of the f-values from 1 ^1S. Only one electron is excited, however, during transitions from the excited states, and, accordingly, the f-values for the diffuse and subordinate series should sum to unity, as for hydrogen. This conclusion may be tested by calculating and summing the oscillator strengths for these series.

The results are shown in Table 6. The summations from $n = 11$ to $n = \infty$ have been computed from the asymptotic forms of the expressions for f when n is large. The integration over the continuous f-values has been performed numerically by using equations (33), (35), and (36). The final sums for the diffuse series are less than unity, which is to be expected, since we have not included the positive f-values for the 2p − ns series. The sum of these values for hydrogen is 0.111 and appears to be of the same order of magnitude for helium. In the singlet subordinate series the value 0.963 is satisfactorily close to unity, but the triplet sum 0.849 is too small. Probably the device of employing $Z = 1.10$, while suitable for the discrete transitions, is invalid when applied to the continuum.

TABLE 6

He I f-VALUES

n	$2\,{}^1S-n\,{}^1P^o$	$2\,{}^3S-n\,{}^3P^o$	$2\,{}^1P^o-n\,{}^1D$	$2\,{}^3P^o-n\,{}^3D$
2	0.389	0.542	.....	.....
3	.157	.0826	0.755	0.553
4	.0570	.0270	.118	.129
5	.0252	.0123	.0416	.0512
6	.0136	.00665	.0199	.0260
7	.00813	.00404	.0112	.0152
8	.00528	.00264	.00705	.00968
9	.00369	.00182	.00471	.00658
10	0.00263	0.00132	0.00333	0.00469
$\sum_{n=11}^{\infty} f_n$	0.004	0.005	0.006	0.018
$\int_0^{\infty} f\,d\kappa$	0.297	0.163	0.157	0.291
Sum	0.963	0.849	1.124	1.105
$-f_{2p-2s}$	.....	.....	−0.130	−0.181
$-f_{2p-1s}$	.....	.....	−0.116	0.924
	.....	.....	0.878	.....

The writer is pleased to acknowledge his indebtedness to Professors D. H. Menzel and P. M. Morse for numerous profitable discussions of the wave-mechanical problems treated in this paper.

HARVARD OBSERVATORY
May 1939

THE NUMBER OF LINES IN A SERIES AS A FUNCTION OF ELECTRON PRESSURE

FRED L. MOHLER

ABSTRACT

In an intense discharge the higher lines of a series merge into a continuous spectrum at a value of the effective quantum number n_m which depends upon the electron concentration N_e. A previous paper by the author gives values of the electron concentration for the caesium discharge for a wide range of vapor pressures and current densities. The number of lines in the D and F series have been determined for this range of conditions. The maximum quantum number for the red component of the D series and for the F series is given by the equation $\log N_e = 23.06 - 7.5 \log n_m$.

This relation agrees well with theoretical results for hydrogenic spectra and has been applied to stellar spectra. For main-sequence Ao stars the electron pressure in atmospheres is 0.4×10^{-4} at the Balmer limit; 0.7×10^{-4} at the Paschen limit, and 1.8×10^{-4} at 4340 A. The star α Cygni has a pressure of about 1×10^{-6} At. at the Balmer limit, while for white dwarfs the pressure exceeds 10^{-2} At.

I. INTRODUCTION

In the spectrum of an intense discharge the successive lines of a series are increasingly broadened until they merge into a continuous spectrum at a fairly definite interval from the theoretical series limit. The width of lines is a complicated function of temperature, pressure, and ionization, but for the higher lines of a series in an intense discharge the ionization broadening must be of primary importance. Consequently, the number of lines in a series should be a function of the electron concentration alone for a discharge of high-current density. Since states of high quantum number are hydrogenic, the relation between the number of lines and the electron concentration will be nearly the same for all elements. Because of the generality of the relation, the number of lines in a series should be a useful basis for estimating the concentration of electrons where other methods cannot be used. To preserve the generality of the results the effective quantum number (the square root of the Rydberg denominator) should be used.

Recent work[1] on the caesium discharge under conditions of nearly

[1] F. L. Mohler, *J. Res. Nat. Bur. Stand.*, **21**, 697, 1938.

complete ionization affords a basis for determining the number of lines in a series for a wide range of electron concentrations. It is an important advantage to have the percentage of ionization high enough so that other types of broadening are negligible, while measurements over a wide range minimize the effect of experimental uncertainties.

II. EXPERIMENTAL PROCEDURE

The apparatus and procedure have been described before.[1] Current densities sufficient to maintain a high percentage of ionization were obtained by running a discharge through a section of capillary tubing. The capillary was viewed from the end and was photographed with a three-prism Steinheil spectrograph with a focal length of 72 cm. Exposures were timed to give measurable photographic densities for both the lines and the continuous spectrum between the lines near the ends of the series, and a series of exposures to a calibrated strip lamp gave a scale of relative intensity. Exposure times ranging from 0.01 sec. to many hours were required. Values of the electron concentration for a given current density and vapor pressure were taken from the previous paper.[1] These values are based largely on the absolute intensity of the continuous recombination spectrum.

Plate VI shows some typical spectra. The theoretical limits of the F series are at 5950 and 5920 A and of the D series at 5100 and 4950 A. For the highest pressure and current the D series ends near the sixth doublet, 5635 and 5466 A, and there are no F-series lines in the range of the plate, while for the lowest current density there are over 20 doublets in each series. The violet component of the D series extends beyond the other series and is easiest to measure. The end of this series has been determined in all cases, and a few measurements have been obtained for the red component of the D series and for the F series.

Figure 1 illustrates the method used to determine the end of the series. The intensity at the center of a line and for the continuous spectrum near the line was measured for a few lines near the end of the series. The log of the intensity ratio of line to background was plotted against the log of the quantum number, and a straight line

PLATE VI

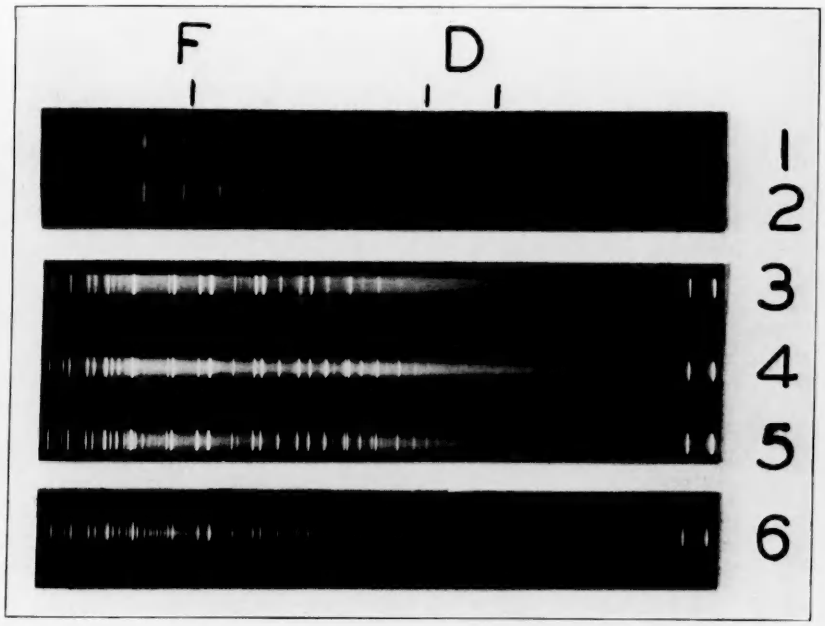

CAESIUM SPECTRA FROM 6500 A (*left*) TO 4500 A

Letters indicate the theoretical series limits. Electron concentrations: 1: 1.2×10^{16}; 2: 5×10^{15}; 3: 1.0×10^{15}; 4: 3.6×10^{14}; 5: 1.4×10^{14}; 6: 2×10^{12}.

was drawn through the points. The intercept of this line at $\Delta \log J = 0$ is taken as the maximum quantum number. In some cases the points seem to fall on a curve which is concave upward, but in all cases a straight line has been drawn neglecting the toe of the curve. Numbers over the curves give vapor pressures in millimeters, and the electron pressures are about half of these numbers.

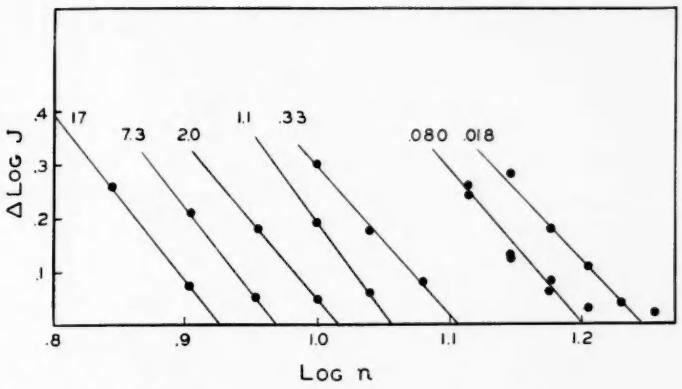

FIG. 1.—Plots of relative intensity of line to background versus quantum number on a logarithmic scale for lines near the end of the violet component of the D series. Numbers above curves are vapor pressures in mm.

Figure 2 is a logarithmic plot of the maximum effective quantum number n_m as a function of electron concentration. Dots are values for the violet component of the D series measured under conditions of over 50 per cent ionization. Circles are some measurements with low currents and low ionization. For this case the series are very long, and both instrumental resolution and pressure broadening may influence the results.

The lower straight line through the dots has a slope of 0.140, and the equation for log n_m for the violet component of the diffuse series can be written

$$\log n_m = 3.156 - 0.140 \log N_e . \qquad (1)$$

Some measurements of n_m for the red component and for the F series give n_m about half a unit higher than for the violet component. The

upper line of Figure 2 has been drawn half a unit above the first line and the equation of the line is

$$\log n_m = 3.175 - 0.140 \log N_e . \qquad (2)$$

The difference between the two components of the D series seems to come from the fact that the violet components of the D series are superposed on the strong continuous spectrum near the limit of the

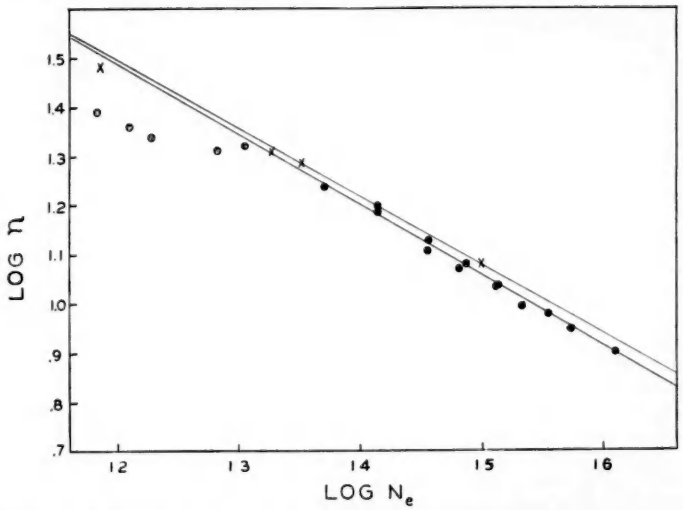

FIG. 2.—The maximum effective quantum number versus electron concentration on a logarithmic scale. Dots and circles: the violet component of the D series; upper line: red component of D series and of F series; crosses: theoretical values for Balmer series of hydrogen.

red component. The second equation is probably more nearly representative of the case of a simple hydrogenic series. It is of interest that the F and D series end at nearly the same value of n_m. An inspection of some spectrograms of other elements indicates that it is generally true that different series end at about the same effective quantum number.

III. COMPARISON WITH THEORY

A paper by Inglis and Teller[2] covers the theory of the effect. A very general but elementary treatment of the effect both of collisions

[2] P. 439 of this *Journal*.

and of Stark effect by Sugita[3] gives relations between the number of lines and electron concentrations that are not in good agreement with theory, for it gives values of n_m about five units larger than observed.

Recently, Pannekoek[4] published detailed computations of the intensity distribution near the limit of the Balmer series for various values of the random field of ions and electrons. The results are presented as plots of spectral intensity distribution, and from these plots n_m can be determined by the graphical method shown in Figure 1. The points fall on curves that are definitely concave upward, but the same criteria have been used as before to determine the intercept. These results are shown as crosses in Figure 2 and are seen to agree accurately with the upper line.

Inglis and Teller[2] have investigated the theory in a more general way and derive the following equation for the ion density,

$$N = 1.84 \times \frac{10^{23}}{n_m^{7.5}}. \tag{3}$$

They show that this relation will remain approximately true for different series and for alkali-type spectra as well as for hydrogen. For temperatures less than $10^5/n_m$ degrees absolute, electrons contribute to the Stark effect, and N of equation (3) is $2N_e$. At higher temperatures the effectiveness of electrons decreases.

Most of these measurements have been made at temperatures less than the critical value, and for comparison with experiment $2N_e$ should be used in equation (3). Plotted on the scale of Figure 2, equation (3) gives a line so close to the experimental lines that it is confusing to include it in the figure. It is coincident with the upper line of Figure 2 at $\log N_e = 16$, and 0.02 units below this line at $\log N_e = 14$. The slight difference in slope may be a real temperature effect but is less than the estimated experimental uncertainties. Equation (3) with $N = 2N_e$ can be written

$$\log N_e = 22.96 - 7.5 \log n_m. \tag{4}$$

[3] *Proc. Phys. Math. Soc.* (Japan), **16**, 254, 1934. [4] *M.N.*, **98**, 694, 1938.

A line of this slope but coincident with the upper experimental line at $\log N_e = 15$ gives

$$\log N_e = 23.06 - 7.5 \log n_m . \qquad (5)$$

Equation (5) will be used to estimate electron pressures in stellar atmospheres. The electron pressure in atmospheres is

$$1.35 \times 10^{-22} TN_e$$

or

$$\log P_e = 1.19 + \log T - 7.5 \log n_m . \qquad (6)$$

The electron concentration in stellar atmospheres covers nearly the range of Figure 2, and the temperature is roughly twice the temperature used in laboratory experiments. This will somewhat exceed the critical temperature $10^5/n_m$, with the result that the effective ion concentration is somewhat less than $2N_e$. The error is not serious, for the number of lines in a series gives necessarily an insensitive measurement of N_e. An experimental uncertainty of at least 20 and probably of 40 per cent in the absolute values of N_e is to be expected.

IV. APPLICATION TO STELLAR SPECTRA

Pannekoek has used his computed curves of intensity distribution near the Balmer limit to estimate the electron pressure in the solar chromosphere, and the results are in satisfactory agreement with estimates by Menzel and Cillié made on the basis of the intensity of the continuous spectrum.[5]

Sugita[3] has used his theoretical relations to estimate electron pressures in some class A and B stars on the basis of the number of absorption lines in the Balmer series as measured by Ching Sung Yü.[6] These values tend to be higher than estimates based on other considerations. This comes in part from the errors in his approximations, but the method can only set an upper limit to the electron pressure. Instrumental resolution, Doppler effects from thermal agi-

[5] *Ap. J.*, **85**, 88, 1937. [6] *Lick Obs. Bull.*, No. 422, 1930.

tation and stellar rotation, and pressure broadening from neutral atoms will all tend to make the computed pressure too high.

Some high-dispersion stellar spectra published by Merrill and Wilson[7] reduce observational uncertainties to a minimum. They give quantitative intensity measurements for the Balmer and the Paschen series of five stars. In Figure 3 their data for the intensity ratio of background to absorption line have been plotted against n on a

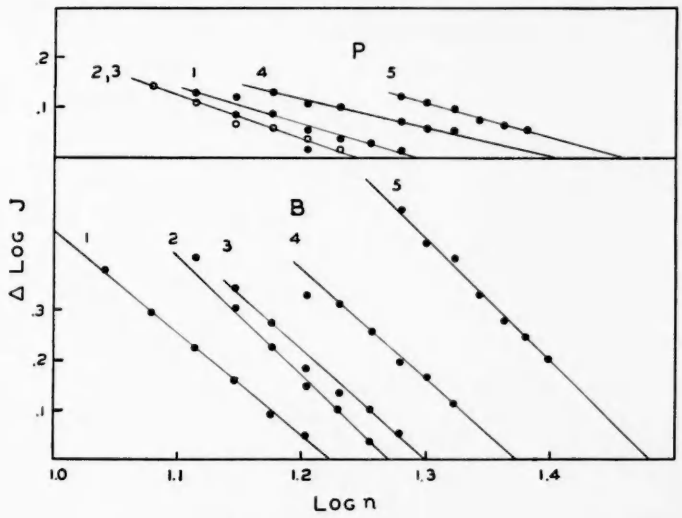

FIG. 3.—Relative intensity of background to line versus quantum number on a log scale for stellar absorption spectra. *Above:* Paschen series; *below:* Balmer series. 1: α Leonis; 2: α Canis Majoris; 3: α Lyrae; 4: β Orionis; 5: α Cygni.

logarithmic scale. The plots are strikingly similar to the plots of Figure 1 for caesium emission spectra in spite of the fact that the physical significance of the ordinates is quite different in the two cases. The intercepts of these plots should give values of n_m directly comparable with values from the caesium emission spectrum. For some series the intensity data are incomplete, but in all cases the intercepts of Figure 3 agree within a unit with the estimates given by Merrill and Wilson for the ends of the series. Figure 3 shows that the contrast between line and background is much smaller in the

[7] *Ap. J.*, 80, 1, 1934.

Paschen series than in the Balmer series, but this does not necessarily make n_m less.

Table 1 lists the stars, their spectral types and temperatures, the values of n_m from Figure 3 and the values of P_e obtained from equation (6). The significance of P_e requires consideration. At a given wave length the light comes from an effective depth in the stellar atmosphere which depends upon the opacity of the atmosphere at that wave length. Values of P_e derived from the number of

TABLE 1

ELECTRON PRESSURES IN STELLAR ATMOSPHERES

STAR	CLASS	TEMP.*	n_m		P_e (ATMOSPHERES)		
			Balmer	Paschen	3650 A	8200 A	4340 A
α Can Maj.	Ao	9400°	18.6	17.5	0.42×10^{-4}	0.69×10^{-4}	1.8×10^{-4}
α Lyrae....	Ao	9400	20	17.5	0.26×10^{-4}	0.69×10^{-4}	1.8×10^{-4}
α Cygni....	cA2	8450	30	28.5	1.1×10^{-6}	1.6×10^{-6}	4.1×10^{-6}
β Orionis...	cB8	10000	23.5	25.0	8.1×10^{-6}	5.1×10^{-6}	13×10^{-6}
α Leonis....	B8n	10000	16.7	19.5	.....	.....	.....

* Payne, *The Stars of High Luminosity* ("Harvard Obs. Monographs," No. 3), 1930.

lines in the Balmer and the Paschen series pertain to the electron pressures at the photosphere at or near the Balmer and the Paschen limits, respectively. In an isothermal hydrogen atmosphere the total pressure will vary inversely as the absorption coefficient, and by Saha's equation the electron pressure will be inversely proportional to the square root of the absorption coefficient.

Russell[8] has given a detailed analysis of stellar opacity assuming that opacity comes entirely from *Grenz-Continua* and from the absorption of free electrons and ions. He has derived values for the electron pressure at the photosphere near 4340 A. Between the Paschen limit and 4340 A the electron pressure is assumed to vary inversely as the 3/2 power of the wave length. Hence,

$$P_e\,(4340\text{ A}) = 2.6\,P_e\,(8200\text{ A})\,. \qquad (7)$$

The last column of Table 1 is computed on this basis. Russell's theory gives a value of $P_e = 0.8 \times 10^{-4}$ At. for main-sequence Ao

[8] *Ap. J.*, **78**, 295, 1933.

stars. This is to be compared with the value of 1.8×10^{-4} At. for both α Canis Majoris and α Lyrae.

The difference between values of P_e for the Balmer and the Paschen limits depends upon the difference in opacity at the two limits. Assuming that the absorption comes entirely from the two *Grenz-Continua*, Gaunt's absorption equation[9] and the Boltzmann equation give the relation

$$\frac{P_e^2(8200)}{P_e^2(3650)} = \tfrac{8}{27} e^{(E_3 - E_2)/kT}, \tag{8}$$

where E_2 and E_3 are the energies of the second and third states. Equation (8) gives the electron pressure at the Paschen limit as 1.7 times the pressure at the Balmer limit at 9400° K, while Table 1 gives the ratios as 1.6 and 2.7 for α Canis Majoris and α Lyrae, respectively. The effect of continuous absorption from infrared series and free-free transitions is to reduce the ratio of $P_e(8200)/P_e(3650)$, and except for the case of α Leonis the observed ratios are in the range to be expected.

The c stars are supergiants of very low density and surface gravity. The electron pressure varies as the square root of the surface gravity for an ideal isothermal atmosphere, and on the basis of the data of Table 1 the surface gravity of α Cygni is 1/1600 that of α Canis Majoris. On other grounds the surface gravity of α Cygni has been estimated to be about 1/300 that of a main-sequence star.[10] In stars of class n all the lines are diffuse, and Doppler effect from stellar rotation is recognized as a probable cause of this.[11] If there is rotational broadening, the number of lines in a series does not give directly the electron pressure in class n stars. Because the Doppler width in frequency units is proportional to the frequency, the number of lines in the Paschen series will be less affected by Doppler effect than those in the Balmer series. The observational results for α Leonis can be explained if it is assumed that the equatorial velocity in the line of sight is 180 km/sec and that the ionization broadening is the same as for the class c supergiant β Orionis. This is not a

[9] *Proc. R. Soc.*, **126A**, 654, 1929.

[10] Payne, *The Stars of High Luminosity* ("Harvard Obs. Monographs," No. 3), 1930.

[11] Rosseland, *Theoretical Astrophysics*, Oxford, 1936.

unique solution, but a velocity less than 180 km/sec cannot explain the observed difference in n_m for the Balmer and the Paschen series, while a velocity much greater than 180 km/sec would be quite exceptional and would also imply that the intrinsic line-width was unusually small.

The white dwarfs have very wide Balmer lines, and random Stark effect is recognized as the probable cause.[12] The spectrum of 40 Eridani B (class Ao) shows $H\zeta$ distinctly while $H\eta$ is doubtful, so that n_m is about 9. Equation (6) gives the electron pressure 1.1×10^{-2} At., or about 260 times the pressure at the Balmer limit for Sirius.

On the basis of estimates quoted by Russell, Dugan, and Stewart[13] for the mass and radius of Sirius and of 40 Eridani B, the ratio of electron pressures would be 43, assuming that the mass absorption coefficients of the atmospheres are the same. In the spectrum of the dwarf van Maanen 1166 (class F),[14] the Balmer lines are more diffuse, but the end of the series is at nearly the same point, indicating that P_e is not much greater. Data quoted by Russell, Dugan, and Stewart indicate that P_e is 63 times that of Sirius. The spectrum[15] of Ci. *20* No. 398 (class A) is very similar to 40 Eridani B, except that the Balmer series ends near $n = 8$. This gives a value for P_e of about 2.6×10^{-2} At.

The number of lines in the Paschen and Balmer series offers a very direct but somewhat insensitive measure of the electron pressure at the photosphere of A and B stars. Results give values ranging from 1.1×10^{-6} At. for the supergiant *a* Cygni to 2.6×10^{-2} At. for the dwarf Ci 20 No. 398. The results are in all cases of the magnitude to be expected but cover a somewhat wider range than estimates based on other methods. However, all comparisons with other data involve simplifying assumptions as to the nature of stellar opacity and give in no case a direct check of the method.

NATIONAL BUREAU OF STANDARDS
June 13, 1939

[12] Pannekoek and Verwey, *Proc. K. Acad. v. Wetens. Amsterdam*, **38**, 479, 1935.

[13] *Astronomy*, **2**, 740, Boston, 1927.

[14] Öhman, *M.N.*, **92**, 71, 1931; this paper includes also a densitometer tracing of the spectrum of 40 Eridani B.

[15] Asklof and Ramberg, *Arkiv Mat. Astron. och Fysik*, **26**, B8, 1938.

IONIC DEPRESSION OF SERIES LIMITS IN ONE-ELECTRON SPECTRA

D. R. INGLIS AND E. TELLER

ABSTRACT

The effect of ionization of the surrounding atmosphere in broadening the high-series terms of the alkali spectra so that they form a continuum down to a quantum number n, is discussed theoretically. It is shown that the ion density is proportional to $n^{-7.5}$. The effect of the mobility of the electrons is investigated.

It is observed both in stellar atmospheres and in the laboratory, under conditions involving high density of ions, that the series limits of hydrogen-like spectra are depressed, the spectrum remaining normal up to a certain quantum number, after which the lines quite suddenly merge into a continuum.[1] The quantum number of the last discrete level is known to be a function of ion density. Comparison of laboratory and astrophysical observations may be used as a means of determining stellar ion densities. For this purpose it is, however, imperative that the possible variation of the phenomenon with temperature, as well as with ion density, be understood.

The problem has been attacked by several authors,[2,3,4] among whom Sugita has pointed out explicitly the superposition of the Stark effect of the (heavy) ions and the short-life broadening or collision broadening due to the bombardment of the more mobile electrons. His treatment of the Stark effect was, however, based on Kudar's simplified consideration of the possibility of an electron merely spilling over the top of the potential barrier formed by the atomic and external fields. And the treatment of electron bombardment used much too small a collision cross-section, namely, the area of the atomic orbit. His conclusion that the Stark effect is more important than the collision effect is, however, quite correct, as will be shown hereinafter.

[1] F. L. Mohler, preceding paper. We are indebted to Dr. Mohler for informing us of this problem while reporting his experiments and for a critical reading of the manuscript.

[2] H. P. Robertson and J. M. Dewey, *Phys. Rev.*, **31**, 973, 1928.

[3] M. Sugita, *Proc. Phys. Math. Soc.* (Japan), **16**, 254, 1934.

[4] A. Pannekoek, *M.N.*, **98**, 694, 1938.

Pannekoek has treated the termination of the series in the hydrogen spectrum as due to a merging of the lines broadened by the Stark effect. His very thorough calculations seem to us to take into account the essential reasons for the termination, and his results do indeed agree satisfactorily with experiment. His discussion does not include, however, collision broadening. It is, therefore, not quite clear whether the free electrons cause a broadening in the same way as do the heavy ions or whether they act primarily through a collision mechanism. In addition, in order to facilitate direct comparison with laboratory experiments, it seems desirable to extend the treatment to include the hydrogen-like spectra also.

ESTIMATE OF THE STARK EFFECT

Since we shall be interested in the region of high principal quantum numbers ($n \approx 20$), the correspondence principle allows the concept of electron orbits, and our treatment is partly classical. The radius (or, more strictly, the semimajor-axis) of the orbit is

$$a = n^2 a_0, \qquad a_0 = 0.53\ 10^{-8}\ \text{cm}, \tag{1}$$

and the energy (in a coulomb field) is

$$E = \frac{e^2}{2a}. \tag{2}$$

The separations of the higher states become very small:

$$\Delta E = \frac{e^2}{na}. \tag{3}$$

The perturbation energy (first-order Stark effect) of an external field F is of course equal in order of magnitude to aeF. A better value to use for the maximum displacement (half of the spread) of a line is $(3/2)aeF$, as will be shown by a more quantitative discussion below. The field F required to make the lines merge into one another may thus be had by putting $(3/2)aeF = \Delta E/2$, or

$$F = \frac{\frac{e}{3a_0^2}}{n^5}. \tag{4}$$

The critical value of n is here seen to be an extremely insensitive function of the applied field, so we may expect a rather abrupt termination of the series even if the effective field varies considerably, as for an atom in an atmosphere of ions.

The field F produced by a concentration of N singly charged ions per cubic centimeter is, in very rough approximation,

$$F \backsim eN^{2/3},$$

where $N^{-1/3}$ has been taken as the distance to the effective ion. Holtzmark[5] has studied carefully the fluctuations in such a field and finds that the most probable value of the field is

$$F = 3.7\, eN^{2/3}.$$

Substituting this in equation (4) leads to the approximate relation

$$Nn^{15/2} = 0.027 a_0^{-3}. \tag{5}$$

This gives the ion density N as a function of the principal (effective) quantum number n of the last term observed in the series.

DISCUSSION OF THE STARK EFFECT

The Stark effect energy of hydrogen, obtained from a treatment by the parabolic co-ordinates best suited to the problem, is[6]

$$\epsilon = \frac{3}{2} n(n_2 - n_1) a_0 eF, \qquad n_1, n_2 = 0, 1, 2, \ldots, n-1. \tag{6}$$

The various choices of the electric quantum numbers n_1 and n_2 give a variation of ϵ between the limits $\pm(3/2)n(n-1)a_0eF$. The curve giving the distribution of states in the energy spectrum is shaped like a symmetrical triangular peak, since the number of ways of forming the factor $(n_2 - n_1)$ varies linearly between the limits n for $\epsilon = 0$, and 1 for maximum ϵ.

The limits of ϵ in (6) may be visualized without the use of parabolic co-ordinates by considering the Stark energy as a small perturbation

[5] *Phys. Zs.*, **25**, 73, 1924.

[6] P. S. Epstein, *Phys. Rev.*, **28**, 695, 1926; E. Schrödinger, *Ann. d. Phys.*, **80**, 437, 1926.

of the elliptic orbits of the electron. The perturbation is a maximum for orbits having their major axes along F. The maximum average radius corresponds to the case of rectilinear motion along a radius between the limits 0 and $2a$, the speed being $v = em^{-1/2}(2/r - 1/a)^{1/2}$. The average radius is, then, $r_{av} = \int dr(r/v)/\int dr/v = (3/2)$ n^2a_0eF, agreeing with equation (6) for large n. Such a simple graphic treatment does not give any more of the details of equation (6), one reason being that the angular momentum l is not a constant of the motion and there are many states with different values of l and the same n which are degenerate in hydrogen and are strongly mixed by the perturbation. The energies in equation (6) would be the result of a number of rather complicated secular problems, one for each m, if we should carry out the perturbation problem using the states described by spherical harmonics.

In the alkali spectra we do not find such complete degeneracy. However, states of a given n with $l \geqslant 2$ are practically degenerate, but the s and p levels of that n may be even lower than most of the levels with next lower n. These nondegenerate levels will not be strongly mixed with the others until the perturbation is of the order of magnitude of their separation. We wish to show in the following paragraph that the matrix elements responsible for the mixing are not greatly affected by the lack of degeneracy.

Corresponding to the selection rule $\Delta l = \pm 1$, there exist nondiagonal matrix elements of $r \cos \theta$ only between states of adjacent values of l. The evaluation of the matrix elements of r depends on an integration over r involving the radial-wave functions. The usual polynomials for these are rather complicated for large n and small l. We may, however, think of the wave functions as the result of integrating the radial-wave equation inward from infinity. The equation contains a centrifugal-force term which depends upon l, but which differs very little between states of slightly different l, except at values of r much smaller than a. Because of the increasing curvature for smaller distances, the radial function has its highest maximum outside of its first node, in the neighborhood of a. The integration depends essentially on the energy. In two degenerate states which differ slightly in l the radial functions are practically the same throughout the region of large r, which is important in

determining a matrix element of r, and the matrix elements between them are about equal to the diagonal elements or to the mean value of r. For two states differing in energy the integrations differ at large r, which reduces the matrix element of r between them. The rate at which this energy difference becomes important may be judged by the fact that in hydrogen an energy difference of ΔE is sufficient to make the radial functions orthogonal. The orthogonality, by introducing cancellation and reducing the integrand in magnitude, reduces the matrix element of r considerably. For energy differences less than ΔE the reduction of the matrix element of r is essentially quadratic in the energy difference (since it has the same sign on both sides of zero). Since a difference ΔE would not quite reduce it to zero, a difference $\Delta E/2$, such as one might find in an alkali atom, would leave a nondiagonal element of r somewhat larger than three-fourths of a diagonal element.

We may consider that a high p-level is separated from the nearest degenerate set of levels with larger l by about $\Delta E/2$, though it may happen to be closer. (We consider the nearest degenerate set because there is no selection rule for n.) As long as the p–d nondiagonal matrix element of the perturbing energy, H'_{pd}, is small, the degree of admixture is about $H'_{\mathrm{pd}}/(\Delta E/2)$. This ratio is a measure of the probability of a series transition involving the degenerate set of states, in violation of the selection rule which defines the series. As the ratio approaches unity, the states of the set become increasingly involved in the series transitions, and, at the same time, their energies are spread out enough to merge with other sets. Similar considerations apply to the s-states of the sharp series. The s- and p-states may also be displaced by about $(H'_{ab})^2/(\Delta E/2)$ by the quadratic Stark effect. Here H'_{ab} contains the fluctuations of the ion field, so this also tends to merge the series lines. Each of these effects tends to merge the lines of the sharp and the principal series of the alkalis when the Stark perturbation becomes about equal to the separation of the levels, and their combined result should be a termination of the series which is even more abrupt than in hydrogen. The less abrupt termination of the series in hydrogen and in the alkali series of higher angular momentum l is due to a broadening of the lines below the series limit by the linear Stark effect, which

depends on the degeneracy in l. (For an s-state, the perturbation might become effective still more abruptly than for a p-state, for it is necessary for a p-state to act as an intermediary in mixing it with the degenerate states of higher angular momentum, unless the inhomogeneity of the ionic field becomes important). Despite the more complex mechanism of terminating the series in the alkali spectra, equations (4) and (5) remain valid.

ESTIMATE OF COLLISION BROADENING

Effect of the close collisions.—In comparing the collision broadening[7] with the Stark broadening, it is of interest to note that the merging of the lines due to Stark effect might have been derived in another way. Essentially, we have put the energy due to the dipole moment about equal to half of the energy difference ΔE between states,

$$eFa = \tfrac{1}{2}\hbar\omega\,, \tag{7}$$

where ω is the (average) angular speed of the orbit, according to the correspondence principle. Instead, we might consider the momentum. The uncertainty principle gives the momentum difference between states as $\Delta p = |\Delta p| = \hbar/a$. During the time $1/\omega \approx a/v_n$, the orbital motion is approximately rectilinear, so the increments of momentum are additive. If the transfer of momentum during this time is as great as $\frac{1}{2}\Delta p$, then it is as likely as not that a transition occurs during each cycle, and the states are not stationary. This transfer of momentum to the atomic electron is the force *times* the time, so the field necessary to destroy stationary states is given by

$$\frac{eF}{\omega} = \frac{\frac{1}{2}\hbar}{a}\,. \tag{8}$$

Thus, consideration of momentum leads to the same result as does consideration of energy.

We employ the transfer of momentum in a similar manner in treating the collision broadening. We consider an electron passing

[7] A fundamental discussion of collision broadening has been given recently by L. Spitzer, *Phys. Rev.*, **55**, 699, 1939. For our present purpose the following qualitative considerations seem to be adequate.

an atom along a straight line (neglecting the reaction) at a distance r and at a speed v. The time during which practically the maximum force is effective in transferring momentum to the atomic electron is either the "collision time" r/v or the "atomic time" $1/\omega$, whichever is the shorter. Here we wish to confine our attention to small-distance encounters, defined by the condition that they should each cause a transition with practical certainty. For that the collision parameter r will have to be less than a value r_1. If the length of the encounter is limited by the atomic time, we have, by consideration of the momentum, $(e^2/r_1^2)/\omega = \hbar/a$, or $r_1 = (av_0/\omega)^{1/2}$, where $v_0 = e^2/\hbar$ = velocity in the first Bohr orbit. The discussion leading to equation (8) shows that encounters closer than this r_1 cause a merging of the lines, and it is merely a matter of language whether we consider it to be a collision effect or the static Stark effect.

If the length of the encounter at r_1 is limited by the collision time, we have $(e^2/r_1^2)\ (r_1/v) = \hbar/a$ and $r_1 = av_0/v$. The collision broadening is obtained roughly from the uncertainty principle, $\epsilon\Delta t = \hbar$, or

$$\epsilon = \hbar \text{ (number of collisions per second)} = \hbar N\sigma v = \hbar N\pi r_1^2 v$$

$$= \frac{\pi\hbar N a^2 v_0^2}{v}. \qquad (9)$$

The factor v^{-1} in r_1 means that a decrease of v is favorable for large ϵ in equation (9), down to the point where the collision time is equal to the atomic time, or $r_1/v = 1/\omega$. The speed most favorable to a large collision effect is thus also the critical speed below which the electrons cause essentially a static Stark effect. For this speed then, $r_1 = v/\omega$, and also $r_1 = av_0/v$. This determines the critical v for a given n as

$$v = (v_0 a\omega)^{1/2} = (v_0 v_n)^{1/2}, \qquad (10)$$

where v_n is the velocity in the nth Bohr orbit. For higher velocities we may properly speak of a collision broadening. For the case of smaller velocities, $v < (v_0 v_n)^{1/2}$, the electrons will contribute to the merging of the lines through the Stark effect, and one will have to substitute for N in equation (5) the total number of electrons plus ions, that is, double the number of positive ions under ordinary con-

ditions. For higher velocities the collision effect of the electrons by itself will decrease with v^{-1}, so that for very high velocities the effect of the positive ions alone would remain.

The temperature corresponding to the velocity v in equation (10), obtained by setting $mv^2/2 \approx 3kT/2$, is

$$T = \frac{T_0}{n}, \tag{11}$$

where $T_0 \approx 10^5$ degrees absolute corresponds to v_0. This is fulfilled by the values $n = 20$, $T = 5000°$, for example. This corresponds to about the largest value of the product nT occurring in Mohler's experiments. We see, thus, that the velocity at which the electrons start to contribute through the collision effect rather than through the Stark effect is actually attained experimentally.

Effect of the more remote collisions.—Inclusion of the slow encounters in the ion density considered by Holtzmark disposes of them for large as well as for small values of the collision parameter r, but for fast electrons it is necessary to consider the remote collisions separately.

First, we consider those collisions for which $r > r_1$ but for which the collision time is less than the atomic time. These collisions are non-adiabatic and may be treated by time-dependent perturbation theory. The time-dependent wave function of the perturbed atom may be expressed in terms of the stationary states as

$$\psi = \psi_0 + \sum a_k \psi_k ,$$

where the coefficients a_k are slowly varying functions of the time. For the non-adiabatic case we have

$$\dot{a}_k = \frac{i}{\hbar} H'_{k0} ,$$

where H'_{k0} is a matrix element of the perturbing Stark effect energy. Thus, at the end of the collision a_k will have the value $(i/\hbar)H'_{k0}r/v$. The probability that a transition has occurred is

$$\left(\frac{r}{v\hbar}\right)^2 \sum (H'_{k0})^2 .$$

According to the rule of matrix multiplication, the sum is $(H'^2)_{00}$, for which one may write approximately $(ae^2/r^2)^2$, making the transition probability $(ae^2/rv\hbar)^2 = (av_0/rv)^2$.

For collisions at still greater distances, for which the atomic time is greater than the collision time, we may use the adiabatic approximation. The energy of a state is associated with a time wave, the phase of which is shifted by an amount $\delta = (\epsilon/\hbar)t = (\epsilon/\hbar)\, r/v$ by a collision, where we may consider ϵ as ae^2/r^2, due to linear Stark effect. If the time wave was $e^{i\nu t}$ before a collision, it becomes $e^{i(\nu t+\delta)} \approx e^{i\nu t}\,(1 + i\delta)$, for $\delta << 1$. Here $i\delta e^{i\nu t}$ can be interpreted as the new wave caused by the collision which is out of phase with the original wave. Since δ is the amplitude of this wave, $\delta^2 = (av_0/rv)^2$ corresponds to a transition probability. This is the same as the transition probability in the non-adiabatic case.

The number of collisions per second between r and $r + dr$ is $2\pi Nvrdr$, and they cause $(2\pi Na^2v_0^2/v(dr/r)$ transitions per second. Considering the broadening effect of the most remote collisions, we must, however, take into account the fact that the cancellation of fields of the various electrons will render the collisions ineffective for values of the collision parameter greater than some value r_m. It is probably sufficient to determine r_m by the requirement that only one collision with $r < r_m$ (lasting a time r/v) shall be in progress, in the average, at any instant. This gives $r_m = (\pi N)^{-1/3}$. Integrating from r_1 to r_m and adding to equation (9), we have the approximate collision broadening, for large v,

$$\epsilon = \frac{\pi\hbar N(av_0)^2}{v}\left(1 + 2ln\frac{r_m}{r_1}\right). \qquad (12)$$

$r_1 \to 0 \quad \left(-1 + 2\ln r_m\right)$

We now evaluate this broadening for the case of that line n which the Stark effect of the heavy ions is just able to merge into its neighbors. According to equation (5), $Na^3 = .027n^{-3/2}$. With $\omega = v_0/na$ and with the notation $x = v/(v_0v_n)^{1/2} = n^{1/2}v/v_0$, we obtain

$$\epsilon = \frac{.027\pi\hbar\omega}{x}\,(1 - 2ln\ 0.3\pi^{1/3} + 2lnx).$$

This has a maximum value $\epsilon_m = .24\hbar\omega$. This is, indeed, considerably less than the broadening $\frac{1}{2}\hbar\omega$ of this line caused by the Stark effect of the heavy ions.

SUMMARY

It is found that the principal cause of termination of the series is the static Stark effect broadening which merges the lines into one another. This confirms the applicability of the detailed calculations of this effect made for hydrogen by Pannekoek.

The quantum number n of the line with which the series terminates may be correlated with the ion density N by the formula $Nn^{7.5} = .027a_o^{-3}$, where a_o is the Bohr radius (eq. [5]).

This equation may be applied to the alkali spectra as well as to hydrogen. The continuum should set in more abruptly in the sharp and principal series of the alkalis, the lines near the end of the series being less diffuse in these cases.

For temperatures lower than $10^5/n$ degrees absolute the electrons contribute to the broadening through the static Stark effect rather than through a collision mechanism. In this case the total number of ions, positive and negative, enters equation (5).

At higher temperatures, the positive ions alone cause static Stark effect, the electrons contributing by means of collisions. The collision broadening is smaller than would be the Stark effect of the same electrons at a lower temperature, the broadening decreasing as $T^{-1/2}$. At very high temperature equation (5) applies with N representing the positive ions alone.

JOHNS HOPKINS UNIVERSITY
BALTIMORE, MARYLAND

GEORGE WASHINGTON UNIVERSITY
WASHINGTON, D.C.